Fall 12-3-2014

Single- and Dual-Porosity Calibration and Long-Term Modeling of Highly Conductive Floodplain Soils in the Ozark Ecoregion

Ryan P. Freiberger
University of Nebraska-Lincoln, rfreibe1@gmail.com

SINGLE- AND DUAL-POROSITY CALIBRATION AND LONG-TERM MODELING OF HIGHLY CONDUCTIVE FLOODPLAIN SOILS IN THE OZARK ECOREGION

by

Ryan P. Freiberger

A THESIS

Presented to the Faculty of

The Graduate College at the University of Nebraska

In Partial Fulfillment of Requirements

For the Degree of Master of Science

Major: Agricultural and Biological Systems Engineering

Under the Supervision of Professor Derek M. Heeren

Lincoln, Nebraska

December, 2014

SINGLE- AND DUAL-POROSITY CALIBRATION AND LONG-TERM MODELING OF HIGHLY CONDUCTIVE FLOODPLAIN SOILS IN THE OZARK ECOREGION

Ryan P. Freiberger, M.S.
University of Nebraska, 2014
Advisor: Derek M. Heeren

Phosphorus (P) is a critical nutrient for agriculture, but is also responsible for surface water enrichment that leads to toxic algal growth. While P loading to surface waters has traditionally been thought to occur from surface runoff, contributions from subsurface transport can also be significant. While P transport through many soil types is well-documented, the presence of highly conductive gravel outcrops and macropore networks can have a significant, yet poorly-documented effect on P movement to groundwater. Floodplain soils in the Ozark ecoregion generally contain coarse chert gravel layers that exhibit preferential flow behavior. Previous research has evaluated short-term P transport in plot trials ranging from 1 m^2 to 100 m^2 across many Ozark ecoregion floodplain sites. Traditional methods of estimating P loading and soil saturation do not account for macropore flow and likely underestimate P transport to the water table.

Long-term P modeling was performed in HYDRUS-1D and 2D using data collected from short-term plot experiments. Seven model levels were developed to illustrate a wide variety of laboratory and field conditions. Calibration was performed in HYDRUS-2D using single- and dual-porosity models with both

homogeneous and heterogeneous gravel profiles as well as a mesh macropore profile. The dual-porosity model with heterogeneous hydraulic conductivity best matched experimental data, although the dual-porosity model with homogenous soil layers also performed well.

Long-term P transport to a 3 m-deep water table was simulated in HYDRUS-1D and 2D using nine years of both daily and modified 5 minute rainfall data with a P flux consistent with annual poultry litter applications. HYDRUS-1D models produced a wide range of long-term results, while HYDRUS-2D models produced a much narrower range of results. There was little difference between analogous 1D and 2D models, suggesting that HYDRUS-1D may be sufficient to model long-term transport. The lack of distinction between the single- and dual-porosity long-term models could be explained by the large P concentration gradient between the poultry litter leachate and the soil water.

Acknowledgements

This thesis would not have been possible without the help and guidance of many individuals. I would like to take a moment to thank those that contributed to this work.

I would first like to thank my advisor, Dr. Derek Heeren. His guidance throughout this entire research project has been indispensable. His mentoring has also allowed me to grow as a professional and as a person. I feel privileged to have been able to work with Dr. Heeren.

Special thanks go to Dr. Garey Fox at Oklahoma State University. His insight into both this particular research and the greater field of solute transport has been invaluable. His help with obtaining important resources for our work has also been greatly appreciated.

The members of my committee also provided valuable input and useful advice for this research, and I am grateful to all the support and guidance that they have provided.

This thesis is the result of a group effort of all the people above and others. Without all of them and the help they provided, this thesis would have never been possible. I am honored to have been able to work with those that helped me during my graduate program. Thank you for everything that you have done.

Table of Contents

List of Tables

List of Figures

1. Introduction

Phosphorus is an important nutrient for crop growth and development, but overloading of freshwater systems with phosphorus can induce significant algae growth. Algal blooms and cyanobacteria outbreaks contribute to hypoxic waters and fish kills, as well as reduce the quality of water for consumption and recreational use (Lopez et. al., 2008). Phosphorous (P) transport has been assumed to take place primarily in surface runoff, although a growing collection of research indicates that subsurface P transport can be significant (Osborne and Kovacic, 1993; Cooper et al., 1995; Gburek et al., 2005; Fuchs et al., 2009). Large scale streambank storage of P-laden stream water during high flow discharges can result in P-laden groundwater in alluvial aquifers which migrates back to the stream during baseflow conditions (Heeren et al., 2011). These subsurface P transport rates in Ozark floodplains have been shown to be comparable to surface runoff P transport rates (Mittelstet et al., 2011). In many gravelly floodplains, gravel outcrops and macropores are present resulting in high infiltration rates, some of which are reported to be on the order of 10 to 100 cm hr^{-1} (Heeren et al., 2014; Heeren et al., 2013). It has been shown that in porous media with heterogeneous flow properties, the majority of the flow can occur in small preferential flow paths (Gotovac et al., 2009; Najm et al., 2010). Djodjic et al. (2004) performed experiments on P leaching through undisturbed soil columns, and stressed the need to consider larger-scale leaching processes due to soil heterogeneity.

1.1 Poultry litter leaching

Poultry litter is a popular fertilizer option in the Ozark ecoregion, given the wide range of macro- and micronutrients it provides for plants (OCES, 2013). However, improper application of poultry litter, either from overapplication or poor application timing, can cause significant loss of nutrients from runoff or leaching into the soil. Westerman et al. (1983) performed laboratory experiments on small test plots to gauge runoff from soils amended by poultry litter. Runoff rates of sediments and nutrients were influenced by many factors, including the manure characteristics, manure application rate, incorporation into the soil, and time to first rain after application. Edwards and Daniel (1993) performed P runoff experiments on field plots amended with poultry litter. P losses in runoff increased with litter application rates, and large sediment losses were found to increase as litter application and rainfall intensity increased. Sharpley and Moyer (2000) measured P leaching in laboratory poultry litter columns and found that poultry manure and litter leached 20% of its total P in five 7 cm h^{-1}, 30 min events.

1.2 Preferential flow

Rapid leaching of water and solutes through soil profiles to groundwater occurs due to preferential flow in the profile. At the most fundamental level, preferential flow occurs when water and solutes are allowed to move more quickly through a particular region of the soil that has greater transport potential than the surrounding soil. Soils featuring a high degree of heterogeneity, like those found in the Ozark ecoregion, usually exhibit a similarly high degree of preferential flow. Preferential flow can occur over a wide range of velocities in a wide range of pore sizes (Beven and Germann, 2013). This

means that preferential flow is not limited to transition and turbulent flow in large macropores, but can also occur as laminar flow in fluid films with a thickness of less than 100 μm along the sides of smaller pores (Nimmo, 2010).

Regions of high preferential flow may or may not be directly connected to the soil surface or another source of water. Preferential flow regions that are connected to the surface or another water source are supplied directly by "event" water, such as storm water. Regions not connected to a source may receive flow from a redistribution of "pre-event" matrix water (Beven and Germann, 2013). Non-connected preferential flow can also occur under "source-responsive" conditions, where preferential flow deep in the profile can respond quickly to changes in surface water sources (Nimmo, 2010).

Conditions that create preferential flow regions are numerous. Large scale preferential flow regions can be caused by weathering of parent material over long periods of time (karst formation, soil fissures). Smaller scale preferential flow regions can be the result of layered heterogeneity based on alluvial deposits, root growth and decay or animal burrowing activity, or surface cracks formed by clay shrink-swell potential (Beven and Germann, 2013). Allaire et al. (2011) created a risk assessment map of the Canadian Great lakes region for different sources of vertical and horizontal preferential flow for P transport. Featured in the risk assessment were four sources of preferential flow: vertical crack flow caused by clay shrink-swell, vertical burrow flow through earthworm burrows, vertical finger flow caused by heterogeneity in coarse sandy soils, and horizontal lateral flow caused by soil layering and root layers.

1.3 Conceptual preferential flow models

Accurately modeling large macropores and preferential flow in general is a complicated process. Possibly the best currently available means of modeling macroporosity in a soil is through the use of a multi-domain system (Beven and Germann, 1982; Šimůnek and van Genuchten, 2008). Multi-domain models split the soil profile into a fracture (macropore) domain and a matrix domain. Such models account for high flows and solute transport rates that are linked to macroporosity in soils. Multi-domain models express physical transport in several ways. Mobile-immobile (MIM) models define water and solute flow through the macropore space, with solute transport also occurring between the immobile and mobile phases through molecular diffusion (Figure 1a). Dual-porosity models build upon this further by allowing both water flow and solute transport (through advection as well as diffusion) to occur between the mobile and immobile phases (Figure 1b). Dual-permeability models are somewhat different, where mobile and immobile phases are replaced with “fast” and “slow” zones, respectively (Figure 1c). Both zones allow for water and solute transport, but do so at different rates. A last model combines dual-permeability and MIM phases, so that solute transport can also enter an immobile zone and is removed from transport (Figure 1d).

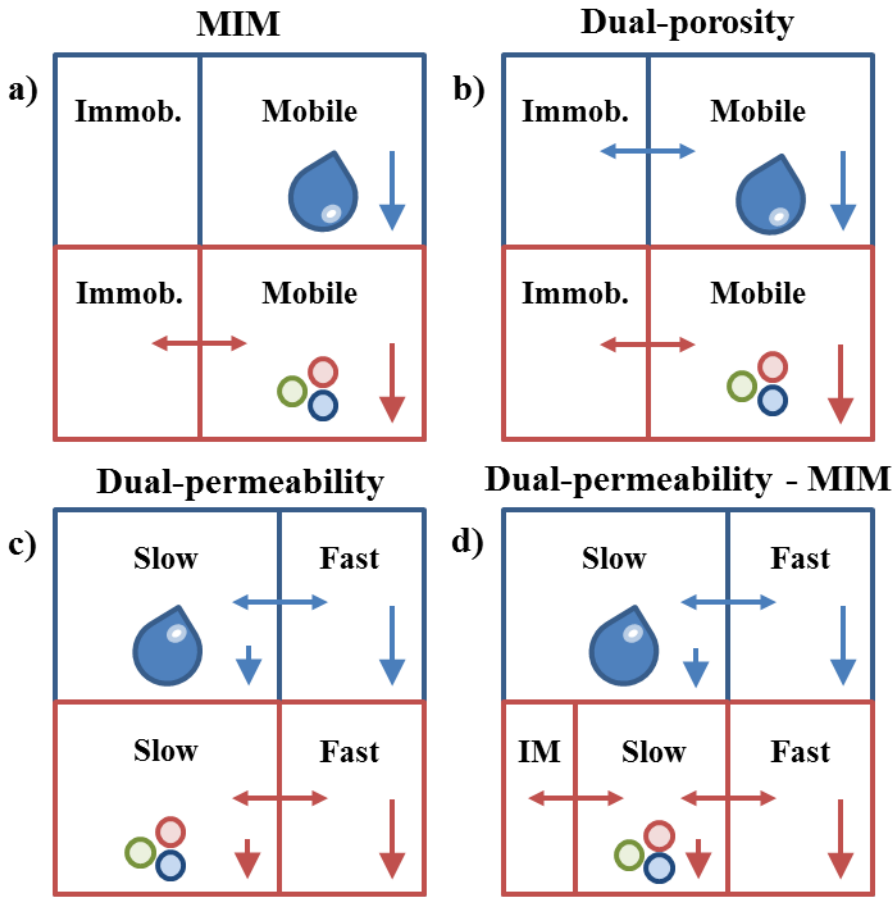

Figure 1. Conceptual models for macroporosity: (a) mobile-immobile, (b) dual-porosity, (c) dual-permeability, and (d) dual-permeability with a solute immobile zone. Adapted from Šimůnek and van Genuchten (2008).

1.4 Flow and transport equations

The one-dimensional Richards equation (Eq. 1, presented in Šimůnek et al., 2003) was developed in 1931 and is a combination of the continuity equation and the Buckingham-Darcy equation:

$$\frac{\partial \theta}{\partial t} = \frac{\partial}{\partial z}\left[K(h)\left(\frac{\partial h}{\partial z} + 1\right)\right] - S \qquad (1)$$

where θ is the volumetric water content [L^3L^{-3}], t is time [T], z is the vertical position with positive upwards [L], h is the pressure head [L], $K(h)$ is the unsaturated hydraulic

conductivity function [LT^{-1}], and *S* is a sink-source term [-]. Two- and three-dimensional versions of this equation have also been developed, but are more complex.

For dual-porosity models featuring MIM components, a modified version of the Richards equation is needed. This modified version breaks the soil matrix into two distinct phases: a mobile phase that is open to water flow and solute transport through advection and dispersion, and an immobile phase that prohibits water flow and solute transport within the immobile zone. Water exchange between the immobile and mobile zones is considered to be an apparent "diffusion" process, and solute exchange occurs by advection with the water exchange as well as molecular diffusion. In soil terms, the immobile phase is the soil matrix, while the mobile phase is made of fractures generated by weathering effects, root action, burrowing animals and insects, or bands of highly conductive materials that cut through the matrix. The θ_m and θ_{im} are complementary portions of the total porosity of the soil, such that:

$$n = \theta_{m,s} + \theta_{im,s} \tag{2a}$$

$$\theta = \theta_m + \theta_{im} \tag{2b}$$

where *n* is the total porosity [L^3L^{-3}], θ is the total unsaturated volumetric water content, $\theta_{m,s}$ and θ_m are the saturated and unsaturated mobile volumetric water contents, and $\theta_{im,s}$ and θ_{im} are the saturated and unsaturated immobile volumetric water contents. This distinction can be used to modify the Richard's equation for multi-domain flow as follows (Šimůnek et al., 2003):

$$\frac{\partial \theta_{mo}(h_{mo})}{\partial t} = \frac{\partial}{\partial t}\left[K(h_{mo})\left(\frac{\partial h_{mo}}{\partial z}+1\right)\right] - S_{mo}(h_{mo}) - \Gamma_w \tag{3a}$$

$$\frac{\partial \theta_{im}(h_{im})}{\partial t} = -S_{im}(h_{im}) + \Gamma_w \quad (3b)$$

where $\theta_{mo,\,im}$ are the water contents for the mobile and immobile phases [L^3L^{-3}], h_{mo} and h_{im} are the mobile and immobile pressure heads, respectively [L], $K(h_{mo})$ is the unsaturated hydraulic conductivity function for the mobile zone [LT^{-1}], t is time [T], z is the vertical coordinate, with positive in the upward direction [L], S_{mo} and S_{im} are mobile and immobile sink terms, respectively [-], and Γ_w is the water transfer rate between mobile and immobile phases [-]. Figure 2 shows the retention curve developed by the van Genuchten equation under mobile-immobile conditions.

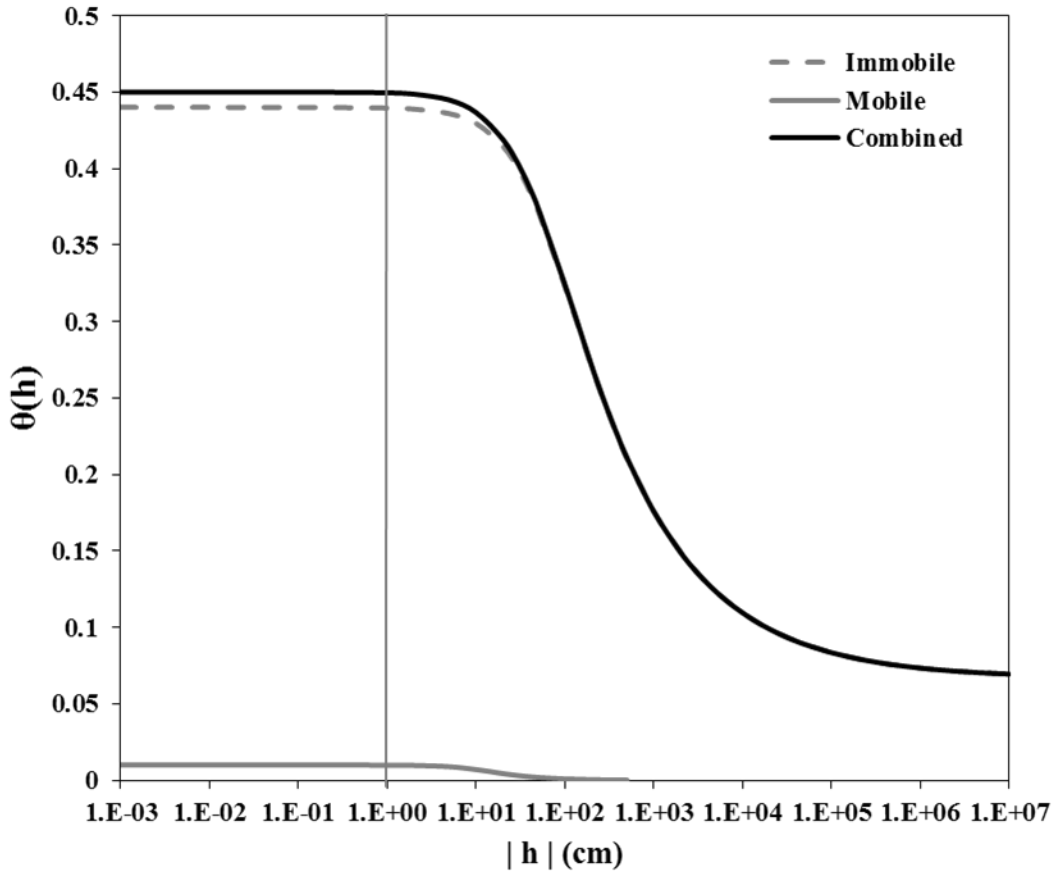

Figure 2. Retention curve developed using the van Genuchten equation under mobile-immobile conditions for the Barren Fork 1x1α silt loam layer.

The advection-dispersion equation (ADE) used by HYDRUS for solute and heat transport is presented in Šimůnek et al. (2003):

$$\frac{\partial \theta c}{\partial t}+\frac{\partial \rho s}{\partial t}=\frac{\partial}{\partial z}\left(\theta D\frac{\partial c}{\partial z}\right)-\frac{\partial qc}{\partial z}-\mu(\theta c+\rho s)+\gamma\theta+\gamma\rho \qquad (4)$$

where θ is the volumetric water content [$L^3\ L^{-3}$], t is time [T], ρ is the soil bulk density [$M\ L^{-3}$], c and s are solute concentrations for the liquid and solid phases, respectively [$M\ L^{-3}$], D is the dispersion coefficient [L^2T^{-1}], q is the volumetric flux density [$ML^{-2}T^{-1}$], μ is a first-order rate constant[T^{-1}], and γ is a zero-order rate constant [$ML^{-3}T^{-1}$]. Like the Richards equation, the ADE can be modified to fit a multi-domain profile (presented in Šimůnek et al., 2003):

$$\frac{\partial \theta_{mo} c_{mo}}{\partial t}+f_{mo}\rho\frac{\partial s_{mo}}{\partial t}=\frac{\partial}{\partial z}\left(\theta_{mo} D_{mo}\frac{\partial c_{mo}}{\partial z}\right)-\frac{\partial q_{mo} c_{mo}}{\partial z}-\varphi_{mo}-\Gamma_s \qquad (5a)$$

$$\frac{\partial \theta_{im} c_{im}}{\partial t}+\left(1-f_{mo}\right)\rho\frac{\partial s_{im}}{\partial t}=\Gamma_s-\varphi_{im} \qquad (5b)$$

where $c_{mo,\ im}$ are the concentrations of solute in the mobile and immobile phases [ML^{-3}], s_{mo} and s_{im} are the sorbed concentrations of solute in the mobile and immobile phases [ML^{-3}], f_{mo} is the fraction of sorption sites in contact with mobile water [-], D_{mo} is the dispersion coefficient for the mobile phase [L^2T^{-1}], $\varphi_{mo,\ im}$ are lump sink-source terms for the mobile and immobile phases, and Γ_s is the mass transfer function, defined as:

$$\Gamma_s=\alpha\left(1-w_{im}\right)\left(c_{mo}-c_{im}\right)+\Gamma_w c^* \qquad (6a)$$

where α is the solute mass transfer coefficient [T^{-1}], w_{im} is the ratio of the volumes of the matrix and the total pore systems, $\theta_{ms}\,\theta_s^{-1}$[-], c^* is equal to c_{mo} for $\Gamma_w>0$ and c_{im} for $\Gamma_w<0$,

and Γ_w is defined as:

$$\Gamma_w = \omega[S_e^m - S_e^{im}] = \alpha_w[h_m - h_{im}] \quad (6b)$$

where ω is the water mass transfer coefficient [T^{-1}], S_e^m and S_e^{im} are the effective saturation values for the mobile and immobile phases [-], h_m and h_{im} are the head pressures of the mobile and immobile phases [L], and α_w is a first-order mass transfer coefficient [T^{-1}][1].

1.5 Preferential flow in HYDRUS-1D and -2D

State-of-the-art modeling programs, such as HYDRUS-1D or HYDRUS-2D/3D, offer these models to allow for maximum flexibility when modeling complex subsurface systems. The HYDRUS suite of software simulates the transport of water, solutes, and heat through simple and complex soil profiles. HYDRUS-1D is limited to one-dimensional transport (vertical or horizontal) and limited options for profile complexity. The HYDRUS-2D/3D software allows for two- or three-dimensional transport, as well as increased complexity within the soil profile and the potential for upscaling to field or even hillslope size models. HYDRUS uses numerical methods to solve the Richards equation for variably saturated water flow and the advection-dispersion equation for heat and solute transport (Šimůnek, 2011). HYDRUS also has the capacity to simulate evapotranspiration (ET) as uptake by roots.

The HYDRUS suite of software has been used in several studies to model flow of water and solutes in soil. Elmi et al. (2012) used HYDRUS-1D and a single-porosity

[1] It is important to note that in this research, the head mass transfer method is used for water transport. The term "α_w" is used in this research, but is referred to as "ω" for consistency with HYDRUS labels and to avoid confusion with other instances of α.

model to simulate PO_4 transport through undisturbed soil cores. Simulated water flow had a good match to the observed data. However, PO_4 sorption was overpredicted by HYDRUS-1D, which suggested that preferential flow was present in the soil columns that was unaccounted for in HYDRUS. The authors also suggested that the Freundlich isotherm used could have also poorly described PO_4 sorption. Naseri et al. (2011) also performed column experiments on soils cores to measure PO_4 transport. In this study, HYDRUS-3D with a single-porosity model was used to simulate transport through the soil columns. Simulated water flow once again matched observed data, but PO_4 sorption was overestimated, leading the authors to conclude that preferential flow could have been present in the soil columns. However, neither of these studies pursued preferential flow any further in HYDRUS.

Some research has been done to simulate artificial macropores in HYDRUS. In this thesis, the term "artificial macropore" is different from "mesh macropore". An artificial macropore is an anthropogenic macropore created in a laboratory soil column. This differs from a mesh macropore, which is defined in this thesis as an expression of a macropore or bundle of macropores in HYDRUS as a single band of highly conductive material built directly into the mesh that allows for flow to bypass low conductivity material. Both of these techniques seek to define preferential flow differently than more traditional multi-domain models that express domains as overlapping continua. Akay et al. (2008) used HYDRUS-3D to simulate soil column studies conducted by Akay and Fox (2007) in which artificial surface-connected and buried macropores were inserted into sandy loam laboratory soil columns and flow to a subsurface drain was measured.

The artificial macropores were simulated in HYDRUS-3D as a cylindrical set of flow boundaries that characterized the flow conditions into such a macropore. Results from flow simulations found excellent matches to experimentally generated curves, suggesting that HYDRUS is well-suited to model macroporous flow. Lamy et al. (2009) performed sand column experiments on water and solute transport through an artificial macropore. The artificial macropore was simulated by defining each node with different material parameters that expressed matrix or macropore behavior. They also used inverse modeling in HYDRUS-2D to optimize parameters and perform a sensitivity analysis. Inverse modeling results showed good matches to column data for the artificial macropore, but the lack of "preferential flow extension" from the macropore to the matrix region in the model caused HYDRUS to underestimate flow through the system and reveals the need to improve macropore-matrix interactions in multi-domain modeling. Furthermore, while these studies had mostly successful results in matching HYDRUS results to experimental data, it should be noted that these artificial macropores had simplified geometries and modeling natural macropores using this technique would be extremely complicated at best.

1.6 Preferential flow in other models

Modeling preferential flow has been done in several other models. Singh and Kanwar (1991) and Kamra et al. (2001) used the basic advection-dispersion equation to model preferential flow. Preferential flow in these studies was described as a combination of the dispersion coefficient and the retardation factor. Both studies evaluated transport through undisturbed soil columns. Singh et al. (1991) used the transport of chloride to

compare the mobile region between no-till and tilled soil profile, finding that no-till land had a higher mobile fraction. Kamra et al. (2001) evaluated transport of bromide and pesticides in soil columns, then used two different models to compare to observed data. The first model calibrated only the retardation factor; the second model held the retardation factor constant while calibrating the dispersion coefficient, mobile fraction, and the mass transfer rate constant. Kamra et al. (2001) also used MIM to evaluate transport, but found that it was not able to illustrate preferential flow adequately. Sheng et al. (2014) modeled iodine, bromide, and nitrate transport in field-scale plot experiments with the Active Region model (ARM). ARM was developed by Liu et al. (2005) and describes preferential flow of water and solutes with fractal, macroscopic properties. Field experiments results were compared to simulated results from ARM and MIM. In general, ARM matched the field-scale data better than MIM and illustrated unstable flow well. However, it was unable to account for the influence of macropores in the soil.

Some research has used multi-domain numerical models other than HYDRUS to model contaminant transport. Jarvis et al. (1999) used the dual-region MACRO model to simulate colloidal particle transport in silty clay loam soils in Sweden. MACRO was developed by Jarvis et al. (1994). MACRO is a dual-permeability variant where transport through the macropore is expressed as a volumetric flux density, and the matrix is expressed as a single-porosity Darcy-Richards domain (Šimůnek et al., 2003; Beven and Germann, 2013). Larsson et al. (2007) simulated P losses to tile drains in clay soils using the ICECREAM model. The ICECREAM model is an adaptation of the CREAMS model, a field-scale non-point source pollution model. The ICECREAM model adds

macropore flow to the CREAMS model and allows adjustments for Nordic conditions. Ahuja et al. (1993) used the Root Zone Water Quality Model (RZWQM) to model atrazine, prometryn, and nitrate transport through macropores. RZWQM is an USDA Agricultural Research Service model that simulates major soil processes in crop production systems. The RZWQM can simulate a wide variety of physical, chemical, and biological processes in a multi-domain system. Ahuja et al. (1993) found that macropore flow was only generated under wet conditions, and that solutes transported with the macropore flow ranged from 0.05 to 8% of surface-applied amounts. Evaporation reduced water flows through macropores, while transpiration reduced water and chemical transport.

1.7 Future research in preferential flow modeling

There are still some areas of growth needed for this field of study. First, there has been little research done that explicitly compares single- and dual-porosity transport. Field-scale research has been conducted and simulated with both single- and dual-porosity models, but again little research has been done comparing the two models, and clear expression of profile heterogeneity is often neglected or oversimplified. Furthermore, limited research has been done using profile data from advanced tools, such as electrical resistivity mapping, at the field scale.

Further advances needed for preferential flow research in general is presented by Beven and Germann (2013). It should be noted that while this thesis makes no attempts to tackle the following issues, they are nonetheless important towards the overall advancement of this field. At the fundamental level, the Darcy-Richards framework that

almost every popular subsurface transport model is based on poorly illustrates many of the complexities that preferential flow creates. The Darcy-Richards framework creates an environment that does not adapt to changes in soil and transport parameters that occur under preferential flow conditions. The use of pedotransfer functions to obtain soil properties and the advection-dispersion equation contribute to this framework. However, despite these shortcomings, the Darcy-Richards framework is popular due to its ease of use with powerful computing tools. Beven and Germann (2013) suggest several alternatives to the Darcy-Richards framework that may prove fruitful for advancing understanding of preferential flow transport, including the use of Stokes flow properties, 2D/3D images of pore arrangements, and particle tracking of water parcels at the profile scale. However, the authors note that these alternatives have seen limited testing or are currently restricted to small scale modeling.

Additional work needs to be done to address the problem of the scale effect in preferential flow modeling. The scale effect, also referred to as the scale effect of dispersion, is the extra dispersion effect added by increasing the spatial and temporal scale of experiments that is not expressed in the basic ADE (Frippiat and Holeyman, 2008). When transitioning from the laboratory to the field scale, dispersion and preferential flow may be added from small pockets of heterogeneity in the soil profile or larger fractures. Transitioning from the field scale to the hillslope scale adds extra complexity by potentially adding significant lateral flow. Accurately mapping the flow networks at this level is difficult, and often requires destructive sampling. (Beven and Germann, 2013). Spatial upscaling methods must be used to properly account for the

added dispersivity or model alternatives to the ADE must be considered (Frippiat and Holeyman, 2008). Potential upscaling techniques include characterizing heterogeneity in the basic ADE with a variance or a characteristic length scale, which are then used to generate a "macroscale" dispersion coefficient. Different model approaches include models using a continuous time random walk approach or MIM modifications (Frippiat and Holeyman, 2008). Little research has been done on the effects of temporal scaling on dispersion and transport.

1.8 Legal considerations

There are also legal complications with preventing P enrichment of Oklahoma surface waters. Several large legal cases in the Ozark ecoregion have been brought before state and federal courts in the last 30 years to address concerns with point and nonpoint source pollution negatively affecting Oklahoma. In that time, several federal pollution programs were put to the test. The 1992 *Arkansas v. Oklahoma* Supreme Court case sought to resolve issues regarding the use of the Clean Water Act (CWA) and National Pollution Discharge Elimination System (NPDES) permits to manage pollution from point sources. The 2003 case of *City of Tulsa v. Tyson Foods et al.* attempted to redefine poultry producers and farmers who apply poultry litter as waste producers to seek damage recovery under the Comprehensive Environmental Response, Compensation, and Liability Act (CERCLA). More recently, the 2009 case of *State of Oklahoma v. Tyson Foods, Inc. et al.* sought punishment for poultry producers under the Resource Conservation and Recovery Act (RCRA). However, no federal program tested in these cases had sufficient language to reduce nonpoint source pollution due to poultry litter

application. A more detailed account of these cases and others and their implications can be found in Appendix A.

The research outlined in this thesis seeks to complete several objectives. The main objectives of this research were to evaluate several methods of representing preferential and macropore flow and transport in a state-of-the-art 2D modeling program (HYDRUS-2D) and develop long-term simulations of water and phosphorus transport using the most effective methods. A second objective of this research was to compare these state-of-the-art model results to those produced by a less complex 1D model (HYDRUS-1D) to develop convenient alternatives to the more complex 2D model.

2. Methods[2]

2.1 Barren Fork Creek Field Site

Plot scale infiltration experiments were performed at the Barren Fork Creek floodplain site (Heeren et al., 2013) located in the Ozark region of northeastern Oklahoma, which is characterized by karst topography, including caves, springs, sink holes, and losing streams. The erosion of carbonate bedrock (primarily limestone) by slightly acidic water has left a large residuum of chert gravel in Ozark soils, with floodplains generally consisting of coarse chert gravel overlain by a mantle of gravelly loam or silt loam (Figure 3). Topsoil depth in the floodplains ranged from 1 to 300 cm in the Oklahoma Ozarks, and generally increased with increasing stream order. Common soil series include Elsah (frequently flooded, 0-3% slopes) in floodplains; Healing

[2] Material in this section was presented previously in Freiberger et al. (2014).

(occasionally flooded, 0-1% slopes) and Razort (occasionally flooded, 0-3% slopes) in floodplains and low stream terraces; Britwater (0-8 % slopes) on high stream terraces; and Clarksville (1-50%) on bluffs.

At the Barren Fork Creek site, located five miles east of Tahlequah, Oklahoma (latitude: 35.90°, longitude: -94.85°) and just downstream of the Eldon U.S. Geological Survey (USGS) gage station (07197000), soils were Razort gravelly loam. The silt loam layer was from 30 to 200 cm thick, and the chert gravel layer, ranging from 3 to 5 m, extended down to limestone bedrock. The gravel subsoil, classified as coarse gravel based on the Wentworth (1922) scale, consists of approximately 80% (by mass) of particle diameters greater than 2.0 mm, with an average particle size (d_{50}) of 13 mm (Fuchs et al., 2009). Estimates of saturated hydraulic conductivity for the gravel subsoil range between 140 and 230 m d^{-1} based on falling-head trench tests (Fuchs et al., 2009). The gravel layer itself is a complex alluvial deposit (Figure 3) that includes both clean gravel lenses associated with rapid flow and transport (Fox et al., 2011) as well as layers of fine gravel that can cause lateral flow in the silt loam and subsequent seepage erosion (Correll et al., 2013). The anisotropic horizontal layering results in a propensity for lateral flow.

The berm infiltration method (Heeren et al., 2014) was used to confine water and solutes at multiple infiltration plots (1m by 1 m to 10 m by 10 m) within the Barren Fork floodplain. A constant head of water and constant solute concentrations were maintained within the plots. Chloride (Cl^-) was used as a conservative (nonsorbing) tracer. Target tracer concentrations were 100 to 200 mg L^{-1} KCl (correlating to 48 to 95 mg L^{-1} Cl^-),

depending on background EC levels. The P (highly sorbing) concentrations of approximately 3 mg L^{-1} (corresponding to 10 mg L^{-1} as phosphate) were used to represent poultry litter application rates (typically used as a fertilizer source in the Ozark ecoregion) in the range of 2 to 8 Mg ha^{-1} (1 to 3 ton $acre^{-1}$). The P concentrations were achieved by adding phosphoric acid (H_3PO_4), which deprotonated to $H_2PO_4^-$ and HPO_4^{2-} in the slightly acidic solution. Observation wells were installed near the plots in order to collect water samples to document solute breakthrough curves. The infiltration data have been presented in Heeren et al. (2013) and the transport data in Heeren (2012). This research used HYDRUS to simulate the 1 m^2 infiltration plot at the Barren Fork Creek site.

Figure 3. Streambank at the Barren Fork Creek field site including the bank profile (top left), a megapore (top right), and a seepage undercut (bottom). Note the sloughed material in the bottom of each picture from recent bank failures. These complex alluvial deposits include both clean gravel lenses associated with rapid flow and transport (top left) as well as fine gravel lenses that can cause lateral flow and seepage erosion.

2.2 Development of HYDRUS Model

2.2.1 Soil profile heterogeneity

The model was developed in HYDRUS using parameters established from previous research at the Barren Fork site. A 2D slice of a soil profile was generated to match electrical resistivity imaging (ERI) data found by Miller et al. (2014) for the

Barren Fork 1x1α site. The profile was divided into four distinct soil layers: a 1.33-m topsoil layer identified by Heeren (2012) and three subsurface gravel layers identified using ERI data (Figure 4). Values for van Genuchten parameters and soil material properties for the soil layers were estimated using the Rosetta Lite (v. 1.1) module embedded in HYDRUS. Gravel soil parameters were estimated using the "sand" classification in Rosetta Lite. However, the saturated hydraulic conductivity (K_s) for soil materials was estimated through different means. The silt loam K_s value was estimated to be 9.6 cm hr^{-1} from infiltration tests done by Heeren et al. (2013). The K_s values for the gravel layers were determined using ERI data and the following relationship developed based on field data from the Barren Fork Creek site and one other floodplain site in the Ozark ecoregion (Miller et al. 2014; Miller, 2012):

$$K_s = 0.11 * \rho \quad (7)$$

where K_s is saturated hydraulic conductivity (m d^{-1}) and ρ is ERI resistivity (Ω-m). The K_s values for points within each gravel layer as determined with ERI data were then averaged to generate an average K_s for that layer. Average K_s values ranged between 130 cm hr^{-1} to 578 cm hr^{-1}.

2.2.2 Soil chemical laboratory data

In order to determine soil physical and chemical properties, soil core samples were collected with a Geoprobe Systems (Salina, KS) 6200 TMP (Trailer-mounted Probe) direct-push drilling machine using a dual-tube core sampler with a 4.45 cm opening. Before P injection experiments, background soil cores were collected during the installation of the observation wells from one to four wells per plot.

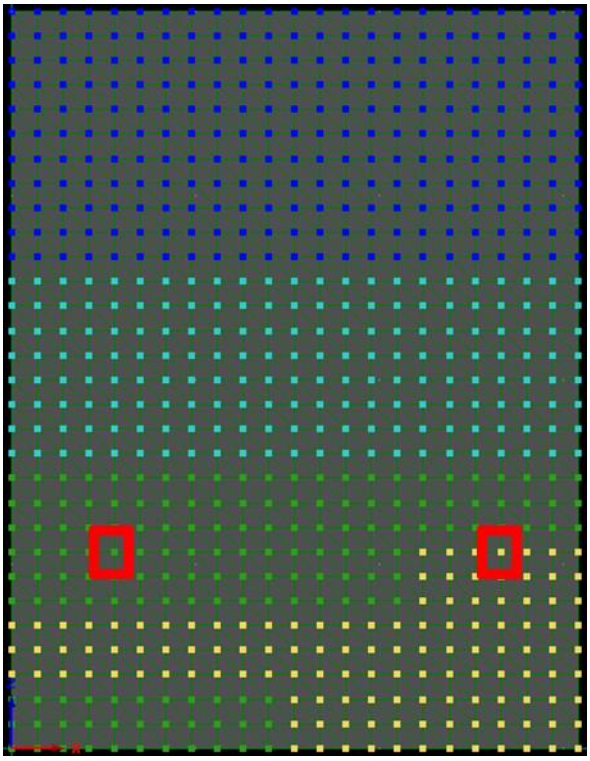

Figure 4. Material distribution represented in HYDRUS-2D. Silt loam topsoil (dark blue) overlays three distinct gravel layers of different *Ks* from lowest (light blue) to highest (yellow). Observation nodes matching placement of observation wells from Heeren et al. (2014) are marked by red boxes.

In the lab soil cores were sliced into approximately 15 cm samples representing different vertical horizons. All soils were air-dried and sieved with an 8 mm sieve prior to analysis. While a 2 mm sieve is commonly used, laboratory analysis showed that P sorption capacity was significant on the 2 to 4 mm and 4 to 8 mm particle size fractions as well as the less than 2 mm size fraction. The greater than 8 mm particle size fraction had only a small capacity for P sorption and was difficult to analyze with regular soil chemistry lab procedures. Therefore, all soil chemistry testing was performed on the less than 8 mm fraction of each sample. Soil pH and electrical conductivity (EC) were determined with a 1:1 soil to de-ionized water solution, stirred with a glass rod and

equilibrated for 30 minutes. All soil samples (approximately 670) were analyzed for water soluble (WS) P, Al, Fe, Ca, Mg, and Mn content (Figure 5). Water extractions were conducted by shaking air dried soil with de-ionized water (soil: solution ratio of 1:10) end over end for 1 h, followed by centrifuging (2500 rpm at 5 min) and filtration with 0.45 µm Millipore membrane. Extracted P, Al, Fe, Ca, Mg, and Mn were analyzed by inductively coupled plasma atomic emission spectroscopy (ICP-AES) (Table 1).

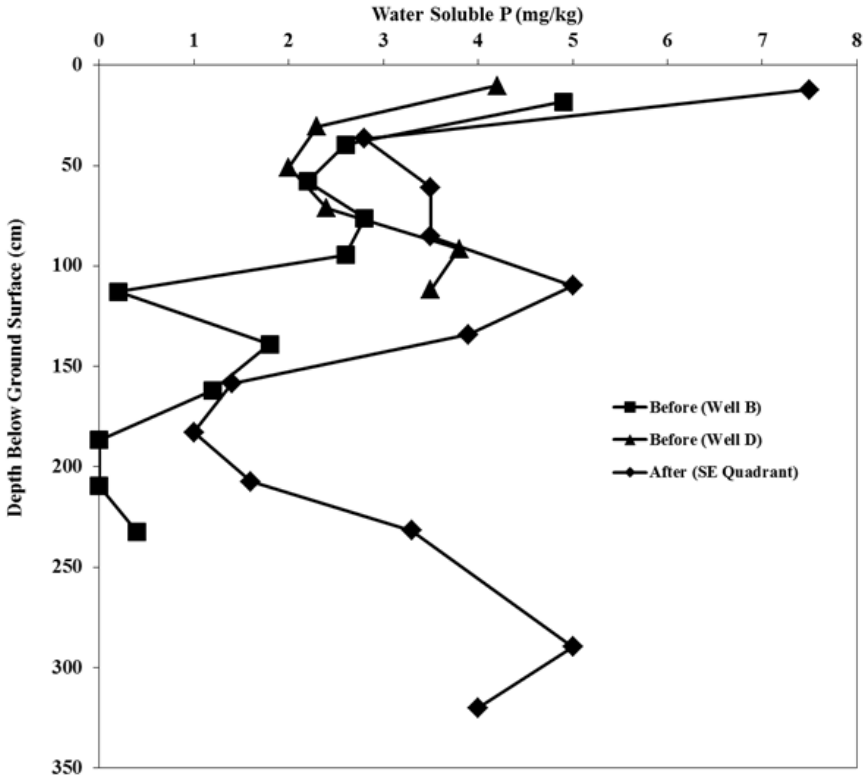

Figure 5. Subsurface soil water soluble P concentrations (mg P kg^{-1} soil) before and after plot experiments. Note the end of the P plume between 160 and 185 cm (Well B).

Oxalate extractable P, Al, Fe, and Mg (P_{ox}, Al_{ox}, Fe_{ox}, Mg_{ox}; 1:40 soil: 0.2M acid ammonium oxalate (pH 3), 2 h reaction time in the dark; McKeague and Day, 1966) were determined for all "topsoil" (approximately the top 10-15 cm of the soil core) samples.

The P, Ca, Mg, K, Al, and Fe from ammonium oxalate extractions were measured using ICP-AES. Amorphous Al and Fe are considered to be the most reactive soil fraction in regard to P sorption. The ratio of ammonium oxalate extractable P to (Al + Fe) (all values in mmol kg^{-1}) was expressed as:

$$DPS_{ox} = \left[\frac{P_{ox}}{Al_{ox}+Fe_{ox}}\right] 100\% \quad (8)$$

where DPS_{ox} is the ammonium oxalate degree of P saturation (Table 1). Note that this is exactly the same as the traditional soil degree of phosphorus saturation (DPS) calculations (Pautler and Sims, 2000) except without the empirical constant α which is used to relate soil P sorption capacity to Al_{ox} and Fe_{ox} and the denominator acts to express the effective total soil P sorption maximum. The α value was unknown, so no α value was used. Beauchemin and Simard (1999) noted that various studies have applied an α value of 0.5 to all soils, regardless of soil properties. The authors claimed that the α value is empirical and needs to be determined for each soil type and experimental conditions. In addition, Beck et al. (2004) recommended that the α value be omitted from the DPS calculation.

Phosphorus adsorption isotherms were performed on background vadose zone samples from both the silt loam and the gravel subsoil. The P adsorption isotherms were conducted by adding different levels of P (0.0, 0.5, 1.0, 10, and 20 mg P L^{-1}) to 2 gram soil samples, equilibrating for 24 hr (shaking), and measuring P in the equilibrated, centrifuged, and filtered samples by ICP-AES.

While P isotherms are nonlinear and often characterized by the Langmuir

equation, they typically exhibit linearity at low concentrations. Therefore, the low concentration data (less than 8 mg/L) were fit with a linear isotherm:

$$q=K_{d,<8mm}C_{eq}+y_{int,<8mm} \quad (9)$$

where q is the mass sorbed (mg P kg^{-1} soil), $K_{d,\ <8mm}$ is linear sorption coefficient for the fine fraction (L water mg^{-1} P), C_{eq} is the equilibrium solution P concentration (mg P L^{-1} water), and $y_{int,\ <8mm}$ is where the line intercepts the y-axis (L water kg^{-1} soil). Since the soil samples already had a significant amount of previously sorbed P, desorption occurred at low C_{eq} as indicated by negative values in a plot of q vs. C_{eq} (Figure 6). The y_{int} is an indication (though not equal to because of adsorption-desorption hysteresis) of the amount of P previously sorbed onto the soil sample at the time of sample collection. The equilibrium P concentration (EPC), where neither sorption nor desorption occurred, was calculated as the x-intercept of a logarithmic trendline fit to the entire data set (including high concentrations).

Table 1. Soil chemical properties for the topsoil (approximately the top 10-15 cm of the soil core) at each plot location for both before and after the water and solute infiltration experiments. Data include electrical conductivity (EC) and the Degree of P Saturation (DPS), which was calculated based on the molar concentrations of the ammonium oxalate extract.

Plot	P Injection	n	pH	EC	Water Soluble (mg kg^{-1})				Ammonium Oxalate (mg kg^{-1})				DPS
				($\mu S\ cm^{-1}$)	P	Al	Fe	Mg	P	Al	Fe	Mg	(%)
1x1α	Before	2	6.3	97	4.6	192	40	9	223	621	2,050	101	12.0
	After	1	6.3	325	7.5	71	39	18	300	604	2,296	160	15.3
3x3α	Before	2	6.5	139	5.2	321	66	12	246	704	2,535	102	11.1
	After	3	6.5	134	4.9	198	52	10	269	643	2,373	129	13.1

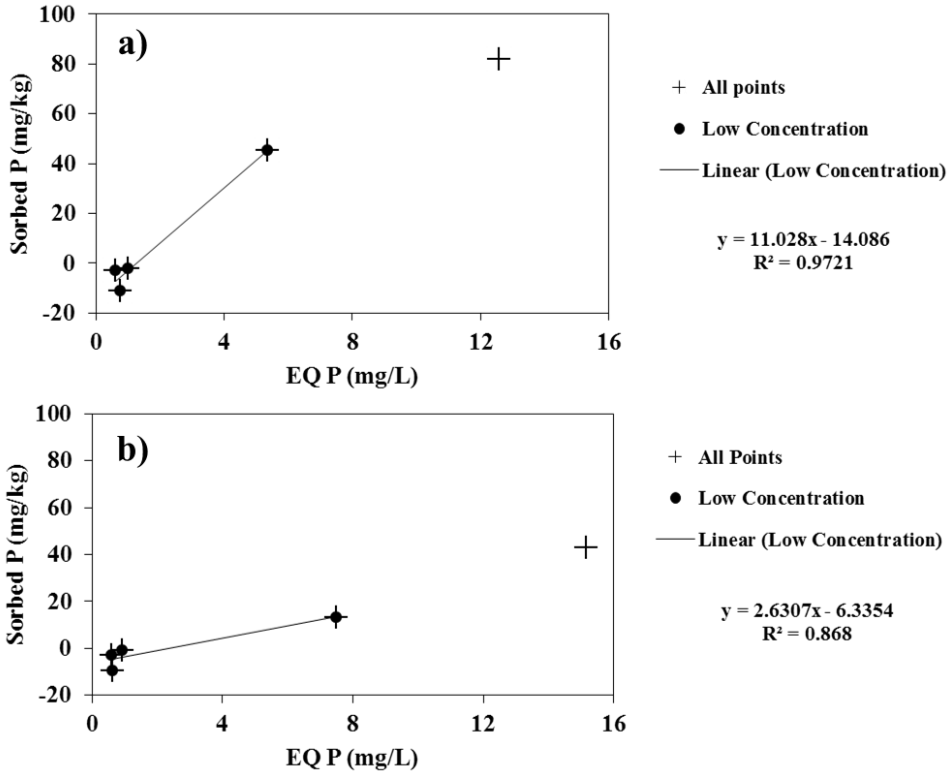

Figure 6. Phosphorus sorption isotherms for the Barren Fork Creek site for (a) silt loam, 64-83 cm below ground surface, and (b) sandy gravel, 142-163 cm below ground surface. See Table 2 for additional data for these samples.

Since the isotherms were performed on the less than 8 mm fraction, parameters were needed that characterized the whole soil sample (Table 2) since HYDRUS calculates P sorption in terms of the entire soil mass. Sorption on the greater than 8 mm size fraction was assumed to be negligible. Therefore, "weighted" linear isotherm parameters were determined by accounting for the fraction of total sample on which testing was performed:

$$K_{d,whole}=f_{<8mm}(K_{d,<8mm}) \quad (10)$$

where $K_{d,\,whole}$ is linear sorption coefficient for the whole soil sample (L water mg^{-1} P), and $f_{<8mm}$ is the fraction of the soil sample that passes an 8 mm sieve (kg kg^{-1}). The

Table 2. Soil physical and chemical properties for samples selected for phosphorus adsorption isotherms from the Barren Fork Creek site. Well B is part of the 1x1α plot, and Well K is part of the adjacent 3x3α plot (Heeren et al., 2013).

Borehole	Depth (cm)								
Soil Physical and P Sorption Characteristics									
						<8 mm fraction		weighted	
		Soil type		8 mm sieve (% passing)	EPC (mg L^{-1})	K_d (L kg^{-1})	y-int (mg kg^{-1})	K_d (L kg^{-1})	y-int (mg kg^{-1})
Well B	64-83	Silt loam, some gravel		94	0.94	11.0	-14.1	10.3	-13.2
Well K	142-163	Sandy gravel		57	1.08	2.6	-6.3	1.5	-3.6
Soil Chemical Properties									
						Water Soluble			
		pH	EC (µS cm^{-1})	P (mg kg^{-1})	Al (mg kg^{-1})	Fe (mg kg^{-1})	Ca (mg kg^{-1})	Mg (mg kg^{-1})	Mn (mg kg^{-1})
Well B	64-83	6.3	26	2.8	799	113.1	74	18	2.7
Well K	142-163	6.4	10	2.7	321	89.4	17	10	1.7

$y_{int,\ whole}$ was weighted in the same way. The EPC is the same for the fine fraction and the entire sample.

2.2.3 Soil chemical properties in HYDRUS

Note that units in these HYDRUS simulations were cm for length, g for soil mass (i.e. bulk density in g cm^{-3}), μg for P mass, and hours for time. Therefore, K_d was entered in units of cm^3/g (e.g. K_d = 10.3 L kg^{-1} = 10.3 cm^3 g^{-1} for the silt loam). The measured K_d for the gravel sample was applied to the whole gravel layer in HYDRUS. Initial conditions in HYDRUS included a soil solution P concentration equal to the EPC for the silt loam layer (0.94 mg L^{-1}) and the top of the gravel layer (1.08 mg L^{-1}). Initial solution P concentration in the gravel below the water table was equal to average of background P concentrations from well samples (0.055 mg L^{-1}). The disparity in these concentrations indicates the presence of a solute front in the soil matrix (from historical P leaching) that has not yet reached the water table, although P leaching through macropores may have reached the water table during rainfall events. Based on the relative location of this solute front which is apparent in the WSP data (Figure 5), a linear interpolation was used for the initial P concentration between 1.08 mg L^{-1} at 160 cm and 0.055 mg L^{-1} at 175 cm (Figure 9). Soil P was assumed to be in chemical equilibrium with the solution.

Calibration runtime parameters were modeled after field experiments done by Heeren (2012). Simulation data in HYDRUS was matched to data collected from selected observation wells at the Barren Fork 1x1α site (Figure 7). Observation nodes were placed at the water table on either side of the plot to represent the selected observation wells (Figure 4). Data from the wells were then used for calibration. Water and solute inflows

were also set to match conditions in the Heeren (2012) research. Chloride (Cl) was used as an indicator for water flow in the Heeren (2012) research due to its nature as a conservative tracer and was simulated in HYDRUS alongside P. For Cl and P calibration, constant concentrations of 50.1 mg L^{-1} and 1.68 mg L^{-1} were used in each respective study. For both studies, a constant head of 6 cm was applied over the plot area.

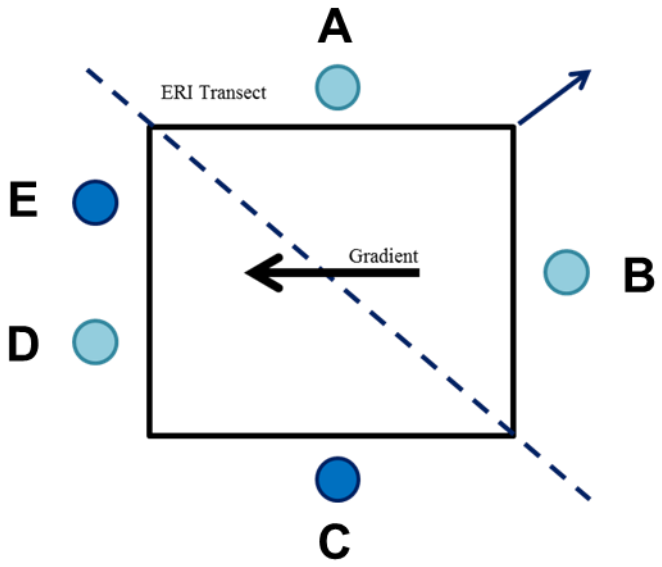

Figure 7. Plot overhead view. Path of ERI transect is indicated. Wells are labeled A-E. Observation wells selected for calibration indicated in dark blue.

2.3 Calibration of HYDRUS model

2.3.1 Single- and dual-porosity models

The θ_m and θ_{im} [L^3L^{-3}] terms represent the mobile and immobile phases of the soil pore space as defined in the modified Richards equation. Tension infiltrometer tests conducted by Heeren et al. (2013) showed that 99% of flow is directed through macropores at the Barren Fork site, and between 85% and 99% at similar sites in the Ozark ecoregion. Simulations conducted by Šimůnek et al. (2003) in HYDRUS

suggested the possibility of such flows occurring through a mere 2.5% of total pore space, which suggested that macropores can have a dominant effect on subsurface flows. Furthermore, Haws et al. (2005) modeled mobile zones in HYDRUS-2D as a small percentage of the total porosity. Reducing the flow domain to such a small space has dramatic effects on mean pore water velocity and would certainly cause water and solutes to arrive much sooner than through simple matrix flow, which is consistent with results found by Heeren (2012). Values of θ_m and θ_{im} were set to reflect the simulation conducted by Šimůnek et al. (2003) and flow effects were evaluated by increasing the mobile phase contribution within the confines of the porosity suggested by the Rosetta Lite function (Table 3).

Table 3. Soil properties and calibration parameters.

Soil Parameters						
		van Genuchten Parameters				
		Mobile			Immobile	
	K_s (cm hr^{-1})	α (cm^{-1})	n (-)	l (-)	α (cm^{-1})	n (-)
Silt Loam	9.6	0.1	2.00	0.5	0.020	1.41
Gravel	130-578	0.145	2.68	0.5	0.145	2.68
Calibration Parameters						
	$\theta_{m,\,s}$ (cm^3 cm^{-3})	*Disp. L.* (cm)	*Disp. T.* (cm)	ω (hr^{-1})	α (hr^{-1})	*Frac* (-)
Silt Loam	0.01-0.45	4-200	0.4-20	0.001-1	0.001-5	0-1
Gravel	0.01-0.43	4-200	0.4-20	0.001-10	0.001-5	0-1

Dispersivity [L] is used to correlate pore velocity to the mechanical dispersion of solutes in soil systems. Traditionally, longitudinal dispersivity has been approximated to be 10% of the sample length in the direction of flow, and transverse dispersivity being approximately 10% of the longitudinal dispersivity (Lallemand-Barres, 1978, as

presented in Fetter, 1999). The flow path length during the field experiments was approximately 400 cm, resulting in a first estimate of longitudinal dispersivity of 40 cm. However, this approximation is based on fitting a trend line to observed data, which can vary from the trendline by half an order of magnitude or more (Lallemand-Barres, 1978, as presented in Fetter, 1999). Transverse dispersivity was not calibrated independently and was considered to be 10% of the longitudinal dispersivity value.

The ω [T^{-1}] and α [T^{-1}] terms are the water and solute mass transfer coefficients, respectively, for the mass transfer function in the modified advection-dispersion equation. Values of α are traditionally believed to be between 0.1 and 5.0 hr^{-1} as presented by Radcliffe and Šimůnek (2010); however, results from Alletto et al. (2006) found α to range between 0.0006 and 0.0424 h^{-1}, and Cheviron and Coquet (2008) reported α values of 0.0192 to 0.6528 hr^{-1}. Given these results, breakthrough curves (BTCs) were analyzed with α ranging over several orders of magnitude (Table 3). The ω term is not as well understood as α within the confines of modeling. One study by González-Delgado and Shukla (2014) could not find any trend matching ω to increasing pore water velocity with Cl tracers, and reported ω values of 0.001 to 0.30 hr^{-1} in loam and 0.20 to 1.02 hr^{-1} in sand. Therefore, BTCs were analyzed with ω ranging over several orders of magnitude with a minimum of 0.001 for both silt loam and gravel (Table 3).

Frac [-] is the fraction of sites available for sorption that are governed by an equilibrium process. The *Frac* variable in HYDRUS-2D/3D has two functions, denoting either the fraction of sites available for instantaneous sorption during chemical non-equilibrium or the fraction of sites in contact with mobile water during physical non-

equilibrium. Given the mobile-immobile nature of this particular model, *Frac* was used to denote the latter. *Frac* was analyzed over the entire range of possible values to get a good understanding of its effect on P sorption (Table 3). Due to the conservative nature of the Cl tracer, this variable was not calibrated when simulating Cl transport.

In addition to calibrating the dual-porosity model with distinct gravel layers, three additional models were considered. Calibration on the Level 3 and 4 models were performed using the default single-porosity van Genuchten-Mualem model in HYDRUS-2D/3D, both with a homogeneous gravel layer (Level 3) and heterogeneous gravel layers (Level 4), as well as a Level 5 model, consisting of a dual-porosity model with a homogenous gravel layer. This was done to evaluate the effects of incorporating macropore flow (dual-porosity) and increasing model resolution (homogeneous gravel vs. heterogeneous gravel layers) on breakthrough time and overall shape of Cl and P BTCs. Soil properties for the homogeneous gravel layer were determined as area-weighted averages of the three distinct gravel layers found using ERI data. Table 4 provides a summary of each model and distinctions between each level.

Table 4. Summary of model levels. Additional information about each model can be found in Appendix B.

				Soil Parameters		
	Model	Simulation	Precipitation	K_s (SiL)	K_s (Gravel)	α, ω
HYDRUS-1D models						
Level 1	SP[a]	LT[c]	Daily[e]	PTF[g]	PSD[i]	N/A
Level 2a	DP[b]	LT	5-min[f]	Plot[h]	ERI[j]	Literature
Level 2b	DP	LT	5-min	Plot	ERI	Cal
Level 2c	DP	LT	5-min	Plot	ERI	Cal*
HYDRUS-2D models						
Level 3	SP	Cal[d]	N/A	Plot	ERI	N/A
Level 4	SP	Cal, LT	Daily	Plot	ERI	N/A
Level 5	DP	Cal	N/A	Plot	ERI	Cal
Level 6	DP	Cal, LT	Daily	Plot	ERI	Cal
Level 7	DP	LT	5-min	Plot	ERI	Cal
Mesh Macropore	SP	Cal	N/A	Plot	ERI	N/A

[a], single-porosity; [b], dual-porosity; [c], long-term simulations; [d], calibration; [e], daily rainfall totals converted to 24-hour intensities; [f], 5-minute rainfall totals converted to 1-minute intensities; [g], the Rosetta Lite pedotransfer function; [h], plot infiltration experiments conducted by Heeren (2012); [i], particle size distribution conducted by Fuchs et al. (2009); [j], electrical resistivity imaging conducted by Miller et al. (2014).

* Calibrated parameters for Levels 2c and higher also include dispersivity

2.3.2 Mesh macropore model

Calibration was also performed on a soil profile containing a mesh macropore to determine the effectiveness of such a model. Research by Akay et al. (2008) and Lamy et al. (2009) has shown that HYDRUS can model macropore flow through large void spaces in the profile instead of using the built-in multi-domain models. These void spaces can be modeled in several ways, including as a soil material with high transport or as a set of boundary conditions that force flow into the macropore region. For this calibration, the mesh macropore region was defined as a 3 cm wide band extending vertically throughout the silt loam mantle (Figure 8). The macropore was simulated in HYDRUS as a porous media material with an extremely high K_s in order to replicate the rapid transport possible in macropores. Mesh elements were adjusted to 1 cm-wide elements within the macropore to allow for the proper width. Given that the macropore was expressed in the geometry of the soil profile, the single-porosity van Genuchten-Mualem model was selected for flow and transport. Finally, the nature of the mesh macropore requires significant lateral transport on the surface of the soil to the macropore. To accomplish this in HYDRUS a 5 cm-thick thatch layer was added to the top of the profile, simulated as gravel with extremely high conductivity and no sorption capacity.

Four parameters were calibrated in the mesh macropore model: Disp. L, Disp. T, the soil mantle K_s, and the horizontal position of the mesh macropore. The K_s values of the macropore and silt loam layer were calibrated together to maintain the average mantle K_s value of 9.6 cm hr^{-1} found in plot infiltration experiments conducted by Heeren (2013). The horizontal position of the macropore was calibrated to compensate for the

asymmetry of Cl and P data in the observation wells.

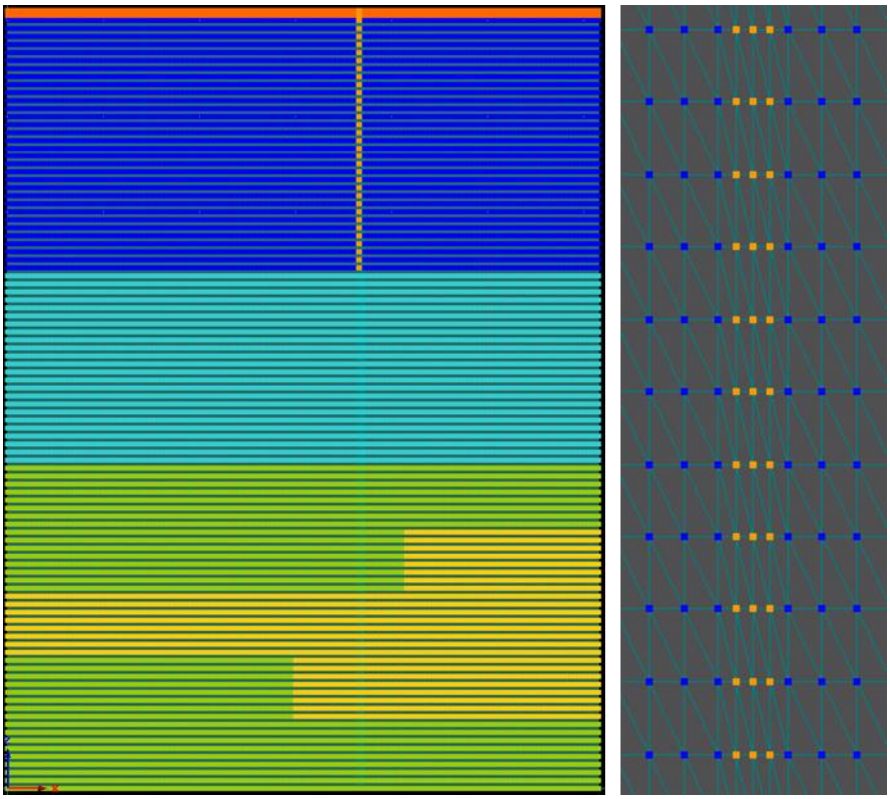

Figure 8. HYDRUS soil profile (left) with a 3-cm wide mesh macropore (light orange) and thatch layer (dark orange). The mesh macropore is defined by smaller, 1-cm elements (right).

2.4 Long-term P Modeling:

Long-term P transport was simulated in HYDRUS-1D and -2D following the calibration process. Long-term trials simulated water and P application to a soil profile for a nine year period between March 2004 and March 2013. Evapotranspiration (ET) was identified as being an important component to long-term modeling. However, HYDRUS was unable to successfully incorporate ET modeling into the full long-term trials. A separate trial was successfully conducted incorporating ET into a two-year simulation to explore how ET might impact long-term simulation results. This

experiment is explained in more detail in Appendix C.

Phosphorus from poultry litter application was simulated as P applied with infiltrating rainwater. P was applied with infiltrating rainwater starting March 1st of each year to match traditional fertilizer application times. Each year, 619 μg of P per cm of profile width were added to the column. This yearly application of P is consistent with a 2 ton-per-acre application rate of poultry litter on grass and a P content of 12.7 kg P per ton of litter as recommended by the Oklahoma Cooperative Extension Service (2013) and near the range of 13-27 kg P per ton of litter reported by MidWest Plan Service (2001). Initial concentrations of P in the simulated infiltration started at 15 mg L^{-1}, which is consistent with P concentrations in the first post-litter application runoff event found by DeLaune et al. (2004). A linear relationship was developed between concentration and cumulative rainfall to simulate a decreasing water concentration from the poultry litter throughout the year at the soil surface:

$$C=I-0.182R \tag{11}$$

where *C* is the concentration (μg cm^{-3}) at the given time step, I is 15 mg L^{-1}, the initial leachate concentration at March 1st of each year (μg cm^{-3}), and *R* is the cumulative rainfall (cm) since March 1st of each year. Once the cumulative applied P reaches 619 μg, no more additional P was added to rainwater for that year. In the event that rainfall was insufficient to remove all P from the surface for a given year, the excess P was added to the next year and a new linear relationship was developed to reflect the additional P. Although likely to be nonlinear, this relationship was modeled as linear for simplification purposes. There may also be conditions where a small amount of rainfall may result in

now P desorption from the poultry litter, but that was not considered here.

2.4.1 HYDRUS-1D long-term modeling

Four long-term simulations were performed in HYDRUS-1D, designated as either Level 1 or Level 2 models. The Level 1 one model was designed to use the level of data that would be available from a quick site visit, including visual observation of silt loam and gravel layering on the streambank, a bucket sample of gravel (from the streambank) to determine the particle size distribution, and soil coring in the floodplain to determine depth of the silt loam, soil texture, water soluble P, and P sorption isotherms. If successful, this model would require significantly less effort compared to the plot infiltration experiments. The Level 1 model evaluated P transport using daily rainfall data, in which daily rainfall totals were converted to constant rainfall intensities (cm hr^{-1}) over the entire 24 hour period.

Level 2 models differed from the Level 1 model in several ways. First, Level 2 models were designed to use data collected from an in-depth study of the research site, similar to research by Heeren (2012). This in-depth study would include plot infiltration experiments to get topsoil transport parameters, collecting ERI transect data to evaluate heterogeneity of the subsurface layers, and a detailed soil chemical analysis. The Level 2 models also acknowledge the presence of high preferential flow and adopt the dual-porosity model to simulate macropore flow. Finally, Level 2 models evaluated P transport using high-resolution rainfall data, defined as rainfall totals collected on a five minute basis. These five minute totals were interpolated to 1-minute intensities (cm hr^{-1}) to prevent calculation errors in HYDRUS. Given the large volume of rainfall data points,

simulations were limited to one year at a time, with initial and boundary conditions imported from the previous year to effectively simulate nine continuous years of rainfall. All rainfall data was obtained through the Oklahoma Mesonet.

For Level 1, the soil profile featured a 1.33 m silt loam mantle and a single 1.66 m gravel layer. Soil characteristics for the silt loam were defined solely by the Rosetta Lite pedotransfer function for silt loam in HYDRUS-1D. Most of the soil characteristics for the gravel layer were defined as sand by Rosetta Lite, although the K_s value was determined using data collected by Fuchs et al. (2009) for the Barren Fork site. The Level 1 model evaluated transport through this soil profile using the standard van Genuchten-Maulem single-porosity model. Three Level 2 models were also evaluated. For Level 2 models, a new soil profile was developed. The gravel layer was broken into three distinct layers to create a 1D version of the profile used during the calibration step. K_s values for all three gravel layers and the silt loam were also set to match those used during the calibration step. The Level 2a model evaluated transport through this profile while maintaining the accepted literature values for transfer rate constants and other parameters. The Level 2b model evaluated transport with calibrated values for these rate constants, and the Level 2c model evaluated transport with calibrated values for the rate constants and profile dispersivity.

2.4.2 HYDRUS-2D long-term modeling

For HYDRUS-2D modeling, a 100-cm wide, 300-cm deep 2D column was developed, corresponding to the vadose zone of the soil profile directly under the 100-cm wide plot used in calibration. Long-term P transport to the water table, situated at the

bottom of the profile, was of interest. Boundary conditions were set so that the sides of the column were no-flow boundaries, the bottom of the column was a constant head boundary set to maintain a constant long-term water table elevation, and the top of the column was set as a variable flux boundary to simulate rainfall events. Initial conditions set the soil water in the column at hydrostatic equilibrium with the water table, and initial concentrations remained the same as those used for P calibration (Figure 9). Long-term simulations in HYDRUS-2D were performed on the Level 4, Level 6, and Level 7 models to get results for single-porosity models featuring daily rainfall data and dual-porosity models featuring both daily and modified 5-minute rainfall data.

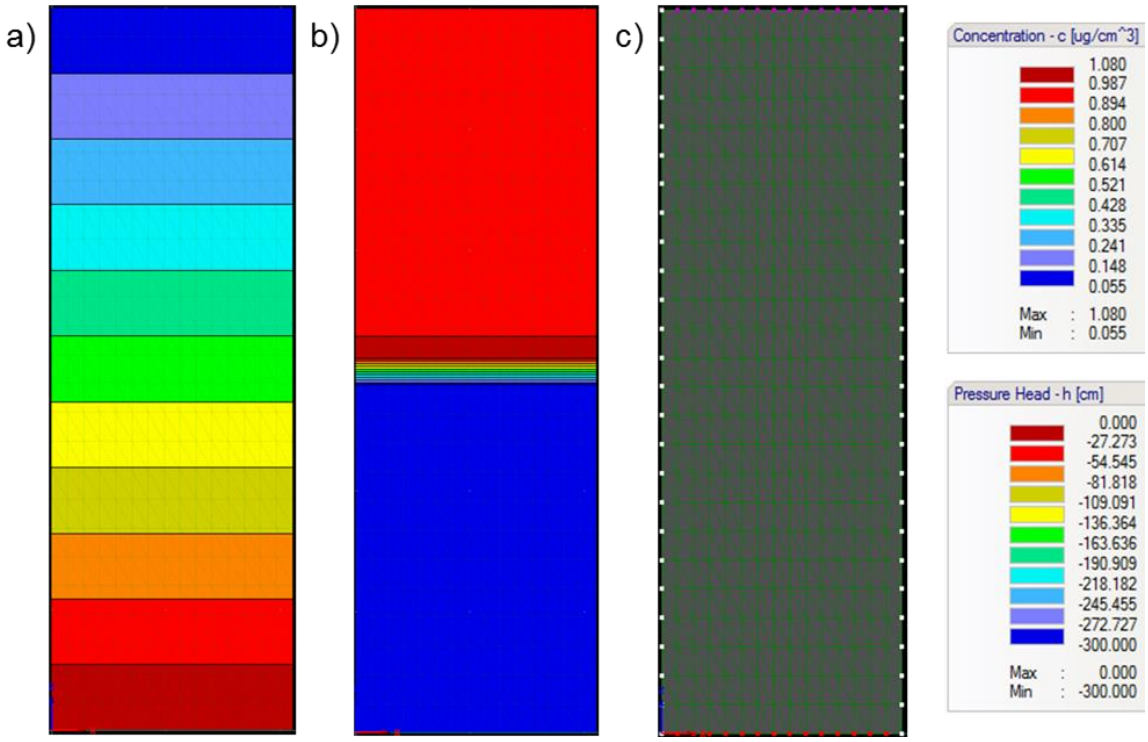

Figure 9. Initial and boundary conditions of the vertical soil profile for long-term P modeling in HYDRUS 2D. Initial conditions for (a) pressure head and (b) mobile P concentration are shown, as well as (c) boundary conditions for variable flux (magenta) and constant head (red).

3. Results

3.1 Calibration Results

Calibration was performed for Levels 3-6 for both Cl and P transport Goodness-of-fit for this calibration step was determined by analyzing two criteria. First, initial breakthrough time of HYDRUS simulation curves needed to be similar to those seen in observation wells. For Cl, breakthrough times were analyzed for t_{15}, or the time needed for the Cl concentration to exceed 15 mg L^{-1}. For P, breakthrough times were instead analyzed for $t_{0.12}$, or the time needed for the P concentration to exceed 0.12 mg L^{-1}.

Target concentrations match critical points seen in the observation wells. The second criterion analyzed was simulation curve differentiation. Due to heterogeneity in the profile, observation wells did not see the same results. HYDRUS simulation curves were analyzed for how well they exhibited these differences in transport. The best-fit model needed to show acceptable matches to these criteria for both solutes.

Level 6 achieved the best calibration was used to set the baseline parameter values for sensitivity analysis and long-term testing (Figure 10). Best-fit parameter values can be found in Table 5. Simulations adequately matched observed data from the Barren Fork 1x1α site. The effects of minimizing and maximizing ω and α on the shape and timing of the breakthrough curve were also illustrated (Figure 11). One limitation of the model was the inability to match observed data with reasonable *Frac* values. Predicted values of *Frac* were about 0.03, which is consistent with the percent macropore composition of the soil profile. However, simulated values of *Frac* had to be set close to 1 to achieve reasonable breakthrough times for P and remain consistent with Cl calibration results.

Calibration results were limited in matching the model to observed data. Breakthrough times were difficult to match for the Cl and P simultaneously. While breakthrough times for Cl were relatively short, breakthrough times for P were relatively long. Balancing parameters that managed water flow, such as ω, was a difficult task as changing these parameters to better match one solute caused a poor match with the other. Solute transport parameters, such as soil isotherm properties, were not enough to balance the Cl and P perfectly. In some cases, better results were seen with lower values of α and

ω; however, these values were at or below the lower limit of what would be physically realistic for α and ω, and it was determined that curves generated with these values may reflect physical conditions too poorly to be useful.

In addition to this, HYDRUS was unable to fully simulate the differentiation between observation wells C and E. Observation data showed that both wells received some level of Cl, but only well C recorded any significant P increase. While the P increase simulated by HYDRUS in well E was reduced by comparison to well C, the increase simulated was still far above the trend defined by observed data (Figure 10).

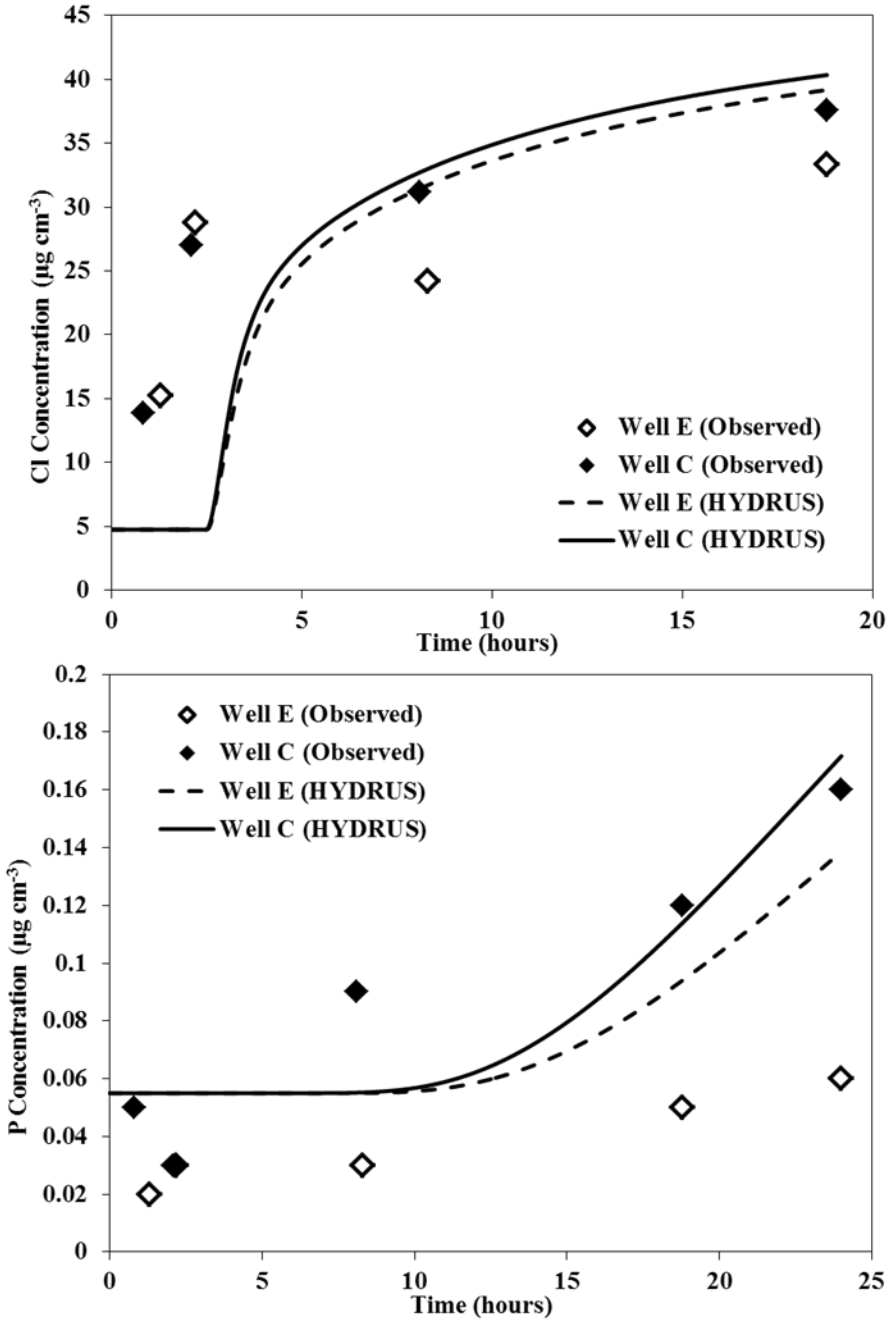

Figure 10. Calibration results for Cl (top) and P (bottom) for the Level 6 model. Curves are HYDRUS-generated BTCs, points are observed data from Heeren et al. (2012).

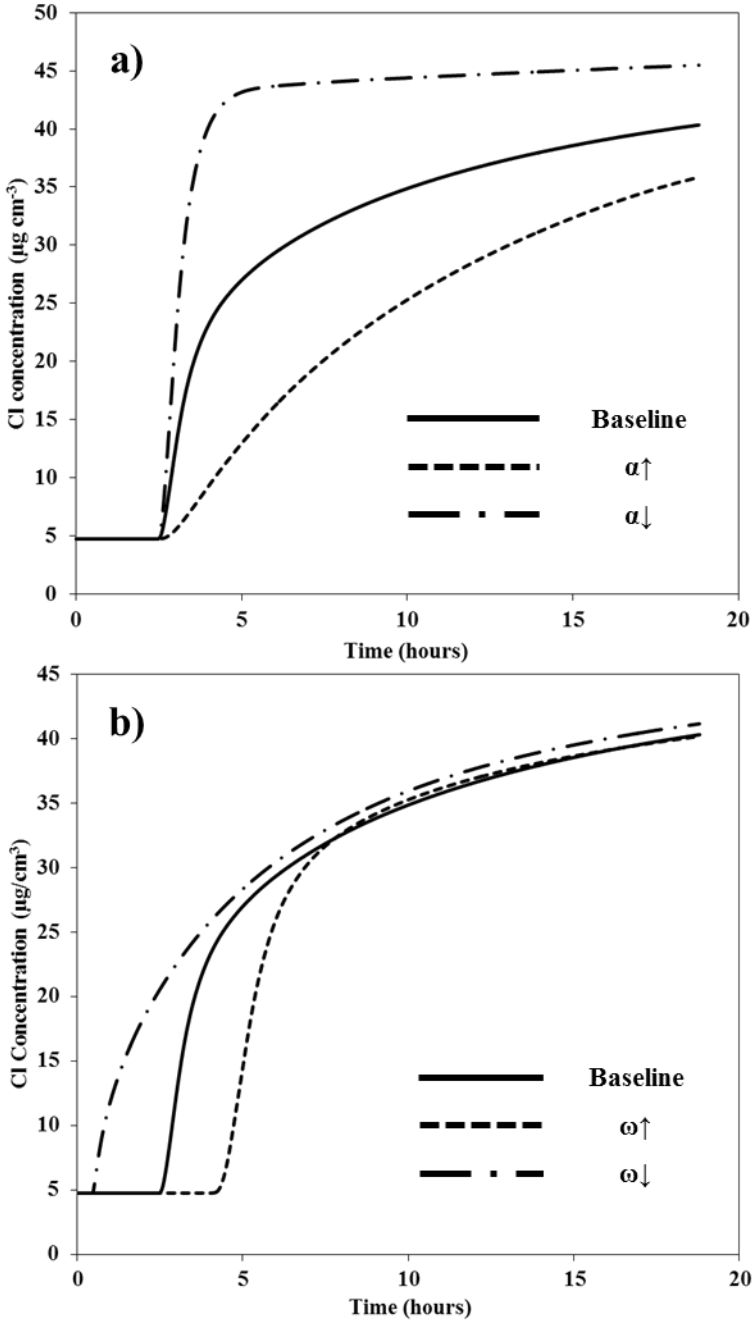

Figure 11. Analysis of Cl changes with (a) *α* and (b) *ω*, and P changes with (c) *α* and (d) *ω*. Note that decreasing *ω* increased breakthrough time for both Cl and P, and increasing *ω* had the opposite effect. Effects of *α* were more complex; decreasing *α* made Cl breakthrough sharper, but had little effect on breakthrough time, but increasing *α* affected both time and shape of Cl breakthrough. No significant effect was seen in P breakthrough. Analysis was performed on Well C data.

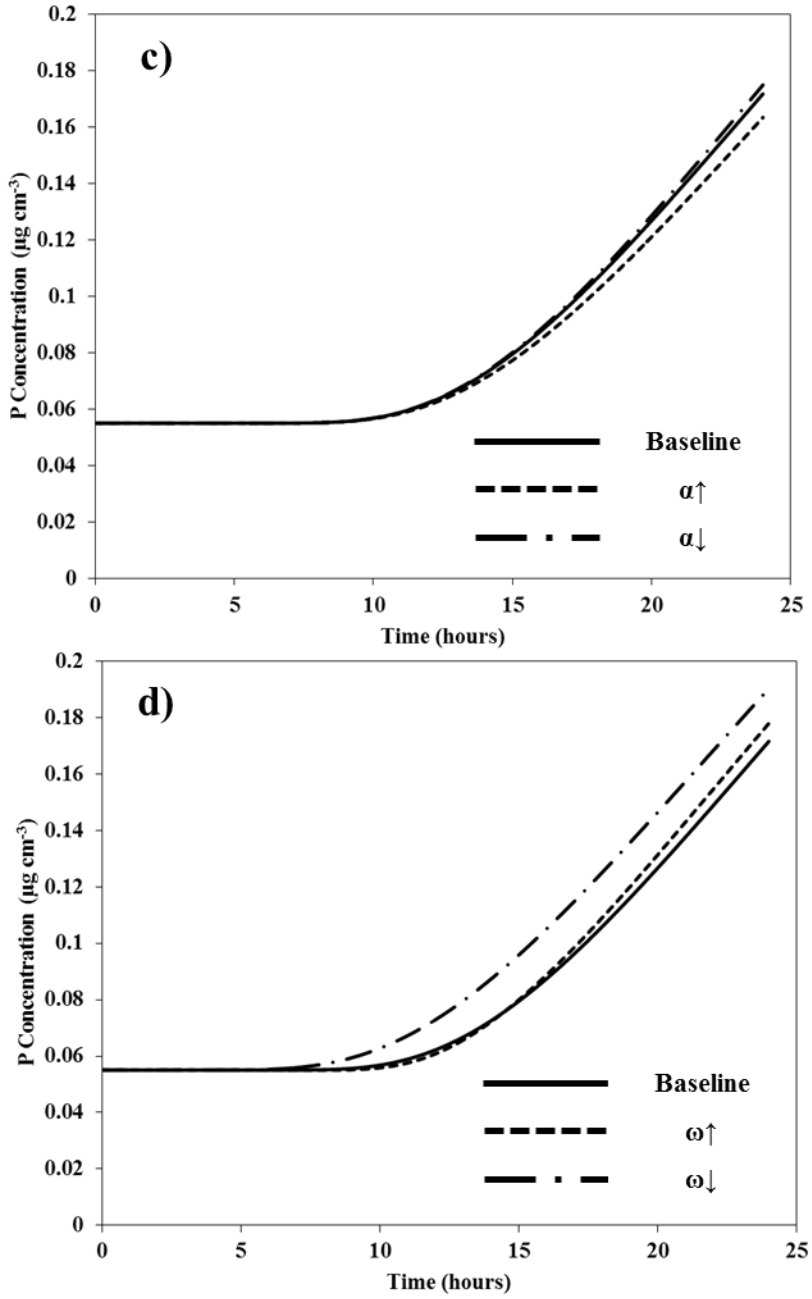

Figure 11 (Continued)

Mass balance information for the calibration was also collected. Peclet and Courant numbers were analyzed for potential model instability. Peclet numbers for the Cl

and P were between 0.22 and 0.23, which is lower than the maximum Peclet number of 5 recommended by Radcliffe and Šimůnek (2010). Courant numbers for the Cl and P were below 0.003, which is less than the maximum Courant number of 1 recommended by Radcliffe and Šimůnek (2010). Water mass balance error for the Cl and P calibrations were near 24%, and adjustments to mesh size, time steps, or iteration criteria were unable to reduce this imbalance. Water mass balance remains a potential limitation of this particular model. Solute mass balance errors were far more favorable, with a Cl mass balance error of 1.4% and a P mass balance error of 0.02%.

Table 5. Best-fit parameter values from calibration results for the Level 6 model.

Calibration Parameter Results						
	$\theta_{m,\,s}$ ($cm^3\ cm^{-3}$)	Disp. L. (cm)	Disp. T. (cm)	ω (hr^{-1})	α (hr^{-1})	Frac (-)
Silt Loam	0.01	100	10	0.01	0.2	1
Gravel	0.01	200	20	0.1	0.01	1

Calibration results for three additional models were also analyzed within HYDRUS (Figure 12) and compared to the Level 6 model. The single porosity (van Genuchten-Mualem) model with a homogeneous gravel layer (Level 3) produced BTCs with longer breakthrough times, reduced peak concentrations, and poor differentiation between the two observation wells (Figures 12a and 12b). The single porosity model with heterogeneous gravel layers (Level 4) performed slightly better; while still having poor breakthrough times and peak concentrations, this model showed better differentiation between the two observation wells (Figures 12c and 12d). Calibration parameters for these two models were limited to the longitudinal and transverse dispersivity for the silt loam; all other variables either belong to the dual-porosity model or were already set to

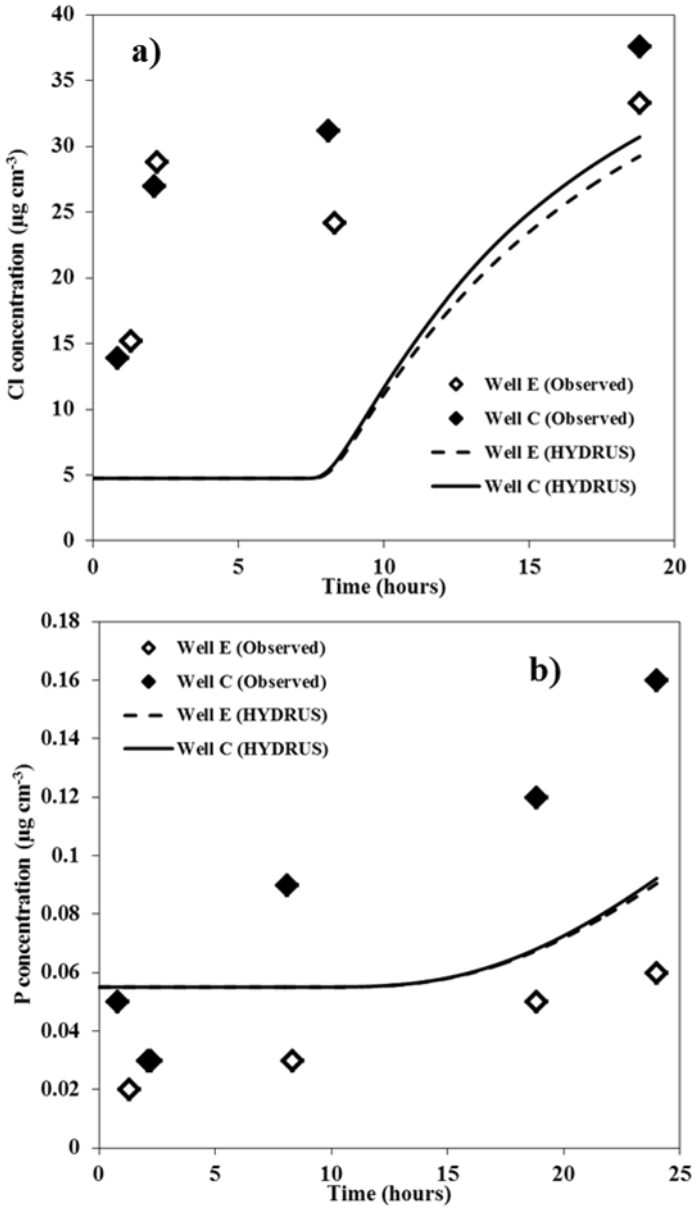

Figure 12. Calibration of Cl (a, c, e) and P (b, d, f) for three additional models in HYDRUS-2D/3D. Simulations included the Level 3 model: a single porosity (van Genuchten-Mualem) model with a single average gravel layer (a, b); the Level 4 model: a single porosity (van Genuchten-Mualem) model with three distinct gravel layers defined by ERI data (c, d); and the Level 5 model: a dual-porosity model with a single averaged gravel layer (e, f). The dual porosity with three distinct gravel layers defined by ERI data is shown in Figure 8 and was selected for the long term simulations.

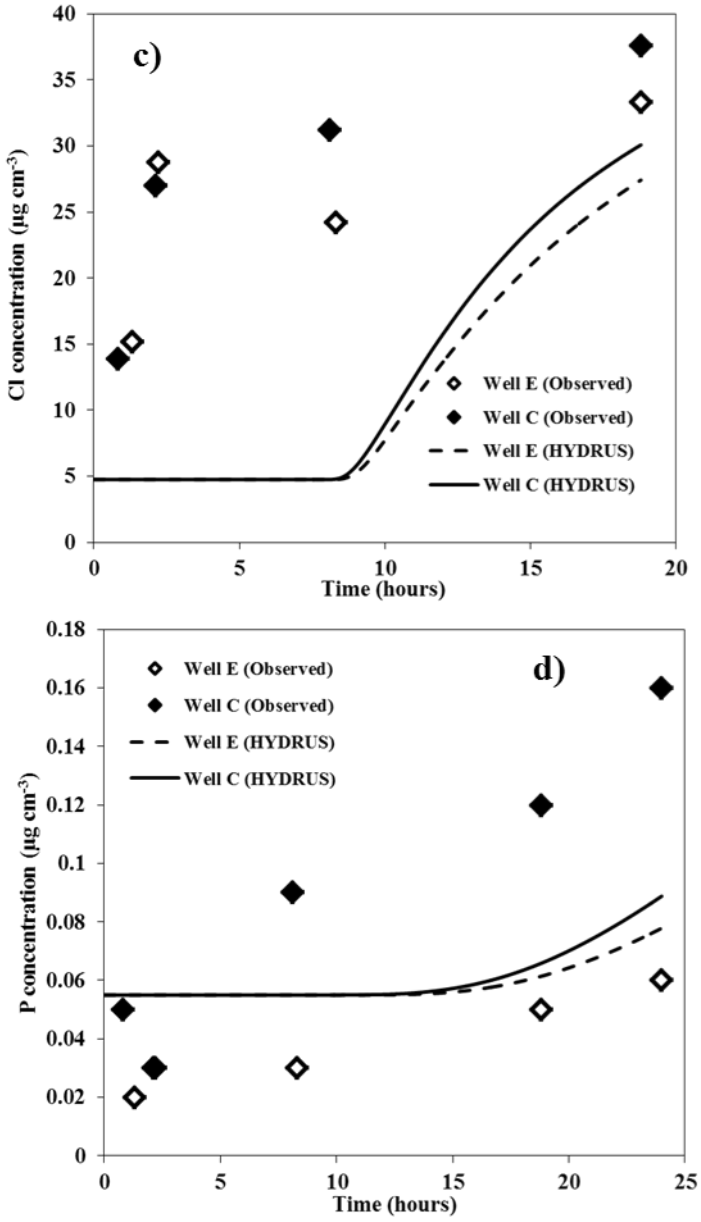

Figure 12 (Continued)

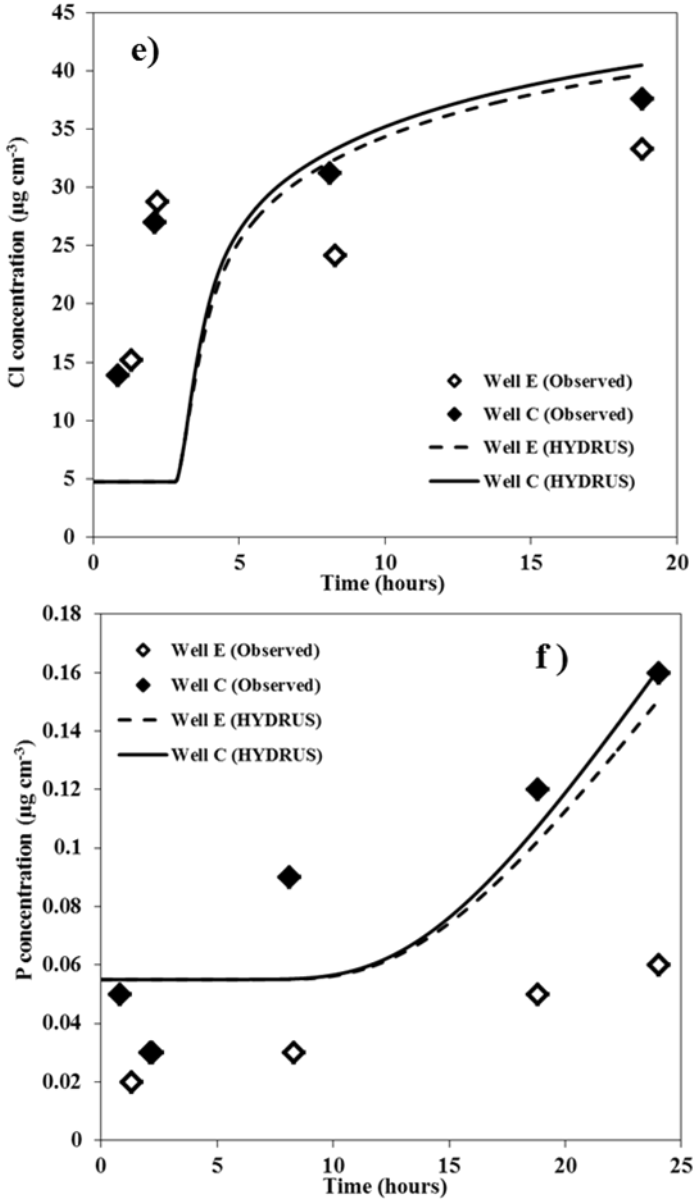

Figure 12 (Continued)

their maximum value prior to calibration. Silt loam Disp. L. and Disp. T. were set to maximum value established in Table 3 to produce these results.

The last model evaluated was the Level 5 dual-porosity model with a homogeneous gravel layer (Figures 12e and 12f). Most of the parameters remained consistent with the Level 6 model used for the long-term simulations; however the mobile sorption site fraction was re-calibrated for this model. Breakthrough times and peak concentrations for Cl were similar to the "standard" dual-porosity model, although breakthrough time lagged behind by about 30 minutes and differentiation between the wells was poorer. The P calibration was much closer to the Level 6 model, with the added benefit of having a lower Frac value of near 0.75. Despite this, there is still poor differentiation between observation wells and the Frac value is still not low enough to consider using this model over the Level 6 model.

Calibration was also performed on the mesh macropore model for both Cl and P transport. Results of the modeling are shown below (Figure 13a-d). Goodness-of-fit was established in a similar manner to the previous calibration step, but also focused on reducing over-estimation of peak Cl and P values and well differentiation. The mesh macropore was able to produce excellent matches to observational P transport data. However, calibrated parameters for P transport produced poor matches to observational Cl transport data, and no acceptable calibrated parameters were found that could reconcile both solutes to their observational data simultaneously. While previous research has been successful in modeling mesh macropore flow (Akay et al., 2007, Lamy et al., 2009), there is most likely not enough information available about the geometry and placement to accurately model a mesh macropore for both solutes in this profile.

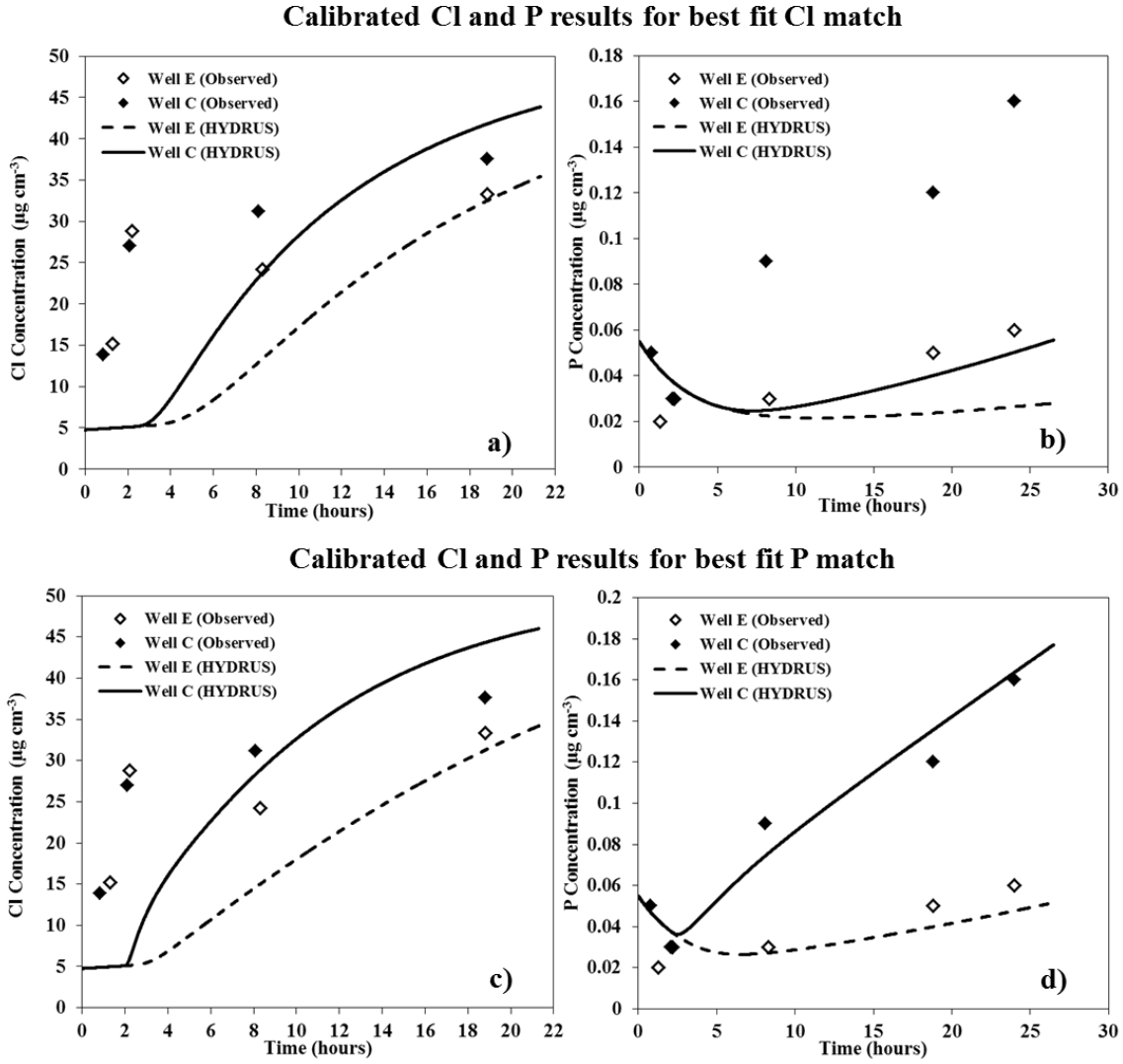

Figure 13. Calibration results of the mesh macropore profile. Calibration was performed to match Cl data (a, b) and to match P data (c, d).

3.2 Sensitivity Analysis

A sensitivity analysis was performed standard model to determine the impact of each parameter on breakthrough time for both Cl and P transport. Each solute simulation was analyzed with respect to the time taken for water at the well C observation node to reach a concentration of 15 mg L^{-1} for Cl (t_{15}) or 0.12 mg L^{-1} for P ($t_{0.12}$). Parameters were then increased or decreased and the percent change in t_{15} or $t_{0.12}$ was recorded.

Results were plotted as percent change in the parameter from the baseline value against percent change in time to the target concentration (Figures 14 and 15).

For Cl modeling, longitudinal dispersivity and immobile pore fraction had an inverse relationship to t_{15}, while α and ω had a positive relationship to t_{15}, although both α and ω seemed to display asymptotic behaviors at large percent increases in the variable. The most sensitive parameters for the Cl analysis were $\theta_{s,\,im}$ for both the silt loam and the gravel, with a maximum increase in t_{15} of 77% and 167%, respectively. The least sensitive parameter was α for the silt loam, which despite seeing a 400% increase in value only produced a 4% increase in t_{15} (Figure 14).

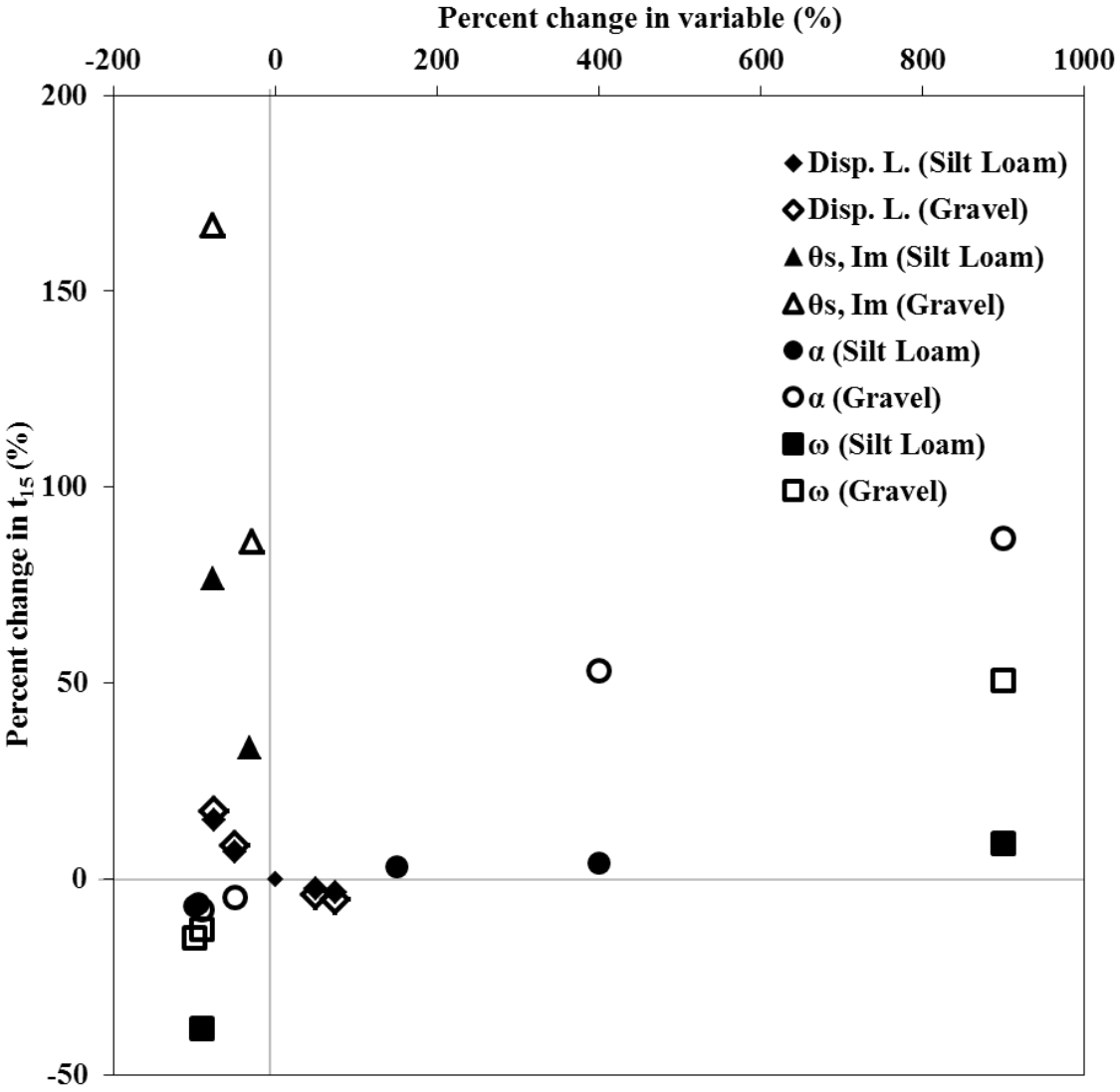

Figure 14. Sensitivity analysis of the Level 6 model for Cl calibration.

For P modeling, gravel mobile sorption site fraction and gravel adsorption isotherm coefficient had a positive relationship to $t_{0.12}$. Neither mobile site sorption fraction or adsorption isotherm coefficient for the silt loam layer had any significant effect on $t_{0.12}$. Although soil chemical analysis showed that the soils were not close to P saturation (DPS < 16%, Table 1), initial solution P concentration in the silt loam (0.94

mg L^{-1}) was high relative to the plot inflow P concentration (1.68 mg L^{-1}). This initial condition would significantly reduce the impact of silt loam-dependent parameters, as sorption sites are already mostly filled with P for the inflow concentration. The gravel mobile sorption site fraction was the most sensitive parameter, with a maximum of 70% decrease in $t_{0.12}$. The least sensitive parameters were gravel adsorption isotherm coefficients, with changes between -20% and 20% in $t_{0.12}$ over a wide percent change in the variable (Figure 15).

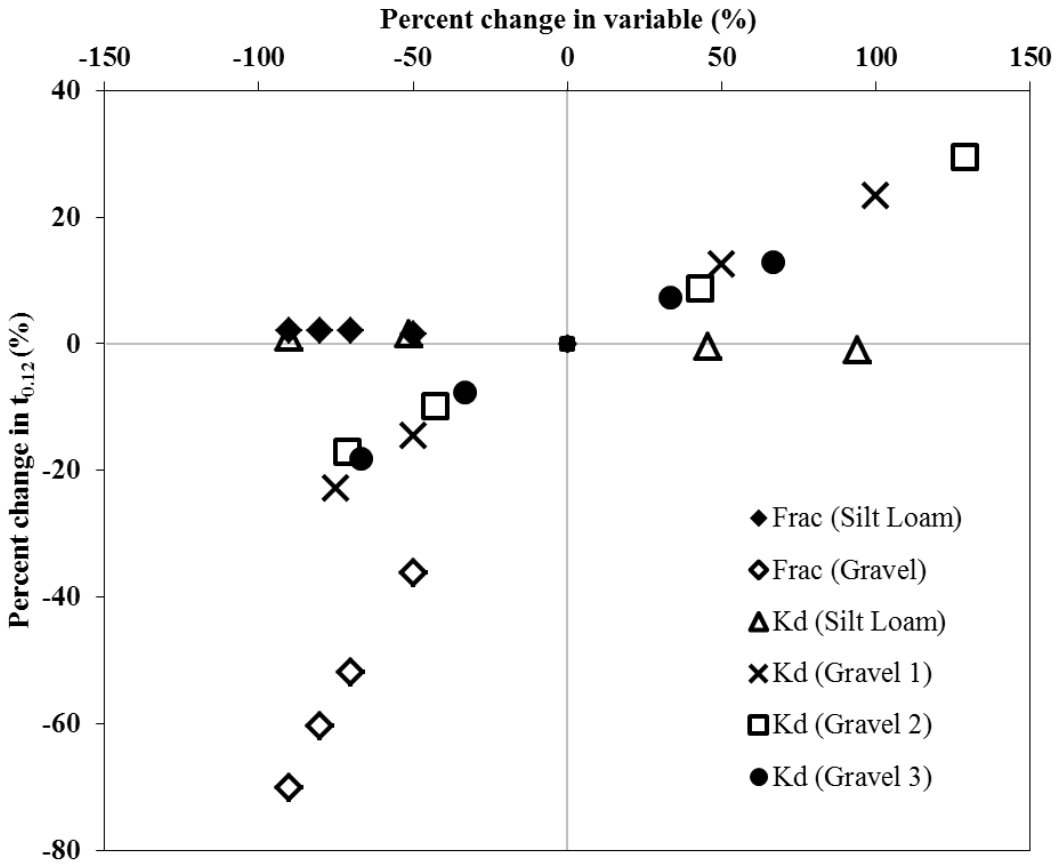

Figure 15. Sensitivity analysis of the level 6 model for P calibration.

Table 6. Summary of long-term results for HYDRUS-1D and 2D. Cumulative P delivery and final P concentrations shown are those taken at the water table at the end of each simulation.

				Error[b]	
	Cumulative P delivered[a]	WT P Concentration[a]	P delivery ratio	P delivery ratio	P Concentration
	(kg ha^{-1})	(mg L^{-1})	(%)	(%)	(%)
HYDRUS-1D					
Level 1	0.2	0.05	0.04	-99.8%	-96.8%
Level 2a	52.1	0.89	10.2	-40.0%	-48.8%
Level 2b	54.4	0.98	10.1	-40.6%	-43.6%
Level 2c	88.5	1.67	16.5	-2.9%	-4.0%
HYDRUS-2D					
Level 4	87.1	1.64	16.0	-5.9%	-5.7%
Level 6	91.7	1.74	16.8	-	-
Level 7	89.7	1.70	16.4	-3.5%	-2.3%

[a] at the end of the 9 year simulations, which did not include ET
[b] percent error based on difference from the Level 6 model

3.3 Long-term P modeling with HYDRUS-1D

Table 6 provides a summary of results for each long-term model evaluated. The percent error for each model compared to the Level 6 model has also been calculated. Additional information about each trial is provided in the sections below. It is important to note that these trials do not take evapotranspiration or root water uptake into account. An analysis of potential ET effects on model results is explored in Appendix C.

Long-term modeling was conducted in HYDRUS-1D to determine the P loading to the water table between March of 2004 and March of 2013. Long-term simulations of the Level 1 model as well as the Level 2a, 2b, and 2c models were performed.

The Level 1 model found that a negligible amount of P (0.2 kg ha^{-1} P) of the 556 kg ha^{-1} P applied as rainfed fertilizer crossed the water table after nine years of simulation (Figure 16). Concentration at the water table did not change in any significant way during the simulation.

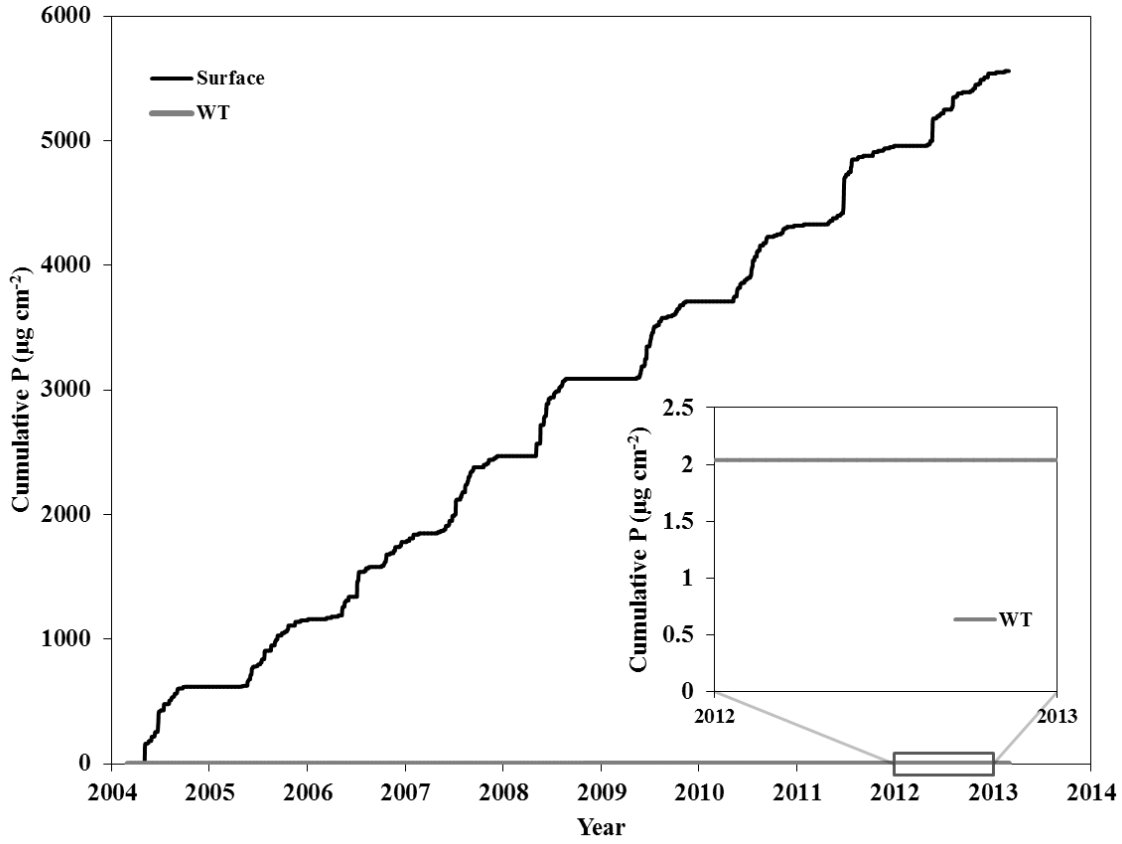

Figure 16. Cumulative P flow for the Level 1 model. The inset is a magnified view of the water table P flux for 2012.

The Level 2a model adopts the heterogeneous gravel layer system developed with ERI from Miller et al. (2014) and the plot infiltration K_s for the Barren Fork silt loam found by Heeren et al. (2013). Of the 509 kg ha^{-1} of P applied with rainwater, 52.1 kg ha^{-1} was delivered to the water table over the nine year simulation, resulting in a P delivery ratio of 10.2% (Figure 17a). The maximum P concentration at the water table was 0.89 mg L^{-1} (Figure 17b).

The Level 2b model adopts previously calibrated values for α and ω over accepted values for these parameters. Of the 534 kg ha^{-1} of P applied to the surface over nine years, 54.4 kg ha^{-1} was delivered to the water table. This results in a P delivery ratio of

10.1% (Figure 18a) and similar to the results yielded by the Level 2a model. The maximum P concentration at the water table was slightly higher than the Level 2b model at 0.98 mg L^{-1} (Figure 18b). These results suggest the importance of properly calibrated α and ω values for expressing water table concentration.

The Level 2c model builds on the Level 2b model by adopting calibrated values for the profile dispersivity. The Level 2b model is also the closest comparison to the Level 7 model in HYDRUS-1D; that is, all parameters in the Level 2b model are the same as those in the Level 7 model. The only exceptions to this are the θ_r and θ_s van Genuchten parameters. 88.5 kg ha^{-1} of the 534 kg ha-1 of surface applied P reached the water table over nine years for a P delivery ratio of 16.5% (Figure 19a). P concentration at the water table was also higher than the Level 2b model at 1.67 mg L^{-1} (Figure 19b). These results suggest the importance of calibrating dispersivity for long-term trials.

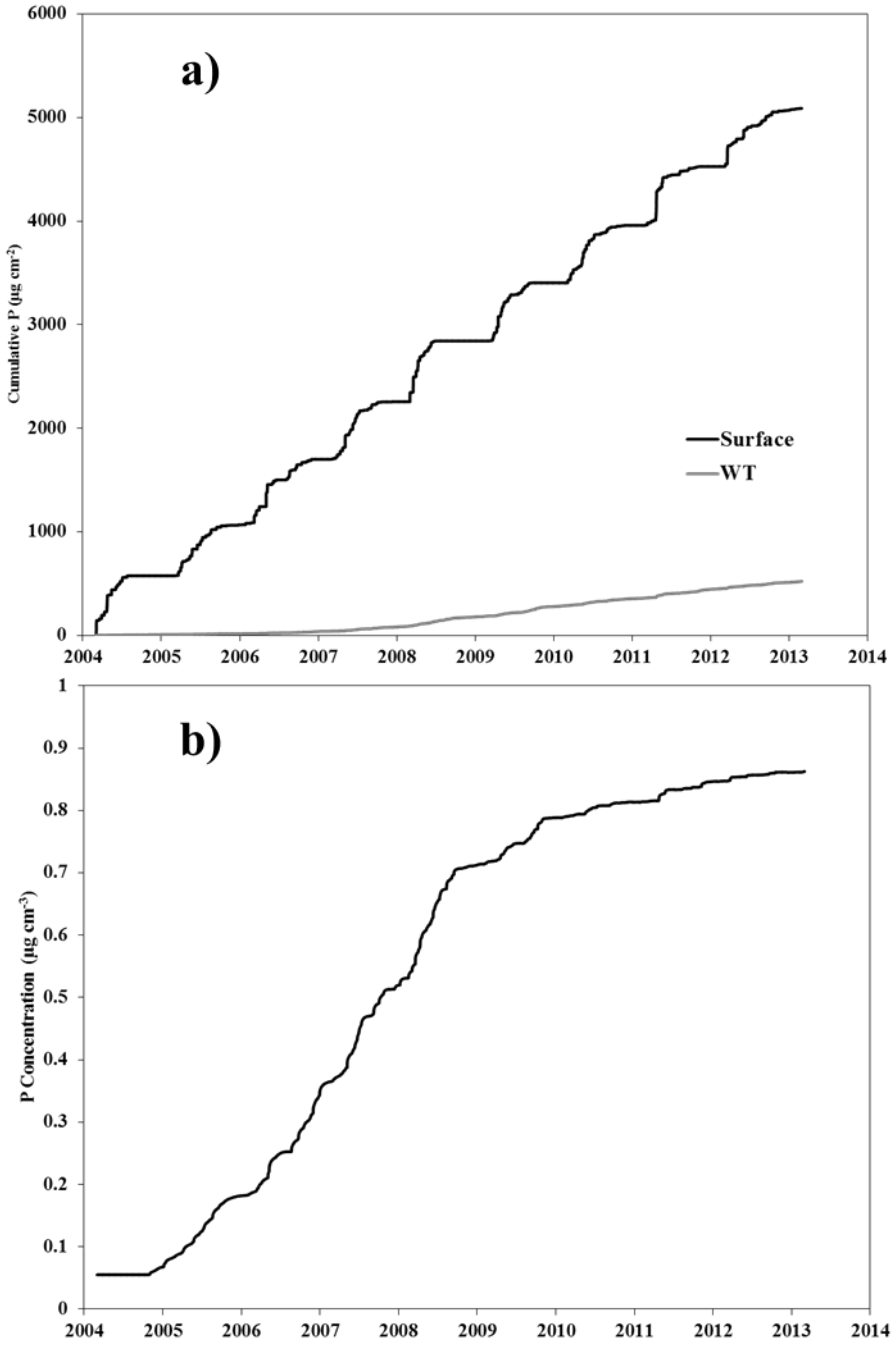

Figure 17. Cumulative P flow (a) and P concentration at the water table (b) for the Level 2a model.

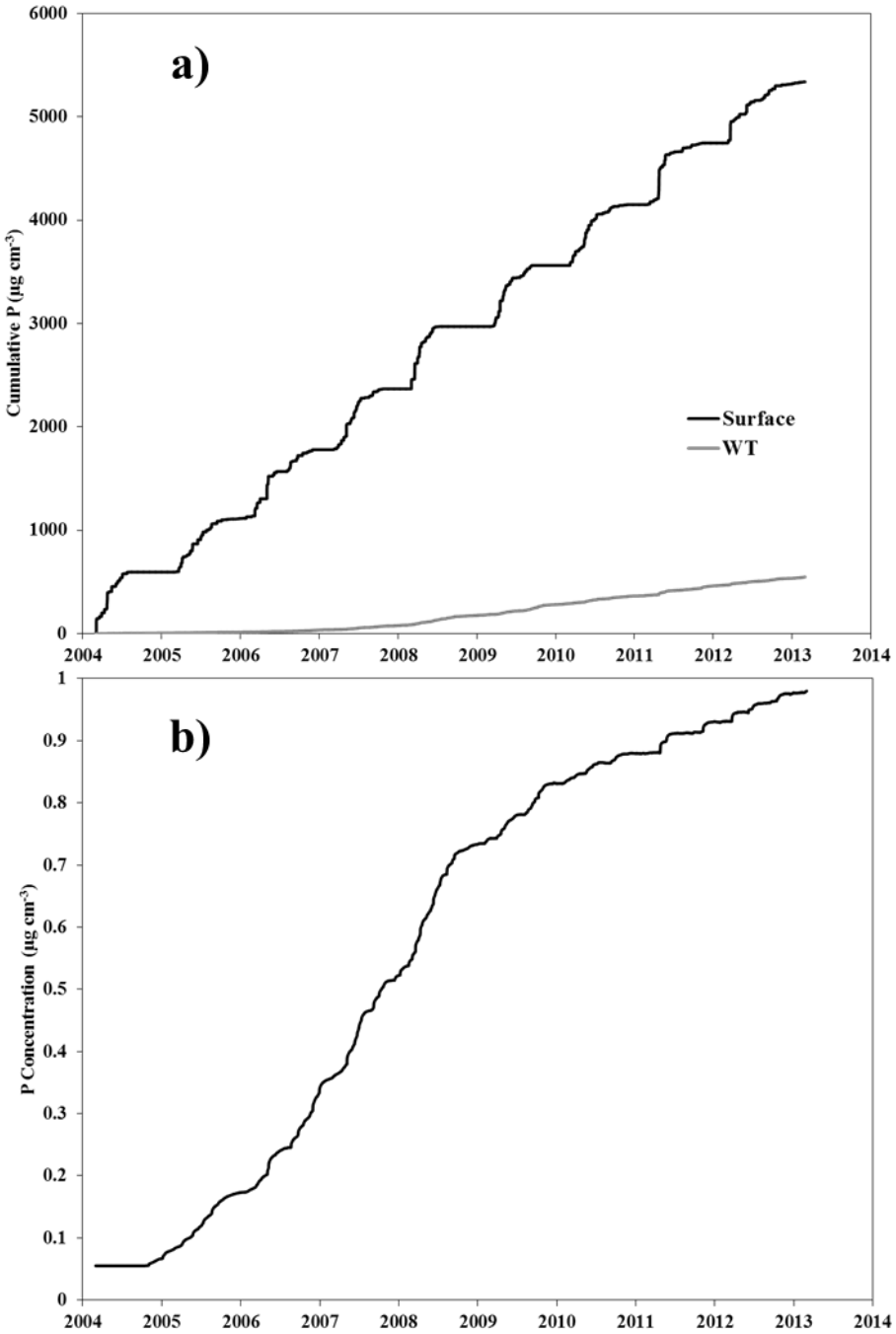

Figure 18. Cumulative P flow (a) and P concentration at the water table (b) for the Level 2b model.

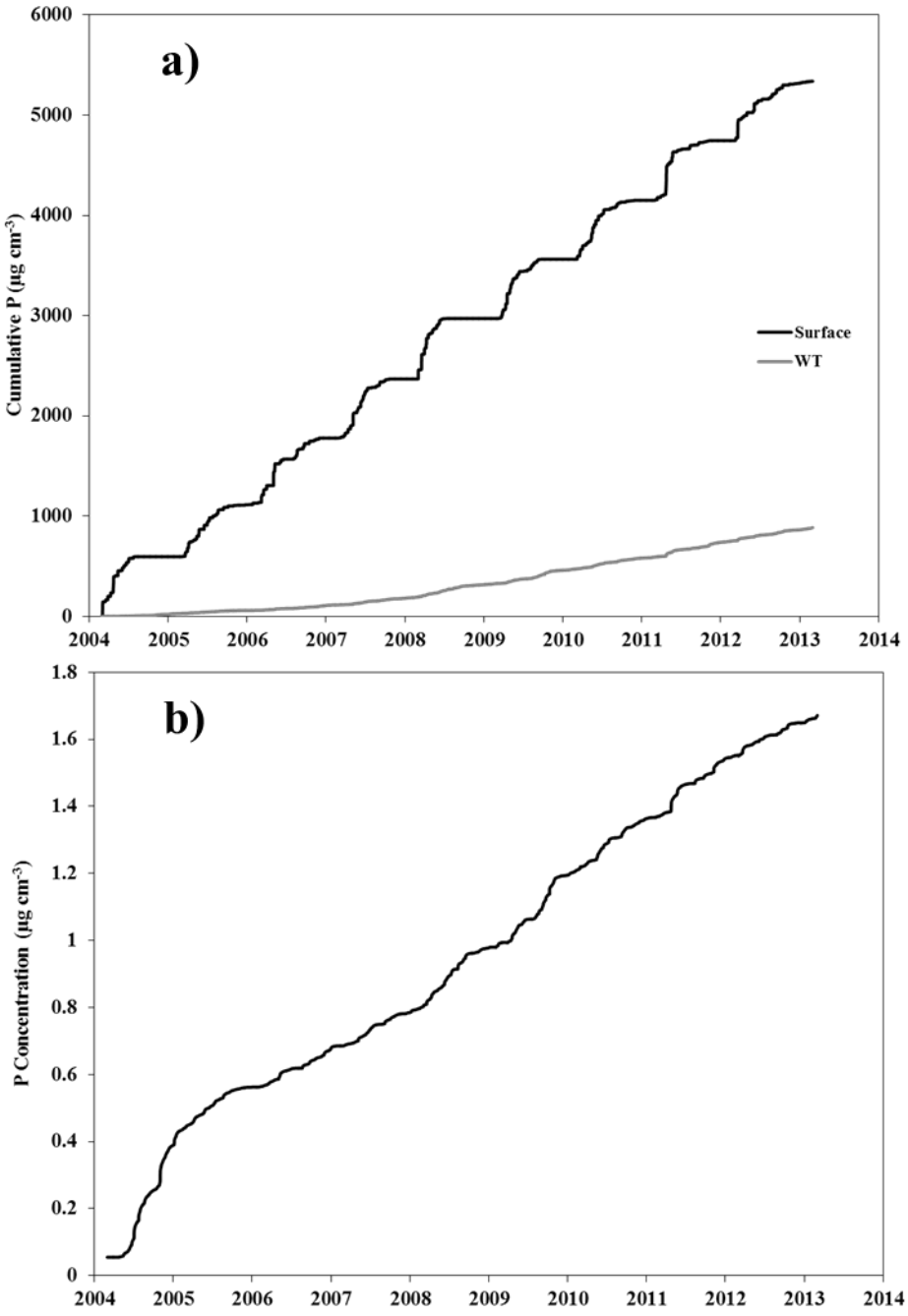

Figure 19. Cumulative P flow (a) and P concentration at the water table (b) for the Level 2c model.

3.4 Long-term P modeling with HYDRUS-2D/3D

Long-term modeling was also conducted in HYDRUS-2D to determine the P loading to the water table between March of 2004 and March of 2013. Long-term simulations of the Level 4, Level 6, and Level 7 models were performed. The Level 6 model simulated P transport using daily rainfall data for the time period of interest. Over nine years, approximately 546 kg ha^{-1} P was applied to the plot area through simulated fertilizer application. P mass was recorded as it crossed the water table boundary. Approximately 91.7 kg ha^{-1} P was lost to the water table, or about 16.8% of applied P (Figure 20). This result is similar to the Level 2c model.

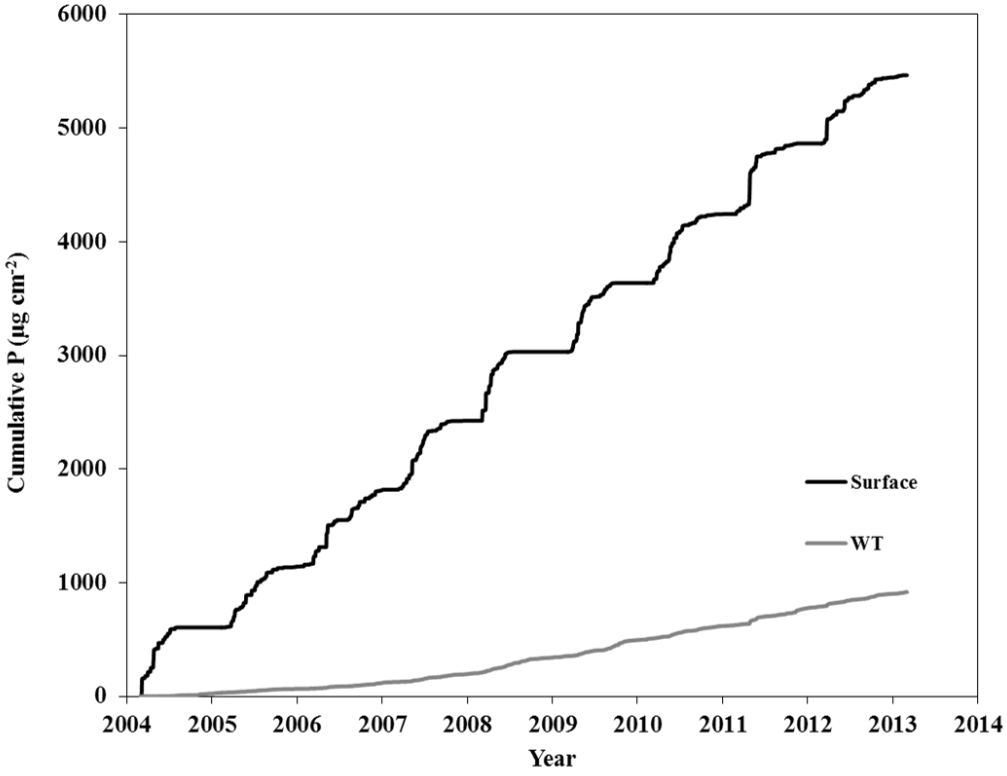

Figure 20. Cumulative P inflow from infiltration and cumulative P outflow to the water table for the Level 6 dual-porosity daily rainfall model.

P concentrations of flow into the water table were analyzed in addition to P mass totals (Figure 21). P concentration of the flow into the water table steadily increased with time, with an end concentration of 1.74 mg L^{-1}. Wet years (2004, 2008, and 2009) saw significantly higher increases in concentration than average and dry years (Figure 21). Sharp peaks seen in Figure 21 were artifacts of the analysis process. The average concentration at the bottom of the profile was obtained by dividing the solute flux by the water flux into the water table. However, exported data from HYDRUS did not have identical time stamps for solute and water fluxes. This resulted in solute fluxes taken at any given time being divided by water fluxes taken a few minutes before or after the given solute flux occurred. This only caused problems during or directly after rain events, when water and solute fluxes were changing rapidly, and the overall trend of concentration increase over the nine year simulation period and over an individual year (Figure 21) can still be clearly seen.

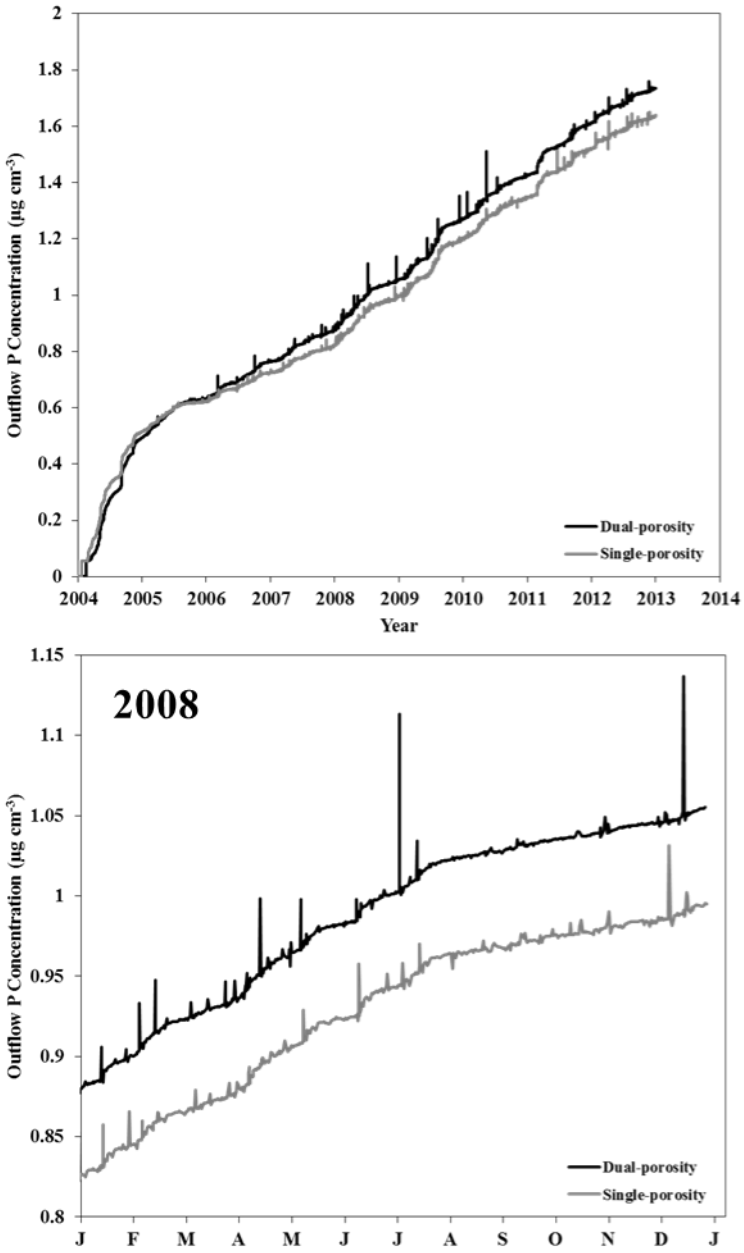

Figure 21. Simulated P concentration over time with the Level 6 dual-porosity daily rainfall model between 2004 and 2013 (top) and for 2008 (bottom). Results for the single-porosity simulation are in gray.

Mass balance information was also collected for the long-term simulations. Peclet and Courant numbers of 0.093 and 0.03, respectively, were reported and are well within the stability ranges recommended by Radcliffe and Šimůnek (2010). Water mass balance

error was acceptable at 0.71%, while P mass balance error was higher at 4.1%, but still acceptable for a complex subsurface system.

Long-term modeling was also done with the Level 4 model. Over 9 years, approximately 87.1 kg ha^{-1} of P was lost to the water table, or 16.0% of applied P. However, the single-porosity model predicted a lower final P concentration at the water table of 1.64 mg L^{-1}, which is 0.1 mg L^{-1} less than the dual-porosity model predicted. (Figure 21). These results are close to the results produced by not only the Level 6 model, but by the Level 2c model, suggesting that no substantial differences exist between single- and dual-porosity models and also between the 1D and 2D models.

Results from long-term dual-porosity simulations using the Level 7 also showed similar results to the dual-porosity and single-porosity daily rainfall models. Over the nine-year period, 89.7 kg ha^{-1} of the 545 kg ha^{-1} of P applied to the surface reached the water table boundary (Figure 22). This corresponded to a P delivery rate of 16.4%.

P concentrations at the water table were recorded over the nine year period for the Level 7 model. The final P concentration was 1.70 mg L^{-1}, which falls between the results of the Level 4 and Level 6 models. These results are also similar to the Level 2c model, the 1D allegory to this model. P delivery ratios were almost identical, and while the Level 7 model had a higher final P concentration, it is still similar to the Level 2c model. The Level 7 model showed a concentration trend similar to the previous long-term 2D models, but was slightly lower than the Level 6 model after 2005 and the gap between the two concentration trends continued to increase with time (Figure 23). Further long-term trials with longer timespans would be needed to confirm this trend. The Level 7 model

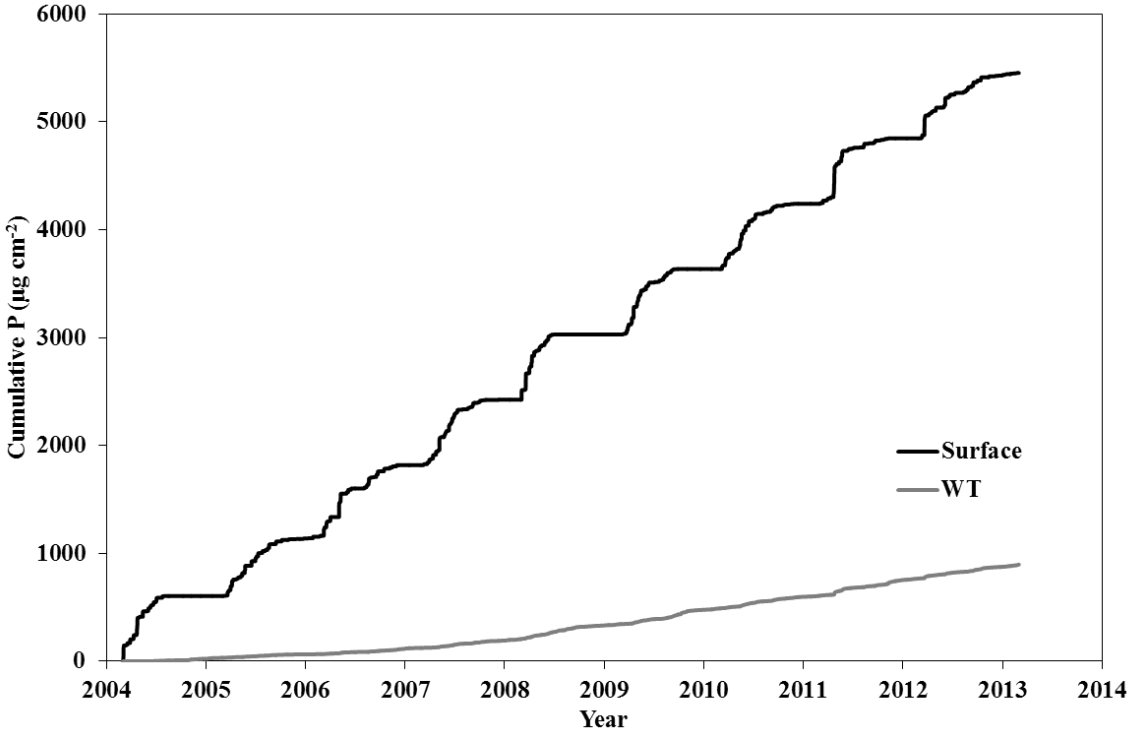

Figure 22. Cumulative P inflow from infiltration and cumulative P outflow to the water table for the dual-porosity modified 5-minute rainfall model.

was analyzed for simulated rapid delivery of P and water through macropores. However, the resolution of the results provided by HYDRUS was not fine enough to detect any rapid delivery instances.

Mass balance error for the Level 7 model had a wide range, between less than 1% and over 100% for both water and solute transport. Solute mass balance error was consistently lower than water mass balance error. However, large errors (above 10%) only occurred in the first 10 to 30 days of simulation for each year and were attributed to model spin-up similar to climatological models (NPS, 2003). After the 10 to 30 day period, mass balance errors dropped below 10% and were often lower than 1%.

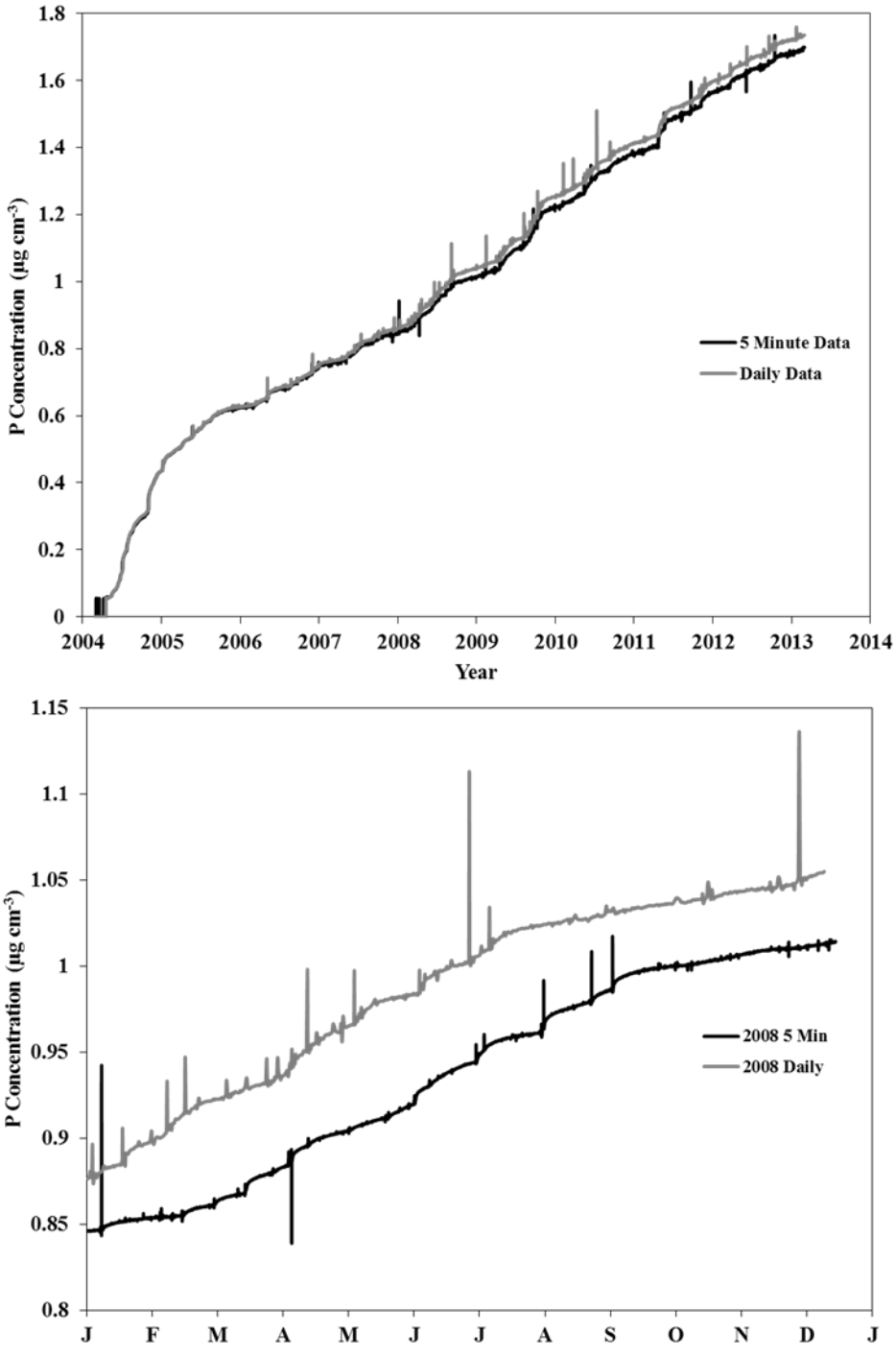

Figure 23. Simulated P concentration over time with the dual-porosity 5-minute rainfall model between 2004 and 2013 (top) and for 2008 (bottom). Results for the dual-porosity daily rainfall model are in gray.

Figure 24 shows how P concentration changes throughout the profile over the nine year simulation. Cross-sections were taken through the center of the soil profile at the end of each year. P concentration at the surface increases significantly over the nine years, but some years show a temporary decrease at the time of sampling. This result is most likely due to rain events near the time of sampling that do not bring additional P into the system. P concentration at the water table increases steadily over time. There also appears to be no significant difference between the three models. This result matches previous findings.

4. Discussion

4.1 Calibration

During the calibration step, there was some difficulty matching HYDRUS simulation breakthrough curves to observed data. It may be due to a lack of soil profile data collected by ERI. It is possible that the ERI survey missed some heterogeneity in the profile near the position of well C, which would have allowed P to reach the well faster than other points in the profile. It is also possible that the ERI data could not provide a fine enough resolution of the soil profile to catch heterogeneity that would have explained why only one well displayed P transport. Another explanation might be that the dual-porosity model simply is not sophisticated enough to model this system, and that alternative modeling techniques might need to be developed to handle profiles dominated by preferential flow (Beven and Germann, 2013).

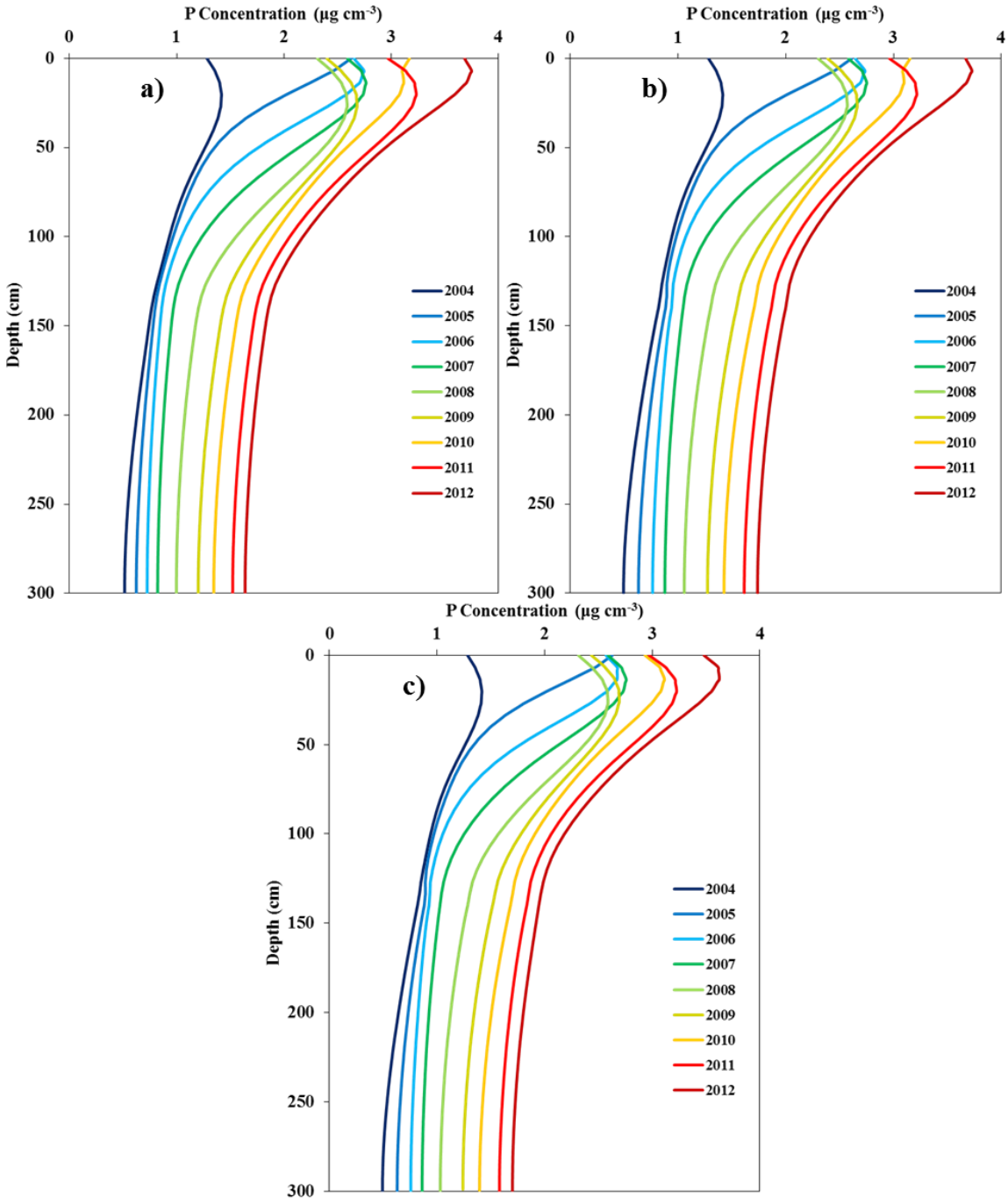

Figure 24. Phosphorus profiles for the Level 4 model (a), the Level 6 model (b), and the Level 7 model (c) over the nine-year simulation. Profiles were collected on March 1st, corresponding to the end of each simulation year. The P concentration between the phases is at equilibrium and increases at the surface and water table during the simulation. No significant differences were seen between the three models.

Despite these limitations, HYDRUS was successful in modeling Cl and P transport. Chloride and P transport were modeled satisfactorily while still keeping the values of soil properties within accepted ranges. The success of this complex model in matching observed data confirms the usefulness of this model and certainly holds it above other subsurface models that cannot account for 2D or 3D flow.

Results of the mesh macropore calibration suggested that it could be useful as an alternative to the multi-domain model approach, but additional information was needed to make it more successful. The mesh macropore was able to closely match observational P data and clearly expressed the differentiation between the two observation wells in a way that was not matched by the dual-porosity model for either solute. However, calibration parameters found with P transport produced poor matches to Cl transport. Furthermore, the mesh macropore model in general was unable to simulate the rapid breakthrough of Cl and the slower breakthrough of P with a single set of parameters. The best placement of the macropore was also difficult to find, and each solute had a different best-fit placement. From these results, it was concluded that the mesh macropore model could not find a set of conditions that matched both solutes with the information that was currently available for calibration. While the modeling of P transport is important as P is the solute of interest for the long-term simulations, the Cl transport is important as a tracer for calibrating water flow through the macropore. A good fit for both Cl and P was required to accept a model for long-term modeling. Mesh macropore models were found to have the potential to simulate porous soil profiles better than the multi-domain model, but more information about macropore geometry and placement and better calibration to

water flow was needed.

The calibration of the three additional models and their comparison to the Level 6 model suggest the usefulness of sampling techniques such as ERI surveying, and the necessity of using some dual-porosity model to accurately represent macropore flow. Results from the calibration suggest that modeling highly conductive and variable soil systems such as these requires the highest resolution data available. In fact, while the ERI survey provided a higher resolution of data than can be found with many other data collection methods, even higher levels of resolution may be needed to more accurately model these complex systems. During calibration, models not featuring a dual-porosity system fell far short of observed data, underlining the need for some kind of multi-domain component to any model used to simulate soils with the level of macropore activity present in alluvial areas within the Ozark ecoregion.

4.2 Long-term Simulation

The HYDRUS-1D long-term models demonstrated the importance of several factors in modeling transport through Ozark ecoregion soils. The Level 1 model demonstrated the importance of collecting detailed soil data. Using Rosetta Lite to define soil properties, especially the silt loam K_s value, together with a single porosity model, created a soil profile that severely inhibited P transport to the water table resulting in a P load over two orders of magnitude smaller than the P load predicted by the standard model (Level 6). Conducting plot infiltration experiments or using a double-ring infiltrometer to obtain soil mantle K_s values are far better options than using PTFs for these soils. The Level 2 models demonstrated the importance of calibrating the α and ω

parameters. While the P delivery ratio for the Level 2a and 2b models were similar, the concentration at the water table shows that properly calibrating these parameters makes some difference in the results. The Level 2c model was substantially different from the other two Level 2 models, delivering more P at a higher concentration to the water table. Given that the only changes between the Level 2b and 2c models were the calibrated dispersivity coefficients, these results suggest that proper representation of the soil profile dispersivity is key to producing successful long-term simulations.

There also does not seem to be a substantial difference between 1D and 2D modeling. The Level 2c and Level 7 models were designed to be 1D and 2D versions of the same model. The fact that they produced similar results suggests that HYDRUS-1D and -2D perform equally as well at long-term simulations. However, this result glosses over an important factor. The HYDRUS-2D long-term model soil profile was designed to mimic a 1D transport profile and the horizontal heterogeneity that was expressed in ERI results and in the calibration step was lost when the profile was simplified. This eliminates almost all of the 2D nature of the profile, leaving only small-scale horizontal transport which did not seem to have much of an impact on transport to the water table. More work needs to be done to investigate whether the HYDRUS-2D long-term model performs differently than the 1D version with profiles featuring more horizontal heterogeneity. Even so, Level 2c cumulative P load and final concentration at the water table were only 2.9 and 4.0%, respectively, lower than standard model results (Table 6).

Comparing the results of the Level 4, Level 6, and Level 7 long-term simulations yielded unexpected results. It was expected that the dual-porosity soil profile in the Level

6 design would deliver more P to the water table than the Level 4 model; while this was technically true, the difference between the two models was not substantially different and could be attributed to model error. It was also expected that the high-resolution rainfall data used in the Level 7 model would increase the macropore flow and delivered P beyond that shown in the Level 6 model. However, results of this model show reduced levels of P delivery, although the difference between the Level 6 and Level 7 models was also unsubstantial.

These unexpected results lead to a few key questions that must be addressed. First of all, an explanation as to why the single-porosity Level 4 model and the dual-porosity Level 6 model produced similar long-term results is needed. This result is somewhat confusing, especially given the significant differences seen between these models during calibration. However, a more detailed analysis of the governing equations used by HYDRUS reveals some insights into this result. Reproduced below from earlier in this work is equation 6a:

$$\Gamma_s = \alpha\left(1-w_{im}\right)\left(c_{mo}-c_{im}\right)+\Gamma_w c^* \qquad (6a)$$

where Γ_s is the solute mass transfer rate between the macropore and matrix phases. One plausible explanation for why additional solute is not reaching the water table in the Level 6 model is that this term is high enough to move most of the solute out of the macropore and into the matrix before solute-laden water reaches the water table. The large value of Γ_s is influenced by two important factors in these simulations. First, the α term for the silt loam mantle is moderately high when compared to ranges found in the literature. Second, the difference between the mobile and immobile concentrations (c_{mo}-

c_{im}) is large. The resulting matrix P concentration at the top of the profile where rainwater enters is relatively low throughout the nine-year simulation period, ranging from less than 1 mg L^{-1} at the start of simulation in 2004 to about 3.5 mg L^{-1} at the end of simulation in 2013. In comparison, rainwater entering the top of the profile contains P concentrations starting at 15 mg L^{-1} at the beginning of each year, and has a higher P concentration than the matrix for most of the year. These two factors combine to create a large gradient that favors solute leaving mobile water in the macropore and entering immobile water in the matrix, forcing the dual-porosity model to exhibit behavior closer to a single-porosity model.

This also explains the large difference between the Level 4 and Level 6 models during the calibration step. The conditions during calibration created a far smaller concentration gradient than the long-term trial, where the inflow concentration was only 1.68 mg L^{-1}. Under these circumstances, the Γ_s term becomes much smaller, and transport of solute in the macropore to the water table is more favored.

Another question that needs to be addressed is the lack of difference between the Level 6 and Level 7 models. Literature suggests that macropores only fully function when under positive pressure conditions, conditions that do not exist under the daily rainfall data model but do exist under the modified 5-minute data model. However, there was no substantial difference in results produced between the two models. The explanation for this is most likely due to the mathematical model used to express macroporosity. One of the key points of the dual-porosity flow model is that water can never flow through the matrix, and that rainfall or other surface fluxes are prevented from

entering the matrix without first entering a macropore. In the field, low-intensity rainfall like the daily rainfall data would enter the matrix directly. Due to the constraints of the model, however, low-intensity rainfall is all forced into the macropore and is required to flow through the macropore region to be transported throughout the profile. This means that intensity of the rainfall has no impact on the total water delivery into the macropore region. It is possible that rainfall intensity still might have an impact on the timing of water delivery to the water table, but the resolution of the HYDRUS results was not fine enough to determine this. Note, however, that the temporal resolution of rainfall would be expected to have a substantial impact on long term simulations with the mesh macropore model or a dual permeability model.

Given the results above, it was also important to confirm that the dual-porosity model was working as intended in the long-term simulations. These results above, combined with no apparent differences in P concentration between the mobile and immobile phases, brought up the question of whether the dual-porosity model was functioning as expected. A special trial was created to verify that dual-porosity models were functioning properly. The 2008-2009 simulation of the Level 7 model was adapted to print results every minute for an 8-hour event near the beginning of the simulation year. Graphical outputs were examined frame-by-frame to find differences between the mobile and immobile concentrations at the top of the profile as P-laden water entered the system. Figure 25 compares the mobile and immobile concentrations of the profile 5.25 hours into the storm event. A clear difference between the mobile and immobile concentrations near the top of the profile can be seen, with concentration differences

between the two phases as high as 0.45 mg L^{-1}. However, concentration quickly approaches equilibrium below the top few layers of elements, with differences between the phases being less than 0.05 mg L^{-1}. This result strengthens previous conclusions about the role of a large Γ_s in these long-term simulations.

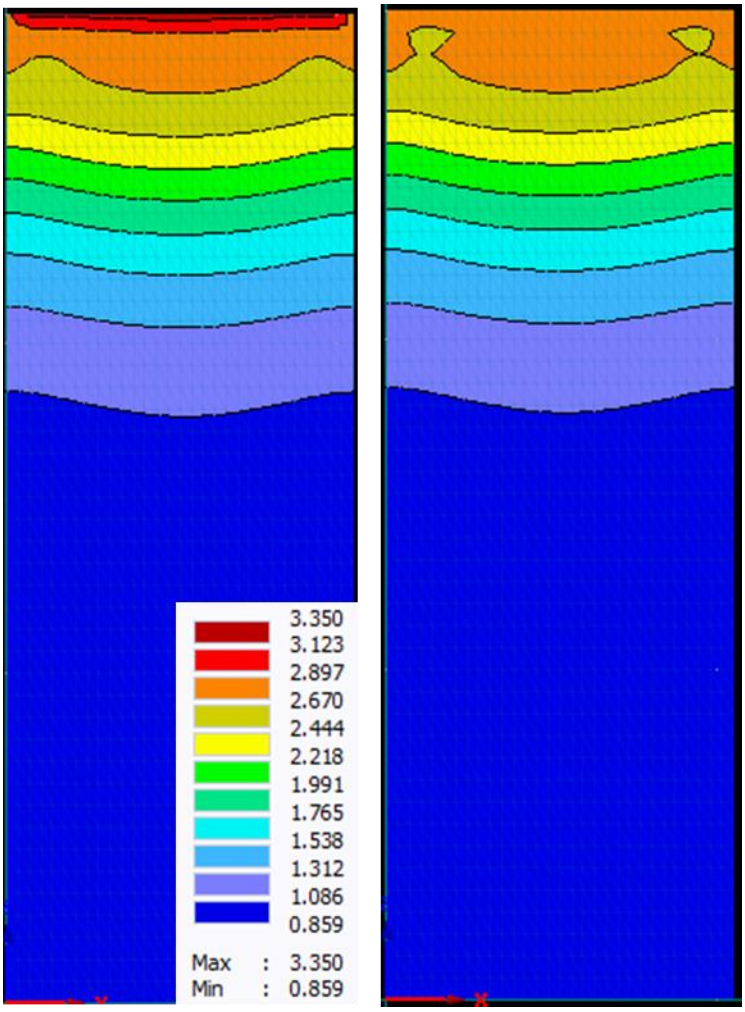

Figure 25. Comparison of Level 7 mobile (left) and immobile (right) concentrations (mg L^{-1}) during an 8-hour rain event, Mar 2-3, 2008. Note the distinction between phases at the top of the profile.

5. Summary

HYDRUS was calibrated to match observed data for Cl and P collected by Heeren

(2012). Of the four model levels calibrated, the Level 6 dual-porosity heterogeneous profile model matched the observed data for both solutes the best. The Level 6 model was used as the "standard" model to compare to all other calibrated models and long-term simulations. Calibration of a mesh macropore profile had an excellent match to P observed data, but poorly matched Cl observed data and was not selected for further testing.

Long-term (nine years) modeling based on historical precipitation data was conducted with several models in HYDRUS-1D. The Level 1 model long-term simulations found that almost no P made it to the water table, despite the moderate level of data collection and field work used to generate parameters used in the model. This suggested that the most convenient model is inadequate, and obtaining detailed soil profile information from in-depth field tests and laboratory experiments is highly useful in modeling, particularly for the silt loam layer. The Level 2a and 2b models tested the importance of calibrating the α and ω rate constants on long-term transport. While both models delivered the same percentage of applied P to the water table (10.2% and 10.1%, respectively), the 2b model with calibrated α and ω parameters had a peak water table concentration closer than the 2a model to the Level 7 model, suggesting that calibrating these parameters or obtaining their values in the laboratory is also useful to long-term modeling. The Level 2c model demonstrated the importance of properly calibrating the dispersivity of the soil profile, and results also suggest that the 1D model may be sufficient to model long-term simulations.

Long-term modeling was also conducted in HYDRUS-2D. The Level 6 model

was simulated over nine years of daily rainfall data. Results suggest that the nature of the soil profile developed during calibration allows for significant P transport to the water table (17%) and water table concentrations of 1.74 mg L^{-1}, grossly in excess of the 0.037 mg L^{-1} P surface water standard set for Oklahoma scenic rivers. It is important to once again note that this result does not reflect ET contributions, which are certainly important and discussed further in Appendix C. This result is especially troubling at sites near bodies of water where stream-groundwater interactions exchange groundwater and surface water. The Level 4 single-porosity model produced a similar result, and it was found that the high concentration gradient between the P inflow and the matrix caused rapid P movement into the matrix from macropores, causing the dual-porosity models to simulate P flux similarly to single-porosity models. The Level 7 model tested the impact of high resolution rainfall data on macropore flow, but found no significant differences between high resolution 5-minute rainfall data and the lower resolution daily rainfall data. This was explained by the nature of the dual-porosity model, which forces all rainfall into the macropore phase regardless of intensity.

Overall, the most important elements for accurately simulating P leaching in the simulated silt loam and gravel soil profile were identified. It was found that modeling was most effective when utilizing field measured hydraulic conductivities for the limiting soil layers and when using properly calibrated dispersivity coefficients. Additionally, the dual-porosity model was found to have a great impact on simulations provided that the solute gradient conditions were kept low.

This research has led to several conclusions about modeling long-term flow

through high preferential flow regions. First, perhaps above all else, it is important to collect comprehensive soil profile information. This includes performing field and laboratory tests to find K_s values for soil layers, mapping heterogeneity in the soil profile, and gathering detailed information about abnormalities in the profile that may contribute to preferential flow. Second, it is important to evaluate the input conditions and the soil profile information of the model to determine if the additional complexity of dual-porosity models is needed. Finally, high resolution precipitation data is not necessary to successfully simulate long-term transport when using a single or dual porosity model. With these conclusions in hand, future modelers of Ozark ecoregion soils will know where to focus their energies and where complexity in the model can be reduced to create a more success long-term model.

6. Future Work

This research has produced some unexpected results and has led to some interesting conclusions about the current state of macropore modeling. The results produced during the course of this research have also pointed to several future avenues that might be taken to further build upon this body of work and progress the science of long-term solute transport through macropores.

The first step that should be taken in the future is to conduct field tests with long-term modeling in mind. Additional data points should be collected during field experiments, both in terms of data density and length of the experiment. While satisfactory matches were made between HYDRUS results and observational data, an increased volume of data points over a longer time frame (48-72 hours) might provide for

a better calibration process. Collecting additional data about plots would also be useful in determining how best to model soil profiles. ERI transect data was an excellent step in the right direction, but additional data from soil cores taken within the plot area and better mapping of large macropores might increase the effectiveness of both the dual-porosity and mesh macropore models.

Future long-term modeling attempts should also take advantage of replicated data from additional plots and sites to create a more comprehensive analysis of each of the models studied in this research. While this work originally planned to model plots in addition to the Barren Fork 1x1α site, the complexities of these additional plots were too great to incorporate them in a timely fashion. Taking the steps suggested in the above paragraph might help to make studying these soil profiles more efficient. Additional information about horizontal heterogeneity and its impact on long-term solute transport at the plot and field scales is also needed.

This research has also suggested the possibility that different models may be better under different scenarios. In this work, there was no substantial difference found between the long-term single- and dual-porosity models due to the specific input and boundary conditions used in simulations. However, other conditions are certainly possible that would reveal large differences between these models, or even favor the use of the mesh macropore model. Therefore, one novel idea for tackling this issue would be the development of a program that would recommend the model components that would be best suited for any set of soil profile, initial, and boundary conditions. This task might be accomplished by performing a sensitivity analysis, using a long term simulation, on

model parameters (α, ω, etc.), soil profile conditions (layer differentiation, pervasiveness of gravel, parent material, soil K_s values, etc.) and input conditions (water and solute fluxes, initial solute concentrations, etc.), and then using those responses to gauge which model or combination of models would be most useful for long-term simulation of that profile. Once completed, users might input key parameters into a software program or use figures and tables to determine exactly which model best fits their needs.

7. References

Ahuja, L. R., DeCoursey, D. G., Barnes, B. B., & Rojas, K. W. (1993). Characteristics of macropore transport studied with the ARS Root Zone Water Quality Model. *Trans. ASAE.* 36:369-380.

Akay, O. & Fox, G. A. (2007). Experimental investigation of direct interconnectivity between macropores and subsurface drains during infiltration. *Soil Sci. Soc. of America J.* 71:1600-1606.

Akay, O., Fox, G. A., & Šimůnek, J. (2008). Numerical simulation of flow dynamics during macropore-subsurface drain interactions using HYDRUS. *Vadose Zone J.* 7:909-918.

Allaire S. E., van Bochove, E., Denault, JT., Dadfar, H., Theriault, G., Charles, A., & De Jong, R. (2011). Preferential pathways of phosphorus movement from agricultural land to water bodies in the Canadian Great Lakes basin: a predictive tool. *Canadian J. Soil Sci.* 91: 361-374.

Alletto, L., Coquet, Y., Vachier, P. & Labat, C. (2006). Hydraulic conductivity, immobile water content, and exchange coefficient in three soil profiles. *Soil. Sci. Soc. America J.* 70(4): 1272-1280.

Beauchemin, S. & Simard, R. R. (1999). Soil phosphorus saturation degree: review of some indices and their suitability for P management in Quebec, Canada. *Canadian J. of Soil Sci.* 79: 615-625.

Beck, M. A., Zelazny, L. W., Daniels, W. L., & Mullins, G. L. (2004). Using the Mehlich-1 extract to estimate soil phosphorus saturation for environmental risk assessment. *Soil Sci. Soc. of America Journal* 68: 1762-1771.

Beven, K. & Germann, P. (1982). Macropores and water flow in soils. *Water Resources Res.* 18(5): 1311-1325.

Beven, K. & Germann, P. (2013). Macropores and water flow in soils revisited. *Water Resources Res.* 49: 3071-3092.

Cheviron, B. & Coquet, Y. (2008). Sensitivity analysis of HYDRUS-1D to transient-MIM parameters: a case study related to pesticide fate in soil. *Second HYDRUS Workshop.* Prague, Czech Republic.

Cooper, A.B., Smith, C. M., & Smith, M. J. (1995). Effects of riparian set-aside on soil characteristics in an agricultural landscape: Implications for nutrient transport and retention. *Agr. Ecosyst. Environ.* 55(1): 61-67.

Correll, D. A., Heeren, D. M., Fox, G. A., Storm, D. E., Penn, C. J., & Halihan, T. April 4-5, 2013. Transient resistivity imaging of a phosphorous tracer test. *Geological Society of America South-Central Regional Meeting*, Austin, Tex.

DeLaune, P. B., Moore, Jr., P. A., Carman, D. K., Sharpley, A. N., Haggard, B. E., & Daniel, T. C. (2004). Development of a phosphorus index for pastures fertilized with poultry litter: Factors affecting phosphorus runoff. *J. Environ. Qual.* 33(6): 2183-2191.

Djodjic, F., Borling, K., & Bergstrom, L. (2004). Phosphorus leaching in relation to soil type and soil phosphorus content. *J. Environ. Qual.* 33: 678-684.

Edwards, D.R. & Daniel, T.C. (1993). Effects of poultry litter application rate and rainfall intensity on quality of runoff from fescuegrass plots. *J. Environ. Qual.* 22: 361-365.

Elmi, A., Nohra, J. S. A., Madramootoo, C. A. & Hendershot, W. (2012). Estimating phosphorus leachability in reconstructed soil columns using HYDRUS-1D model. *Environ. Earth Sci.* 65: 1751-1758

Fetter, C. W. (1999). *Contaminant Hydrogeology, 2nd Ed.* Long Grove, Ill.: Waveland.

Fox, G. A., Heeren, D. M., Miller, R. B., Mittelstet, A. R. & Storm, D. E. (2011). Flow and transport experiments for a streambank seep originating from a preferential flow pathway. *J. Hydrol.* 403: 360-366, DOI: 10.1016/j.jhydrol.2011.04.014.

Freiberger, R. P., Heeren, D. M., Fox, G. A., Penn, C. J., & Eisenhauer, D. E. July 15-17, 2014. Finite element modeling of long-term phosphorus leaching through macropores in the Ozark ecoregion. ASABE Annual International Meeting. Paper No. 1897543, Montréal, Québec, Canada.

Frippiat, C.C. & Holeyman, A.E. (2008). A comparative review of upscaling methods for solute transport in heterogeneous porous media. *J. Hydrol.* 362: 150-176.

Fuchs, J. W., Fox, G. A., Storm, D.E., Penn, C. J., & Brown, G. O. (2009). Subsurface transport of phosphorus in riparian floodplains: Influence of preferential flow paths. *J. Environ. Qual.* 38: 473-484. DOI: 10.2134/jeq2008.0201.

Gburek, W.J., Barberis, E., Haygarth, P. M., Kronvang, B., & Stamm, C. (2005). Chapter 29: Phosphorus mobility in the landscape. In Phosphorus: Agriculture and the Environment, 941-979. Sims, J.T. and A. N. Sharpley, ed. Madison, Wis.: ASA-CSSA-SSSA.

González-Delgado, A. M. & Shukla, M. K. (2014). Transport of nitrate and chloride in variably saturated porous media. *J. Irrig. Drain Eng.* 140(5) 04014006.

Gotovac, H., Cvetkovic, V., & Andricevic, R. (2009). Flow and travel time statistics in highly heterogeneous porous media. *Water Resources Res.* 45, W07402, DOI: 10.1029/2008WR007168.

Haws, N. W., Rao, P. Suresh C., Šimůnek, J., & Poyer, I. C. (2005). Single-porosity and dual porosity modeling of water flow and solute transport in subsurface-drained fields using effective field-scale parameters. *J. Hydrol*. 313: 257-273.

Heeren, D. M., Fox, G. A., & Storm, D. E. (2014). Technical note: Berm method for quantification of infiltration at the plot scale in high conductivity soils. *J. of Hydrol. Eng.* 19(2), DOI: 10.1061/(ASCE)HE.1943-5584.0000802.

Heeren, D. M., Fox, G. A., Storm, D. E., Haggard, B. E., Penn, C. J., & Halihan, T. July 21-24, 2013. Impact of Measurement Scale on Infiltration and Phosphorus Leaching in Ozark Floodplains. ASABE Annual International Meeting, Paper No. 1621213, Kansas City, Mo.

Heeren, D. M. (2012). Subsurface phosphorus transport and scale dependent phosphorus leaching in alluvial floodplains. PhD diss. Stillwater, Okla.: Oklahoma State University, Department of Biosystems and Agricultural Engineering.

Heeren, D. M., Fox, G. A., Miller, R. B., Storm, D. E., Mittelstet, A. R., Fox, A. K., Penn, C. J., & Halihan, T. (2011). Stage-dependent transient storage of phosphorus in alluvial floodplains. *Hydrol. Process.*, 25(20): 3230-3243.

Jarvis, N. J., Villholth, K. G., & Ulén, B. (1999). Modelling particle mobilization and

leaching in macroporous soil. *European J. of Soil Sci.* 50(4): 621-632.

Kamra, S.K., Lennartz, B., Van Genuchten, M.Th., & Widmoser, P. (2001). Evaluating non-equilibrium solute transport in small soil columns. *J. Contam. Hydrol.* 48: 189-212.

Lallemand-Barres, P. & Peaudecerf, P. (1978). Recherche des relations entre la valeur de la dispersivitie macroscopique d'un milieu aquifere, ses autres caracteristiques et les conditions de mesure, etude bibliographique. *Bulletin, Bureau de Recherches Geologiques et Miniéres*, 3/4: 277-287.

Lamy, E., Lassabatere, L., Bechet, B., & Andrieu, H. (2009). Modeling the influence of an artificial macropore in sandy columns on flow and solute transfer. *J. Hydrol*. 376: 392-402.

Larsson, M. H., Persson, K., Ulén, B., Lindsjö, A. & Jarvis, N. J. (2007). A dual porosity model to quantify phosphorus losses from macroporous soils. *Ecol. Modelling* 205: 123-134.

Liu, H.H., Zhang, R., & Bodvarsson, G.S. (2005) An active region model for capturing fractal flow patterns in unsaturated soils: model development. *J. Contam. Hydrol.* 80: 18-30.

Lopez, C. B., Jewett, E. B., Dortch, Q., Walton, B. T., & Hudnell, H. K. (2008). Scientific Assessment of Freshwater Harmful Algal Blooms. Interagency Working Group on Harmful Algal Blooms, Hypoxia, and Human Health of the Joint Subcommittee on Ocean Science and Technology. Washington, DC.

McKeague, J., & Day, J. H. (1966). Dithionite and oxalate-extractable Fe and Al as aids in differentiating various classes of soils. *Canadian J. of Soil Sci.* 46: 13-22.

Miller, R. B., Heeren, D. M., Fox, G. A., Halihan, T., Storm, D. E., & Mittelstet, A. R. (2014). The hydraulic conductivity structure of gravel-dominated vadose zones within alluvial floodplains. *J. Hydrol.* 513: 229-240.

Miller, R. B. (2012). Hydrogeophysics of gravel-dominated alluvial floodplains in eastern Oklahoma. PhD diss. Stillwater, Okla.: Oklahoma State University, Department of Biosystems and Agricultural Engineering.

Mittelstet, A. R., Heeren, D. M., Storm, D. E., Fox, G. A., White, M. J., & Miller, R. B. (2011). Comparison of subsurface and surface runoff phosphorus transport rates in alluvial floodplains. *Agric. Ecosyst. Environ.* 141: 417-425.

MWPS (2001). Manure Storages. MWPS-18, Sec. 2. Ames, Iowa: Iowa State University.

Najm, M. R., Jabro, J. D., Iverson, W. M., Mohtar, R. H., & Evans, R. G. (2010). New method for the characterization of three-dimensional preferential flow paths in the field. *Water Resources Res.* 46, W02503, DOI:10.1029/2009WR008594.

Naseri, A.A., Hoseini, Y., Moazed, H., Abbasi, F., Samani, H.M.V., & Sakebi, S.A. (2011). Phosphorus transport through a saturated soil column: comparison between physical modeling and HYDRUS-3D outputs. *J. App. Sci.* 11(5): 815-823.

Nimmo, J. R. (2010) Theory for source-responsive and free-surface film modeling of unsaturated flow. *Vadose Zone J.* 9: 295-306.

NPS (2003). Model initialization and spin-up. Department of Oceanography, Naval Postgraduate School. Retrieved from http://www.oc.nps.edu/nom/modeling/initial.html.

OCES (2013). Using poultry litter as fertilizer. PSS-2246. Stillwater, Okla.: Oklahoma State University. Retrieved from http://poultrywaste.okstate.edu/Publications/files/pss-2246web.pdf.

Osborne, L. L., & Kovacic, D. A. (1993). Riparian vegetated buffer strips in water quality restoration and stream management. *Freshwater Biol.* 29(2): 243-258.

Pautler, M. C., & Sims, J. T. (2000). Relationships between soil test phosphorus, soluble phosphorus and phosphorus saturation in Delaware soils. *Soil Sci. Soc. of America Journal* 64: 765–773.

Radcliffe, D. E. & Šimůnek, J. (2010). *Soil physics with HYDRUS: Modeling and applications.* Boca Raton, Fla.: CRC.

Sharpley, A. & Moyer, B. (2000) Phosphorus forms in manure and compost and their release during simulated rainfall. *J. Environ. Qual.* 29: 1462-1469.

Sheng, F., Liu, H.H., Wang, K., Zhang, R., & Tang, Z. (2014). Investigation into preferential flow in natural unsaturated soils with field multiple-tracer infiltration experiments and the active region model. *J. Hydrol.* 508: 137-146.

Šimůnek, J., Jarvis, N. J., van Genuchten, M. Th., & Gärdenäs, A. (2003). Review and comparison of models for describing non-equilibrium and preferential flow and transport in the vadose zone. *J. Hydrol.* 272: 14-35.

Šimůnek, J., & Van Genuchten, M. Th. (2008). Modeling nonequilibrium flow and transport processes using HYDRUS. *Vadose Zone J.* 7: 782–797, DOI: 10.2136/vzj2007.0074.

Šimůnek, J. & Šejna M. (2011) HYDRUS 2D/3D Technical Manual. PC-Progress, Prague, Czech Republic.

Singh, P & Kanwar, R. S. (1991) Preferential solute transport through macropores in large undisturbed soil columns. *J. Environ Qual.* 20: 295-300.

Westerman, P.W., Donnelly, T.L., & Overcash, M.R. (1983). Erosion of soil and poultry manure - a laboratory study. Transactions of the ASAE-1983: 1070-1078, 1084.

8. APPENDIX A: Federal regulation of poultry litter and phosphorus pollution of surface waters in the Ozark ecoregion.

Introduction

Nonpoint source pollution from agriculture is a problem that poses serious risk to freshwater and marine systems in the United States. The most devastating pollutant entering our freshwater systems from agricultural fields is phosphorus (P) from applied fertilizer. P is a critical nutrient needed for plant growth, and is considered a macronutrient for plants. For many crops, P influences rapid growth of the plant and healthy root growth (1). However, the land application of fertilizers leaves nutrients vulnerable to removal via storm runoff. This storm runoff eventually makes its way to surface water systems where P and other nutrients promote eutrophication, an ecological response to excess nutrients in surface waters. Eutrophication occurs most frequently in the form of algal blooms. Of these algal blooms, probably the most common and deadliest varieties are cyanobacteria blooms. Cyanobacteria blooms create several negative effects, including hypoxia from large blooms, large-scale fish kills resulting from hypoxic waters, and palatable effects on drinking water and in aquaculture products. Cyanobacteria are also known to produce a wide variety of toxins that are incredibly dangerous and deadly to humans and other animals. These toxins have a range of effects from simple dermatitis to several conditions that lead to death, including cardiac arrhythmia and liver failure (2). Cyanobacteria outbreaks have continued to rise in at least 35 U.S. states, including Nebraska, over the last several years. P inputs into freshwater systems can be directly linked to these blooms, as it is the limiting reactant in algae formation (3). In addition to P loading to surface waters from storm runoff, P can also

make its way to the groundwater via leaching in P-saturated soils, where it can make its way to surface waters via stream-groundwater interfaces.

The Ozark ecoregion is one area where P loading from both overland flow and stream-groundwater interaction are of significant concern for surface water contamination. The Ozark ecoregion is a region of Missouri, Arkansas, and Oklahoma nearly 62,000 km^2 in area and is generally defined by its unique geological features. Specifically, the Ozark ecoregion contains vast quantities of limestone and other carbonite-based bedrocks. These bedrocks have eroded over time from slightly acidic water, leaving behind gravel streambeds and riparian floodplain soils dominated by chert gravel (4). These soils consist of a top layer of gravelly loam or silt loam covering large bands of gravel believed to be old gravel bars. The significance of these soil characteristics is two-fold with regard to P transport. First, the high gravel content of these soils allows P-laden water to infiltrate quickly, sometimes at a rate of nearly 10 cm min^{-1}, and reach the water table in an incredibly short time. Second, the gravelly nature of these soils offers fewer sorption sites for P to adhere to the soil, meaning that more P will reach the groundwater than in other soils, and that these soils will become P saturated more quickly than in other soil types (5).

The Illinois River and the Illinois River Watershed (IRW) are critical water systems within the Ozark ecoregion. The Illinois River is a 100-mile river system that extends from the Ozark Mountains in Arkansas and travels down into Oklahoma into Tenkiller Ferry Lake (6). The river system in Oklahoma has been designated as a scenic river by the Oklahoma Scenic Rivers Commission, and is a popular tourist attraction for

northeastern Oklahoma. As such, the protection of the Illinois River is a prominent concern to Oklahoma residents.

The IRW and the Ozark ecoregion is also home to one of the largest poultry industries in the United States. The Arkansas portion of the IRW contains more than 7,000 poultry farms, which in turn produce more than 5,000 tons of poultry litter on a daily basis (7). This poultry litter, which contains manure from chickens as well as fibrous bedding materials, is rich in nutrients, including P, and is sought after by farmers as a fertilizer. However, due to the economic constraints of transporting litter, most of the land application of this waste occurs within a relatively small proximity to the poultry operations, and is susceptible to losses to the Illinois River and other surface water systems.

The goal of this review is to look at the problem of P contamination in the Ozark ecoregion from a legal perspective and determine how effective the Clean Water Act (CWA), the Comprehensive Environmental Response, Compensation, and Liability Act (CERCLA), and the Resource Conservation and Recovery Act (RCRA) are at regulating point source and nonpoint source pollution of P from agricultural fields. This review will look at three major cases within the Ozark ecoregion to evaluate how each federal program tackles the issue of P contamination and enrichment of surface waters.

Arkansas v. Oklahoma

A fundamental example of how federal laws apply to managing P and other nutrient contamination of surface waters in the Ozark ecoregion is the case of *Arkansas v. Oklahoma*. This case explores both the power of the CWA to hold upstream states to

water quality standards of downstream states, and the power that an agency has in interpreting and applying statutes in laws that they are tasked with managing.

This case focuses on the legality of an NPDES (National Pollution Discharge Elimination System) permit issued by the EPA under the CWA to the city of Fayetteville, AR. NPDES permit No. AR0020010 was issued to the city on November, 5, 1985 for the discharge of treated sewage into both the White River and the Mud River, although the discharge into the White River was not a matter of concern for Oklahoma (8). Oklahoma claimed that the discharge from the sewage plant into the Mud River would cause harm to Oklahoma waterways. Specifically, Oklahoma claimed that discharge from this plant containing P and other contaminants would cause significant further degradation of water quality in the Illinois River system, a system that was already compromised according to Oklahoma water quality standards established in compliance with CWA Sec. 303 (9)(10).

Oklahoma and the "Save the Illinois River" (STIR) interest group appealed to the EPA for an evidentiary hearing to address these concerns. The hearing took place in August 1987. However, the EPA Administrative Law Judge (ALJ) chose to uphold the NPDES permit, citing Oklahoma water quality standards regarding degradation of waterways. The ALJ stated that the effluent from the Fayetteville plant would not produce an "undue impact" on the water quality of the IRW, even under the more stringent water quality standards set forth by the state of Oklahoma. The Oklahoma parties sought an administrative appeal.

Ronald McCallum, Chief Judicial Officer for the EPA, upheld most of the ALJ findings, but disagreed on one important point. The use of the phrase "undue impact" was inappropriately applied from *International Paper Co. v. Ouellette*, a Supreme Court case

that established that the ALJ could refuse the approval of a permit if it had an "undue impact on interstate waters". However, CJO McCallum stated that the Supreme Court never defined the term "undue impact" under the Ouellette case, and that the application of the *de minimis* exception under the Clean Air Act (CAA) to the CWA was inappropriate. Therefore, CJO McCallum required the ALJ to produce discharge estimates to prove that the permit would not cause undue effect on the IRW (8). After further analysis, the ALJ upheld the finding that the Fayetteville plant would produce no "detectable" effect on the IRW and would therefore comply with Oklahoma water quality standards. The ALJ stated that of the 30 pounds per day of P produced by the plant, only 6 pounds would ever reach the Oklahoma section of the Illinois River, and it was concluded that this 6 pounds-per-day increase would have no significant effect on the state of the river. It was further concluded that because the discharge from the plant would be more dilute than anything found on the Oklahoma side of the IRW, the Fayetteville plant effluent would contribute to cleaner water downstream (9).

Oklahoma appealed this decision to the Tenth Circuit Court of Appeals. The court overturned the NPDES permit, stating that the EPA had failed to recognize that the downstream state had waters that were already degraded beyond the water quality standards already in place. Furthermore, addressing the claim that Fayetteville's effluent would actually clean the water in the Illinois River on the Oklahoma side, the court found sufficient evidence to support the idea that the effluent was "expected to contribute to the ongoing deterioration of the scenic river and possibly Tenkiller Lake as well" (11). Arkansas and the EPA petitioned this result to the Supreme Court.

The Supreme Court had to weigh both factual issues, mainly whether the EPA's and the ALJ's finding were indeed correct in determining the status of the IRW and the effect of the effluent from Fayetteville, and legal issues, mainly pertaining to the Tenth Circuit Court overstepping the bounds of its jurisdiction.

With regards to the factual findings, the Supreme Court decided to avoid forming independent factual conclusions about the current and future status of the IRW. The reasoning behind this was that the Court felt that it was not within its jurisdiction to develop these conclusions, a reasoning that the Court felt also extended to the Tenth Circuit Court. In the end, the Supreme Court found that the data and conclusions reached by the ALJ were well-substantiated and agreed that the Fayetteville discharge would not produce adverse effects severe enough to exceed Oklahoma water quality standards. Furthermore it found that the Tenth Circuit Court was wrong in developing conclusions independent of the EPA's findings, stating that such a move overstepped the jurisdiction that the court was allowed (9)(12).

The Supreme Court also identified several legal issues regarding the Tenth Circuit Court decision. First, the court ruled that the Court of Appeals had "exceeded its scope of judicial review by substituting its own reading of the CWA for the EPA's" (9). More specifically, the Court of Appeals had found that "where a proposed source would discharge effluents that would contribute to conditions currently constituting a violation of applicable water quality standards, such proposed source may not be permitted" (11). The Supreme Court found that such an interpretation of the CWA is not based on any current EPA regulation or statute within the CWA, and is therefore an inappropriate overstepping of the Court of Appeal's boundaries. The Supreme Court went on to state

that the Court of Appeals misinterpreted 33 USC § 1342 (h), which is only meant to limit the ability of a publicly owned plant from accepting additional pollutants until it ceases any violations of its NPDES permit. This statute, however, does not apply to the granting of new permits, and cannot be used as evidence to revoke the issuance of a new NPDES permit. The Supreme Court concluded that the "reliance [on the statute] was misplaced" (12).

In addition to this oversight, the Supreme Court also found, on a legal basis, the inappropriateness of substituting its own findings for ones produced by the ALJ. In fact, the Supreme Court identified "at least four times" where the Court of Appeals had presented factual evidence that was contrary to the ALJ. The court went on to say that despite the fact that accepting an agency's findings when there is "substantial evidence" to back up said findings in the standard, the Court of Appeals "turned that analysis on its head". The court stated that "court … should accept the agency's factual findings if those findings are supported by substantial evidence" and that the Court of Appeals "should not supplant the agency's findings merely by identifying alternative findings that could be supported by substantial evidence" (12).

Lastly, the Supreme Court found that the Court of Appeals had been incorrect in their finding that the EPA's decision to uphold the issued permit was "arbitrary and capricious", stating that such a decision was "derivative of the court's first two errors". This designation of "arbitrary and capricious" hinged on the EPA's failure to recognize the already degraded status of the Illinois River. However, the Supreme Court stated that when using the EPA's interpretation of the CWA, which it had already upheld, the

current status of the river need not be considered, rather the standard was whether the new permit would produce a "detectable effect" on the status of the river (12).

With these rulings, the Supreme Court found that the Court of Appeals had "made a policy choice that it was not authorized to make". While it suggested that "it might be wise" to prevent any effluent from entering the Illinois River, presumably for fear that some negative effect may occur, the Supreme Court took the EPA's findings to heart and suggested that it "would be even wiser" to allow for discharge that improved the quality of the water to flow into the river (12).

An interesting result of this case stems from the use of the Chevron doctrine in this decision. The Chevron doctrine pertains to a decision made in the case of *Chevron v. Natural Resources Defense Council* in 1984 regarding the ambiguity left by Congress in some laws and how that ambiguity may be interpreted. In short, when Congress passes a law, and the intent of Congress is clear, no interpretation or adaptation of the law may be made, as the will of Congress is obvious. However, in cases where Congress left a law or statute ambiguous (presumably to allow it to pass through, against opposition), the responsibility of interpreting that statute is left up to the agency tasked with managing that statute. The role of a court in dealing with these ambiguous statutes is only to determine if the agency in question interpreted the law correctly, not to insert its own interpretation of the law (9)(12).

The Chevron test was applied twice to this case. First, it was used in confirming the Supreme Court's opinion that the Court of Appeals overstepped its bounds when it attempted to interpret the law differently than the EPA. The second use, however, is far more interesting from the standpoint of interstate water quality standards. During the

Supreme Court hearing, Arkansas argued that the CWA had no set provisions to require upstream states to comply with the water quality standards of the downstream states. This argument was made to invalidate any claim that Oklahoma might have had in contesting the Fayetteville NPDES permit. During the permitting process, the EPA had in fact required the Fayetteville plant to adhere to downstream water quality standards; although this was essentially neglected, as the EPA had already determined that effluent from the plant would have no detectable negative impact on the Illinois River in Oklahoma. The Supreme Court, however, citing the Chevron doctrine, found that "the EPA's requirement that the Fayetteville discharge comply with Oklahoma's water quality standards to be a reasonable exercise of the Agency's substantial statutory discretion" (12).

City of Tulsa v. Tyson Foods et al.

The case of *Arkansas v. Oklahoma* is a prime example of both the potential positive and negative effects of granting significant power to the EPA under the CWA, showing both the potential power the EPA has in forcing states to work together to maintain waterway health and the fallbacks of giving the EPA the sole power in proving whether or not an NPDES permit will degrade said waterway health.

However, this power only extends to the regulation and management of point source pollution. While the CWA does recognize nonpoint source pollution as a significant source of contaminants to surface waters, it has little power to enforce these sources. Provisions within the CWA require states to identify waters that have been affected by nonpoint source pollution, identify the sources from which the pollutants stem from, and then institute best management practices (BMPs) to control the pollution. However, the CWA does not give the EPA any "authority to design, implement or

enforce control programs to curb nonpoint source pollution" (13). At most, the EPA can withhold current and future grant money set aside for nonpoint source pollution control from a state if it refuses to comply, but there is no language in the CWA that allows for the EPA to withhold any other federal funding from a noncompliant state. In terms of nonpoint source pollution, the "EPA is essentially powerless" (13).

How then should an entity go about pursuing damages from nonpoint polluters? One potential way is through the Comprehensive Environmental Response, Compensation, and Liability Act (CERCLA). Enacted in 1980, CERCLA was created to establish a "Superfund", a trust fund to pay for cleanup costs incurred when cleaning waste sites, and to allow parties affected by the waste site to recover costs of cleanup when a responsible party can be identified. This cost recovery aspect is what allows plaintiffs such as the City of Tulsa and State of Oklahoma in the case of Oklahoma v. Tyson Foods to pursue damage recovery when they were forced to clean surface water systems themselves.

However, there are four key factors that a plaintiff must prove to recover losses. The plaintiff must first show that the waste site in question is a "facility". CERCLA defines a "facility" as:

> (A) any building, structure, installation, equipment, pipe or pipeline (including any pipe into a sewer or publicly owned treatment works), well, pit, pond, lagoon, impoundment, ditch, landfill, storage container, motor vehicle, rolling stock, or aircraft, or
> (B) any site or area where a hazardous substance has been deposited, stored, disposed of, or placed, or otherwise come to be located; but does not include any consumer product in consumer use or any vessel. (14)

Second, the plaintiff must present evidence that shows that the defendant is a "covered person" as:

> (1) the owner and operator of a vessel or a facility,
> (2) any person who at the time of disposal of any hazardous substance owned or operated any facility at which such hazardous substances were disposed of,
> (3) any person who by contract, agreement, or otherwise arranged for disposal or treatment, or arranged with a transporter for transport for disposal or treatment, of hazardous substances owned or possessed by such person, by any other party or entity, at any facility or incineration vessel owned or operated by another party or entity and containing such hazardous substances, and
> (4) any person who accepts or accepted any hazardous substances for transport to disposal or treatment facilities… (15)

Third, the plaintiff needs to show that a "release" of a "hazardous material" occurred. The term release is defined by CERCLA as "any spilling, leaking, pumping, pouring, emitting, emptying, discharging, injecting, escaping, leaching, dumping, or disposing into the environment (including the abandonment or discarding of barrels, containers, and other closed receptacles containing any hazardous substance or pollutant or contaminant)"; however, this definition excludes, among other things, the "normal application of fertilizer" (14). The term "hazardous substance" allows CERCLA to draw upon hazardous waste designations set forth by the CWA and the Solid Waste Disposal Act (SWDA), as well as having its own set of hazardous chemicals. Lastly, the plaintiff must show that the release of the hazardous substance caused damage that resulted in a loss.

In 2003, the city of Tulsa, Oklahoma, and the Tulsa Metropolitan Utility Authority sued six poultry companies, including Tyson Foods and Cargill, and the city of Decatur, Arkansas for pollution of municipal water supplies. The plaintiffs in the case

identified a “Water Supply” which incorporated Lake Spavinaw, Lake Eucha, Lake Yahola, and the Tulsa Mohawk Water Treatment Plant, which received runoff contributions from the 415-square-mile Eucha/Spavinaw watershed. The plaintiffs claimed that in recent years, the Water Supply had seen a significant increase in nutrient loading, particularly P, which had resulted in “excessive algae growth”. This algal growth had reduced the quality of the water significantly with increased odor and taste problems, and that the city of Tulsa had “incurred…substantial treatment costs and other damages in responding to the taste and odor problems” (16). They claimed that the significant increase in P loading to the watershed was due mostly to the application of poultry litter. The plaintiffs stipulated that while the P that had polluted the Eucha/Spavinaw watershed had come from runoff from agricultural fields (for the most part), the poultry companies were ultimately responsible as they were the ones that held contracts with poultry producers in the region who had sold their litter to local farmers (16). In the case of one of the poultry companies and the city of Decatur, the complaint was of a poorly managed NPDES permit that had no formal requirements for effluent water quality, but rather that it be routinely monitored and reported.

The city of Tulsa sought to recover costs under CERCLA. First, they sought to define the Eucha/Spavinaw Watershed as a “facility” as it applies to CERCLA. They claimed that P was a “hazardous substance” and that the P in runoff and discharged from the Decatur point source could be interpreted as a “release” of the hazardous P. Lastly, they sought to identify the poultry companies as the “covered persons” in this case because they filled the role of “arranger” for the disposal and treatment of poultry litter by having contracts with poultry producers.

The defendants, for their part, argued that since the city of Tulsa could not seek damages under CERCLA as they were themselves a responsible party in the worsening conditions of the watershed; the city had been violating NPDES permits and discharging effluents for years, although the plaintiffs argued that this discharge was *de minimis*. They also argued that defining a watershed as a "facility" was too broad and outside the scope of the CERCLA definition for facility, and that they could not be held to the label of "arrangers" for poultry litter disposal, as they had not arranged for any disposal or treatment of a hazardous substance at any facility. Lastly, the defendants asked that the CERCLA claims be dismissed on two accounts. First, they argued, there was no way for the plaintiffs to show a discharge of hazardous substances to the watershed as P in poultry litter could not be labeled as a hazardous substance. Second, the plaintiffs could not show a release of hazardous substances as the application of poultry litter is excluded as the "normal application of fertilizer" clause under CERCLA's definition of release (16)(17).

From these arguments, the court had quite a few issues on which to rule. First, the court had to determine the validity of a cost recovery claim by the plaintiffs, as the defendants had argued that the plaintiffs were also somewhat responsible for the deterioration of the watershed. The court found that, because the plaintiffs had admitted to at least a de minimis contribution to the pollution of the watershed, they were only allowed to pursue an action of contribution, following a precedent set in the case of *Morrison Ent. v. McShares, Inc.* (2002).

A far more interesting ruling was the court's decision on the matter of "facility". The plaintiffs had argued that the watershed should be considered a facility "because the

hazardous substance at issue, phosphorus, is deposited or can be found virtually throughout the Watershed where poultry litter has been land applied". The defendants argued that it could not be considered a facility, as the watershed in question was bigger than the 415 square miles cited by the plaintiffs, and that the plaintiffs could show neither the "the presence of phosphates or phosphorus throughout the entire watershed" nor a "casual nexus between the poultry growers' land application of poultry litter and the alleged contamination of the water supply". In essence, the defendants stated that the plaintiffs would not be able to prove that P could be found anywhere in the watershed, nor could it show a link directly between applying poultry litter and P pollution of the water supply (16)(17).

The court, however, rejected the claims of the defendants. They cited *Nutrasweet Co. v. X-L Eng'g Co.*, a case where contaminants released on the defendant's property had made its way via "surface and groundwater onto plaintiffs property". The court stated that since pollutants could be found on both the plaintiff's and defendant's property, the two combined could be considered one facility; likewise, the application site of poultry litter and downgradient sites harmed by P runoff could be considered linked and one facility. In addition to this, the court cited *U.S. v. Township of Brighton*, where it was ruled that the wording of the statutes suggested that the "bounds of a facility should be defined at least in part by the bounds of the contamination" and that an area "that cannot be reasonably divided into multiple parts or functional units should be defined as a single 'facility', even if it contains parts that are non-contaminated" (16). The court also rejected the defendant's claims that there was no provable connection between the P application and the contamination, citing *Tosco Corp. v. Koch Ind., Inc.*, in which it was

established that a connection could be found simply by the "defendant's identification as a responsible person as defined in § 9607(a)". Despite these findings, the court refused to take the final step in establishing the watershed as a "facility", stating that while "the definition of 'facility' is expansive enough to include the Watershed within its scope", the factual evidence presented to the court regarding the application of poultry litter was "insufficient", "unauthenticated", and "at best admit only to the generation of, and not the land application of, poultry litter in the Watershed" (16).

Another interesting ruling was the court's decision on the matter of "arrangers". The court found that the Tenth Circuit had yet to interpret the phrase "arrange for", which is a key phrase in the CERCLA statutes when determining the arranger status of a party. Instead, the court looked at three different instances where other circuits had defined the phrase. First, the court looked to the Seventh Circuit and the case of *Amcast Ind. Corp. v. Detrex Corp.* The basis of this case looked at an instance of accidental disposal where TCE was accidentally spilled while moving the chemical to storage tanks. The Seventh Court used a narrow interpretation of the phrase "arrange for", and did not find that Detrex, the potential "arranger" did not in fact "'arrange for' those accidental 'disposals'". The court then looked to the Eight Circuit and the case of *U.S. v. Aceto Agricultural Chemicals Corps.* This case looked to the arrangement for the formulation and disposal of pesticides, for which the defendants stated that they were only responsible for the formulation and not the disposal of the pesticide waste. The Eighth Circuit disagreed, stating that since the defendants owned the pesticides throughout the formulation process and that the defendants benefitted from formulating the pesticides,

they could be found as “arrangers” for the disposal of the pesticides as well. This is, by contrast, a rather liberal interpretation of the arranger clause (16).

The court instead turned to the Eleventh Circuit and the case of *South Florida Water Management Dist. v. Montalvo*. In this case, landowners contracted crop dusting of fields with pesticides. These “sprayers” were found to be liable for cleaning the airstrip and storage sites of pesticide contamination and sought to get contributions from the landowners, saying that since the landowners owned the pesticides, they should be held liable for cleanup as well. However, the Eleventh Circuit found that this “would stretch the meaning of ‘arranged for’ too far to hold the landowners liable” (16). The basis for this was that while chemical producers in the *Aceto* case (Eighth Circuit) knew that the chemicals they produced would be hazardous, the landowners in the *Montalvo* case could not have known that the sprayers would spill the chemicals or release tainted rinse water. This establishes a “case-by-case” approach to interpreting the phrase “arranged for” (16). In this case, the court found that it could not “determined as a matter of law whether the Poultry Defendants have ‘arranged for’ the disposal of poultry litter”. It went on to further call into question some of the facts presented about the level of control the defendants had over the “alleged disposal of poultry waste through land application of poultry litter”, and used this as the basis for its noncommittal conclusion on this issue (16).

The court also looked to the determination of whether P in the form of the phosphates lost to the water supply could indeed be classified as “hazardous substances”. The hazardous nature of P in elemental form had been well established in previous cases, to the point where no side debated this fact. Rather, the defendants argued that there was

no listing of “Phosphorus and Compounds” or “phosphates” under the CERCLA registry of hazardous substances. Furthermore, the defendants stated that since phosphates are “found in all living cells” and “is safe and vital to life processes”, it should not be designated as toxic or harmful and therefore not be designated as a hazardous substance under CERCLA.

The court rejected this claim, citing two cases to back up this decision. The first was the case of *B. F. Goodrich Co. v. Murtha*, in which it was found that municipal waste or household solid wastes are not held exempt from being considered hazardous wastes. The second Circuit, which presided over this case, found that even if a waste like “municipal waste” is not expressly listed as a hazardous waste, if its components can be found as a waste under the CWA or the SWDA (along with other hazardous waste listings), it can be found as a hazardous waste under CERCLA. Furthermore, the concentration of a hazardous substance in a mixed waste product has no bearing on whether or not liability under CERCLA can be established (16). The second case cited is that of *U.S. v. Alcan Aluminum Corp.*, where the Third Circuit dismissed claims that “trace levels of generic compounds listed [under CERCLA as hazardous waste] was not a hazardous substance as it posed ‘no real threat to the environment’”. The reasoning behind this was surprisingly wise; the court first ruled that if the release alone resulted in response costs, the release could be considered hazardous regardless of amount; and second, that while a single generator’s impact on the environment may be minimal, they cannot “escape liability” as that minimal impact can be added to other generators to create an actual harmful environmental effect (16). The court in Tulsa concluded from these two cases that “CERCLA is a remedial statute that courts construe liberally to

effectuate its broad response and reimbursement goals" and that the EPA intended phosphorus compounds to be covered under CERCLA when the base P was added as a hazardous substance, stating that "since elemental phosphorus…does not occur free in nature….the EPA likely contemplated liability for phosphorus in real, not theoretical releases". In addition to this, the court ruled that the precedent set forth in Alcan case establishes that a substance need not be toxic or harmful to be listed as hazardous under CERCLA. With these findings, the court found that phosphates found in poultry litter, and poultry litter by association, could be labeled as a hazardous substance under CERCLA (16).

The last interesting decision reached by the court in the City of Tulsa case was the ruling on the "normal application of fertilizer" exclusion set forth by CERCLA. The plaintiffs argued that while the application of poultry litter may be considered to be "normal", the land application undertaken by poultry producers in the watershed goes above and beyond "normal" rates. In deciding this matter, the court was unable to find any instance of the term "normal" being defining, either within CERCLA or in any other court proceeding. Citing *U.S. v. Telluride Co.*, the court stated that it "must construe the term in accordance with its ordinary meaning". While both the plaintiffs and the defendants attempted to define "normal" to help the court reach a decision, the court found that it could not define the term without evidentiary context for the matter. Since neither side was able to present evidence to support their claim on the definition, the court merely dismissed the issue (16).

Other issues were addressed with the case, but they apply to matters too local to be of use at either the level of the entire Ozark ecoregion or on a national level. In

addition to this, the case was settled out of court before proper rulings could be made on the case. This means that none of the precedents that would have come from this case could be set.

State of Oklahoma v. Tyson Foods, Inc. et al.

In 2005, the state of Oklahoma filed suit against eleven poultry companies over land application of poultry litter and the associated negative effects for the Illinois River Watershed (IRW). Oklahoma sought to recover damages and operating costs from the poultry producers under CERCLA. However, it was determined that the Cherokee Nation was a critical party for the proceeding, and dismissed the case. In 2009, Oklahoma filed suit against the poultry companies after reaching an agreement with the Cherokee Nation, this time suing the defendants for violating the terms of RCRA, along with violations of state and federal nuisance laws.

The Resource Conservation and Recovery Act (RCRA) is an amendment of the Solid Waste Disposal Act (SWDA) added in 1976 to address substantial concerns regarding the management and tracking of both hazardous wastes and solid wastes. The program creates a “cradle-to-grave” system that maintains extensive paperwork trails to track a waste production from generation to disposal. The act was put into effect to better manage waste substances and reduce the occurrences of missing waste products and wastes arriving unannounced at disposal sites. RCRA establishes the recordkeeping regulations needed for waste generators, and requires permits for facilities that receive waste products for treatment or storage; these permits are contingent on establishing good recordkeeping and contingency plans for unexpected waste discharges. Lastly, RCRA

sets provisions for how accidental or intentional discharges should be responded to, both for hazardous substances and solid wastes (19).

It was the classification of "solid waste" that the plaintiffs attempted to define poultry litter, and seek recovery costs due to the disposal of poultry litter without a permit. However, the court ruled that poultry litter could not possibly be a "solid waste" product, and dismissed the case. The court called upon several factors in determining that poultry litter was not a solid waste.

First, the court concluded that poultry litter was not a waste product, but rather a marketable commodity of high value for agriculture. This determination was pulled from many sources presented to the court, including farmers who purchased the litter and poultry producers who sell the litter or use it for their own purposes. The value of the litter stems from its use as a fertilizer for cropland and pasture, as well as its usefulness as a soil amendment to improve soil quality in a number of ways, including adding both P and nitrogen (N) to the soil, increasing soil organic matter, and supporting better soil structure (20). Second, the court stated that the plaintiffs did not successfully show that poultry litter was being land applied for the "sole purpose of disposing of it."

Lastly, the court evaluated the term "solid waste" as it pertains to RCRA. 42 U.S.C. § 6903(27) defines "solid waste" as such:

> The term "solid waste" means any garbage, refuse, sludge from a waste treatment plant, water supply treatment plant, or air pollution control facility and other discarded material, including solid, liquid, semisolid, or contained gaseous material resulting from industrial, commercial, mining, and agricultural operations, and from community activities, but does not include solid or dissolved material in domestic sewage, or solid or dissolved materials in

> irrigation return flows or industrial discharges which are point sources subject to [CWA or Atomic Energy Act].

Since the plaintiffs chose not to pursue poultry litter as "garbage", "refuse", or "sludge", the court was left to determine if poultry litter fell into the category of "other discarded material" resulting from "agricultural operations". The court adopted a multistep process to determine whether or not poultry litter could be considered as "discarded".

The court first found that a material cannot be considered as "discarded" if it was "'destined for beneficial reuse or recycling in a continuous process by the generating industry itself'", citing *Am Petroleum Inst. v. EPA*. In addition to this, the court had already found that there were no documented cases of where poultry litter was applied to a field for the express purpose of disposing of or discarding it. The court once again cited its previous finding of poultry litter as a marketable material as further evidence that poultry litter could not be considered a "solid waste".

The court also rejected the plaintiff's argument that poultry litter could be considered as "discarded" when applied on a nitrogen basis. The plaintiff's argument was essentially that applying poultry litter on a N basis applies excess P. Since the excess P is not used, it can be considered to have been discarded. However, the court disagreed, stating that "the fact a field in the IRW may have a high soil test phosphorus" (which is usually a result of the over-application of P) "is not in itself determinative of whether poultry litter has been 'discarded'" (20).

The court also rejected two more claims by the plaintiffs regarding the "solid waste" status of poultry litter. The plaintiffs argued that since the poultry litter was not actually recycled within the poultry growing process, it did not fit the description of

"beneficial reuse". The court rejected this claim on the idea that the waste was being sent to another industry for beneficial use, and that this was not necessarily considered discarding of the waste. The plaintiffs also cited *U.S. v. Seaboard Foods, LP*, where it was ruled that animal manures are "solid wastes" within the confines of RCRA. However, the court rejected this claim as well, stating that the nature of the waste in the *Seaboard* case (waste leaching from storage lagoons) was significantly different from the application of poultry litter and could not be applied so broadly (20).

In the end, the court found insufficient evidence to label poultry litter as a "solid waste" under RCRA, and dismissed the case given that this designation was critical to Oklahoma's argument. This determination was appealed, and is currently awaiting review in a court of appeals.

In the 2013 case of *C.A.R.E. v. Cow Palace, LLC*, the court ruled that a case could not be dismissed simply on the grounds that manure cannot be classified as "discarded" on the basis of over-application of manure and unintentional discharge of manure. This ruling is in direct contention with the ruling in Oklahoma v. Tyson Foods. In this case, the court states that over-applying manure to a field beyond the normal application rate for what is needed could be considered as "discarding" the manure, but that it needed more evidence to support this idea, as the case is ongoing. It would be interesting to see how the results of this case turn out, as they could have a significant impact on how "solid wastes" are defined by RCRA in the future (21).

Conclusions

This paper has investigated three federal programs (CWA, CERCLA, and RCRA) and their potential power to regulate nutrient contamination in the Ozark ecoregion. In

the case of *Arkansas v. Oklahoma*, it was found that the EPA has the power to hold upstream states to the water quality standards of downstream states when issuing NPDES permits for point sources. However, the EPA may have too much control over the evidence presented when issuing permits. In City of Tulsa v. Tyson Foods, Inc., the court granted significant potential power to CERCLA to combat nonpoint source pollution on a watershed scale, namely determining that an entire watershed can be considered a "facility", and that phosphates in poultry litter can be labeled a "hazardous substance" under CERCLA. However, in this case, no precedents were set and the court failed to find poultry companies liable for "arranging" the disposal of litter, despite some convincing evidence to the contrary. Lastly, in Oklahoma v. Tyson Foods, Inc., the court failed to find poultry litter as a "solid waste" under RCRA, again despite some convincing arguments, although the end result of this trial sequence is still pending.

Bibliography

(1) Phosphorus. University of Hawai'i at Manoa, 2007. Web. 16 Nov. 2013.

(2) Lopez, C.B., Jewett, E.B., Dortch, Q., Walton, B.T., Hudnell, H.K. 2008. Scientific Assessment of Freshwater Harmful Algal Blooms. Interagency Working Group on Harmful Algal Blooms, Hypoxia, and Human Health of the Joint Subcommittee on Ocean Science and Technology. Washington, DC.

(3) Correll, D. L. 1999. Phosphorus: a rate limiting nutrient in surface waters. *Poultry Science* 78: 674-682.

(4) Heeren, D. M., Miller, R. B., Fox, G. A., Storm, D. E., Penn, C. J., & Halihan, T.. 2010. Preferential flow path effects on subsurface contaminant transport in alluvial floodplains. *Transactions of the ASABE* 53: 127-136.

(5) Fuchs, J.W., Fox, G.A., Storm, D.E., Penn, C.J., & Brown, G.O. (2009). Subsurface transport of phosphorus in riparian floodplains: Influence of the preferential flow paths. *J. Environ. Qual.* 38: 473-484.

(6) Illinois River Watershed. Environmental Protection Agency, 2 Dec. 2013. Web. 16 Nov. 2013.

(7) Nolan, J. M. 2010. The Oklahoma poultry industry: an industry in the crosshairs of environmental compliance. Drake J. Agric. L. 15(2): 225-256.

(8) United States. Environmental Protection Agency. "Environmental Administrative Decisions: The administrator and judicial officers, April 1985 to October 1989." Environmental Protection Agency, Jan. 1995. Web. 12 Nov. 2013.

(9) Moffett, L. 2004. Arkansas v. Oklahoma: A case of water pollution. *Dartmouth Col. Undergrad. J. of Law.* 11(2): 8-16.

(10) Oklahoma water quality standards. Title 785, Ch. 45. Appendix A.1. 1 Jul. 2013. Web.

(11) State of Oklahoma v. EPA. 908 F. 2d 595. U.S. Court of Appeals, Tenth Circuit. 1990. Leagle, Inc. Web. 12 Nov. 2013.

(12) Arkansas v. Oklahoma. 503 U.S. 91. U.S. Supreme Court. 1992. Leagle, Inc. Web. 12 Nov. 2013.

(13) Adler, R. W. 1999. Integrated approaches to water pollution: Lessons from the Clean Water Act. *Harv. Envtl. L. Rev*. 23: 203-295.

(14) Comprehensive Environmental Response, Compensation, and Liability. Pub. L. 113-36 103 Stat. 9601(9). 11 Dec. 1980.

(15) Comprehensive Environmental Response, Compensation, and Liability. Pub. L. 113-36 103 Stat. 9607(a). 11 Dec. 1980.

(16) City of Tulsa v. Tyson Foods, Inc. 258 F.Supp.2d 1263. U.S. District Court, N.D. Oklahoma. 2003. Leagle, Inc. 13 Nov. 2013.

(17) Pittman, H. M. 2006. Poultry litter and water quality in the Ozark mountains: Allegory for and prelude to the national debate over how best to address water pollution throughout the United States. *J. Food L. & Pol'y.* 2: 157-229.

(18) Warren, D. M. 2006. *City of Tulsa v. Tyson Foods:* CERCLA comes to the farm-but did arranger liability come with it? *Ark. L. Rev.* 59: 169-197.

(19) Resource Conservation and Recovery Act. Environmental Protection Agency, 30 Oct. 2013. Web. 14 Nov. 2013.

(20) State of Oklahoma v. Tyson Foods, Inc., findings of fact and conclusions of law on defendants' motions for partial judgment pursuant to rule 52(c). 05-CV-0329-GKP-PJC. U.S. District Court, N. D. Oklahoma. 2010. American Farm Bureau. 14 Nov. 2013.

(21) CARE v. Cow Palace, LLC. 13-CV-03016-TOR. U.S. District Court, E.D. Washington. 2013. Center for Food Safety. 14 Nov. 2013.

9. APPENDIX B. HYDRUS parameter inputs.

The following table compiles important information about the flow and transport parameters used for every model presented in this thesis. Information about each parameter presented in this appendix is presented below. More detailed information about each parameter is presented in the main body of the thesis.

Table B.1. Variable description and units.

Variable	Units	Description
Water Flow		
θ_r	$[L^3L^{-3}]$	Residual mobile soil water content
θ_s	$[L^3L^{-3}]$	Saturated mobile soil water content
α	$[L^{-1}]$	Parameter α in the Van Genuchten soil water retention function
n	[-]	Parameter n in the Van Genuchten soil water retention function
K_s	$[LT^{-1}]$	Saturated hydraulic conductivity
l	[-]	Tortuosity parameter
$\theta_{r,\,im}$	$[L^3L^{-3}]$	Residual immobile soil water content
$\theta_{s,\,im}$	$[L^3L^{-3}]$	Saturated immobile soil water content
α_{im}	$[L^{-1}]$	Parameter α in the Van Genuchten soil water retention function for the immobile region
n_{im}	[-]	Parameter n in the Van Genuchten soil water retention function for the immobile region
ω	$[T^{-1}]$	Mass transfer coefficient for water flow

Table B.1 (Continued)

Variable	Units	Description
Solute Transport		
Disp. L.	[L]	Longitudinal dispersivity coefficient
Disp. T.	[L]	Transverse dispersivity coefficient
Frac	[-]	Fraction of sorption sites available for instantaneous sorption
K_d	$[L^3M^{-1}]$	Adsorption isotherm coefficient *ks*
Nu	$[L^3M^{-1}]$	Adsorption isotherm coefficient η (for use with the Langmuir isotherm)
Beta	[-]	Adsorption isotherm coefficient β (for use with the Freundlich isotherm)
α (solute)	$[T^{-1}]$	Mass transfer coefficient for solute transport

Table B.2. Model information for all model levels (recreated from Table 4).

	Level 1	Level 2a	Level 2b	Level 2c	Level 3	Level 4	Level 5	Level 6	Level 7	Mesh Macropore
Model Information										
HYDRUS program	1D	1D	1D	1D	2D	2D	2D	2D	2D	2D
Flow model	SP	DP	DP	DP	SP	SP	DP	DP	DP	SP
Simulation	LT	LT	LT	LT	Cal	Cal, LT	Cal	Cal, LT	LT	Cal
Precipitation	Daily	5-min	5-min	5-min	n/a	Daily	n/a	Daily	5-min	n/a
Soil Parameters										
Gravel Layers	1	3	3	3	1	3	1	3	3	5*
K_s (SiL)	PTF	Plot	Plot	Plot	Plot	Plot	Plot	Plot	Plot	Plot
K_s (Gravel)	PSD	ERI	ERI	ERI	ERI	ERI	ERI	ERI	ERI	ERI
α, ω	n/a	Literature	Cal	Cal	n/a	n/a	Cal	Cal	Cal	n/a

* Additional layers are used to express mesh macropore and thatch layers

Table B.3. Silt loam (SiL) water flow parameters for all model levels.

	Level 1	Level 2a	Level 2b	Level 2c	Level 3	Level 4	Level 5	Level 6	Level 7	Mesh Macropore
Water Flow Parameters										
SiL										
θ_r	0.067	0.01	0.01	0.01	0.067	0.067	0	0	0	0.067
θ_s	0.45	0.02	0.02	0.02	0.45	0.45	0.01	0.01	0.01	0.45
α	0.02	0.1	0.1	0.1	0.02	0.02	0.1	0.1	0.1	0.02
n	1.41	2	2	2	1.41	1.41	2	2	2	1.41
K_s	0.45	9.6	9.6	9.6	9.6	9.6	9.6	9.6	9.6	0.61
l	0.5	0.5	0.5	0.5	0.5	0.5	0.5	0.5	0.5	0.5
$\theta_{r,\,im}$	-	0.067	0.067	0.067	-	-	0.067	0.067	0.067	-
$\theta_{s,\,im}$	-	0.44	0.44	0.44	-	-	0.44	0.44	0.44	-
α_{im}	-	0.02	0.02	0.02	-	-	0.02	0.02	0.02	-
n_{im}	-	1.41	1.41	1.41	-	-	1.41	1.41	1.41	-
ω	-	0.1	0.01	0.01	-	-	0.01	0.01	0.01	-

Table B.4. Gravel water flow parameters for all model levels.

	Level 1	Level 2a	Level 2b	Level 2c	Level 3	Level 4	Level 5	Level 6	Level 7	Mesh Macropore
Gravel										
θ_r	0.045	0.01	0.01	0.01	0.045	0.045	0	0	0	0.045
θ_s	0.43	0.02	0.02	0.02	0.43	0.43	0.01	0.01	0.01	0.43
α	0.145	0.145	0.145	0.145	0.145	0.145	0.145	0.145	0.145	0.145
n	2.68	2.68	2.68	2.68	2.68	2.68	2.68	2.68	2.68	2.68
K_{s1}	640	130.66	130.66	130.66	342.3	130.66	342.3	130.66	130.66	130.66
K_{s2}	-	403.75	403.75	403.75	-	403.75	-	403.75	403.75	403.75
K_{s3}	-	578.16	578.16	578.16	-	578.16	-	578.16	578.16	578.16
$K_{s,\ macropore}$	-	-	-	-	-	-	-	-	-	450
l	0.5	0.5	0.5	0.5	0.5	0.5	0.5	0.5	0.5	0.5
$\theta_{r,\ im}$	-	0.045	0.045	0.045	-	-	0.045	0.045	0.045	-
$\theta_{s,\ im}$	-	0.42	0.42	0.42	-	-	0.42	0.42	0.42	-
α_{im}	-	0.145	0.145	0.145	-	-	0.145	0.145	0.145	-
n_{im}	-	2.68	2.68	2.68	-	-	2.68	2.68	2.68	-
ω	-	0.1	0.1	0.1	-	-	0.1	0.1	0.1	-

Table B.5. Silt loam (SiL) solute transport parameters for all model levels. Sorption parameters only apply to P transport.

	Level 1	Level 2a	Level 2b	Level 2c	Level 3	Level 4	Level 5	Level 6	Level 7	Mesh Macropore
Transport Parameters										
SiL										
Disp. L.	30	30	30	100	200	100	200	100	100	40, 150
Disp. T.	-	-	-	-	20	10	20	10	10	4, 15
Frac	1	1	1	1	1	1	0.75	1	1	0.1
K_d	10.3	10.3	10.3	10.3	10.3	10.3	10.3	10.3	10.3	12
Nu	0	0	0	0	0	0	0	0	0	0
Beta	1	1	1	1	1	1	1	1	1	1
α (solute)	-	2	0.2	0.2	-	-	0.2	0.2	0.2	-

Table B.6. Gravel solute transport parameters for all model levels. Sorption parameters only apply to P transport

	Level 1	Level 2a	Level 2b	Level 2c	Level 3	Level 4	Level 5	Level 6	Level 7	Mesh Macropore
Gravel										
Disp. L.	30	30	30	200	200	200	200	200	200	40, 150
Disp. T.	-	-	-	-	20	20	20	20	20	4, 15
Frac	1	1	1	1	1	1	0.75	1	1	0.1
K_{d1}	1.5	2	2	2	1.75	2	1.75	2	2	4.5
K_{d2}	-	1.75	1.75	1.75	-	1.75	-	1.75	1.75	4.5
K_{d3}	-	1.5	1.5	1.5	-	1.5	-	1.5	1.5	4.5
Nu	0	0	0	0	0	0	0	0	0	0.048
Beta	1	1	1	1	1	1	1	1	1	1
α (solute)	-	1	0.01	0.01	-	-	0.01	0.01	0.01	-

10. APPENDIX C. Analysis of evapotranspiration and root water uptake effects in a special two-year simulation.

Evapotranspiration and root water uptake, hereafter referred to collectively as ET, can substantially affect water and solute transport through a soil profile. ET was simulated on the Level 7 model using the Root Water Uptake module in HYDRUS. However, we were unable to successfully incorporate ET into long-term trials. While it is not entirely clear as to why HYDRUS was unable to properly model ET, a likely reason is the combination of the overall complexity of the long-term model combined with low precipitation values for 2005, the second year of simulation that caused the model to fail. Due to time constraints, it was not possible to find a fix for this, and ET was abandoned from the regular long-term models.

Despite this failure, it was still important to determine how HYDRUS simulated ET, and what effect ET might have on the model. Therefore, a special trial was conducted. A two-year simulation was conducted using precipitation data from 2007 and 2008. The model was started using the same initial conditions as the regular long-term trials (meaning that it did not start the 2007 precipitation year with initial conditions from the 2006 precipitation year). A 1 meter root zone was added to the top of the profile, and roots were modeled as those for pasture grasses. HYDRUS provided root water uptake characteristics based on the Feddes model. Evapotranspiration rates for the Barren Fork Creek region were estimated from average annual potential ET obtained from MODIS Global Evapotranspiration Project at the University of Montana.

Results for the two-year simulation can be seen in Figure C.1. The ET model

yielded 1.48 kg ha^{-1} P to the water table of the 129.8 kg ha^{-1} P that entered the profile. This resulted in a P delivery ratio of 1.1%. The model without ET yielded 9.52 kg ha^{-1} P to the water table of the 121.2 kg ha^{-1} P applied, resulting in a P delivery ratio of 7.9%. The comparison between these two models shows that after only two years, the model featuring ET had P yields of nearly seven times less than the model without ET. These results suggest that the ET process is vital to fully understanding and modeling solute transport in these profiles and future work needs to be done to expand ET modeling to the full-length long-term trials in order to accurately assess the magnitude of P leaching to the groundwater.

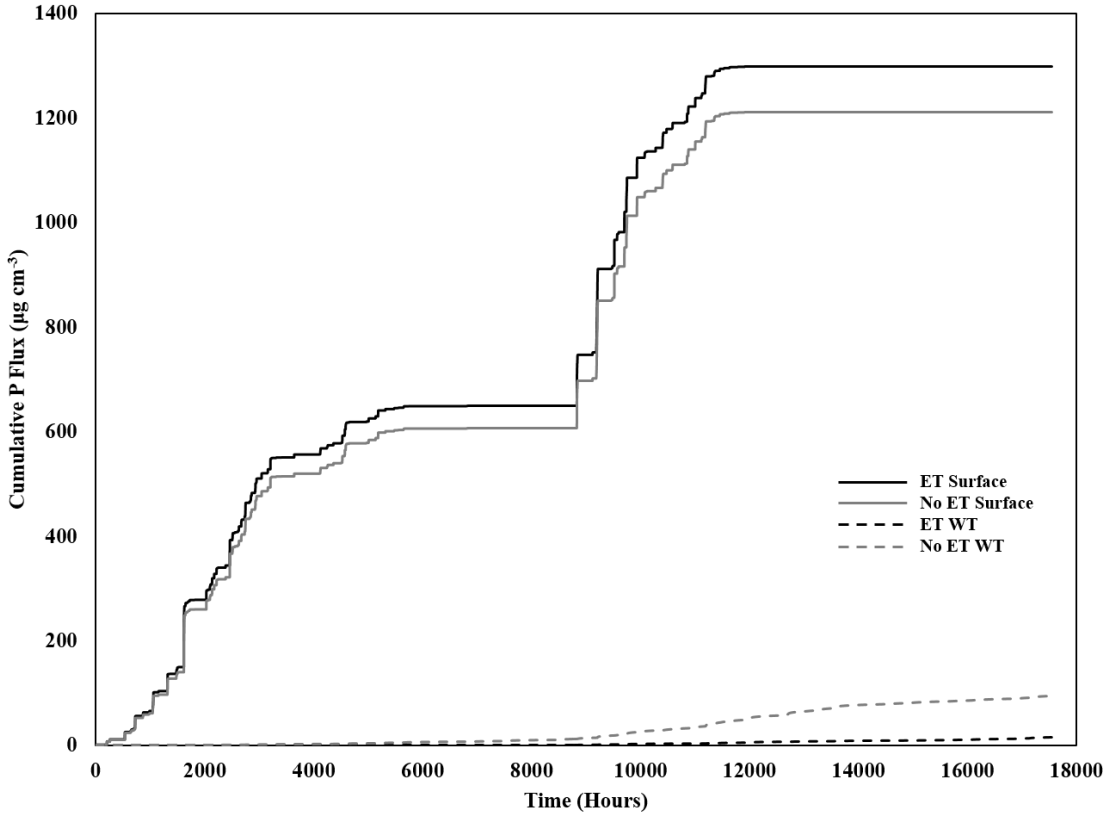

Figure C.1. Simulation results comparing models with and without ET between Mar 2007 and Feb 2009. Time is represented in hours after Mar 1, 2007.